DISCOVERY AND INVESTIGATION OF A NOVEL ROLE FOR MITOCHONDRIAL PROHIBITIN IN MITIGATING ACUTE HEART FAILURE IN ENDOTOXIC SHOCK

By

Taylor Ann Mattox

February 2014

Director of Dissertation: Ethan J. Anderson, Ph.D

Department of Pharmacology and Toxicology, Brody School of Medicine, East Carolina University.

Sepsis results in more than 200,000 deaths annually and is the 10th leading cause of death in the United States (US). In spite of significant advances in medical care the mortality rate for sepsis has continued to rise. Sepsis and the diseases along its continuum (septic shock and multiple organ dysfunction syndrome, MODS) are characterized by excessive production of inflammatory mediators via a feed-forward mechanism that results in a condition commonly referred to as the 'cytokine storm.' This maladaptive inflammatory response, and the subsequent mitochondrial dysfunction that results from it, are thought to underlie the impairment of cardiac function that occurs in the progression from sepsis to MODS. Prohibitin (PHB) is a ubiquitously expressed mitochondrial localized protein, which recent evidence has suggested has a wide variety of roles from transcriptional regulator to a mediator of inflammatory and oxidative signaling.

Here, using a comprehensive series of *in vitro* and *in vivo* experiments, we tested the hypothesis that PHB confers cardiac protection during endotoxic shock (i.e., cytokine storm

induced by LPS) through 1) preservation of mitochondrial integrity 2) attenuated inflammatory signaling, primarily through NFκB and 3) augmented Nrf2 signaling and antioxidant capacity. As expected, LPS and cytokines disrupted mitochondrial function and integrity in both our models. In rats, LPS injection reduced PHB expression in whole heart while simultaneously concentrating the remainder in the nucleus. Interestingly, serum levels of PHB were transiently elevated 3-fold by LPS, but were restored to normal levels within 24 hours. Similarly, whole cell PHB expression was reduced and nuclear accumulation of PHB was increased in cardiomyocytes following TNFα/IL1β treatment *in vitro*. Overexpression of PHB (oPHB) and treatment with recombinant PHB (rPHB) protected cardiomyocytes from TNFα/IL1β-induced toxicity by preserving mitochondrial function, suppressing oxidative stress and ultimately mitigating cytokine-induced cytotoxicity. We further observed that oPHB and rPHB attenuated the TNFα/IL1β-induced transcription of pro-inflammatory genes in cardiomyocytes, while augmenting Nrf2 nuclear transactivation and up-regulation of Nrf2-mediated genes.

Next, using wild-type (WT) and Nrf2-/- mice we tested the hypothesis that cytokine generation and inflammatory signaling induced by LPS challenge would be suppressed by rPHB treatment in a Nrf2-dependent manner, leading to protection of cardiac mitochondria and recovery of cardiac function. Following LPS challenge, endogenous levels of PHB transiently increased dramatically in WT but not Nrf2-/- mice. Treatment with rPHB following LPS challenge suppressed circulating levels of IL6 and TNFα in WT and Nrf2-/- mice, resulting in decreased NFκB and STAT3 activation in heart and complete attenuation of proinflammatory cytokines and iNOS in this organ. Additionally, rPHB treatment reversed the LPS-induced decrease in mitochondrial ATP generation in heart, simultaneously leading to rapid recovery of cardiac function within ~12 hours. Interestingly, rPHB treatment mitigated the LPS-induced

inflammatory response and cardiac dysfunction to similar extent in both WT and Nrf2-/- mice, suggesting the effects of rPHB are independent of Nrf2.

Collectively, these findings suggest that PHB is a mitochondrial inner-membrane protein that acts as a mobile signal transducer, capable of moving from mitochondria to nucleus and also between cell and tissue compartments, to suppress inflammation and cytotoxicity during severe inflammatory stress. They further suggest that PHB may be critical to alleviating the maladapative host response to infection and represents a novel therapeutic target for the treatment of sepsis-associated cardiac dysfunction. Future studies directed at exploiting the pleiotropic functions of PHB to mitigate inflammation and oxidative stress in other cardio-metabolic disease models will be important to building on the knowledge that the present studies have established.

DISCOVERY AND INVESTIGATION OF A NOVEL ROLE FOR MITOCHONDRIAL PROHIBITIN IN MITIGATING ACUTE HEART FAILURE IN ENDOTOXIC SHOCK

A Dissertation

Presented To

The Faculty of the Department of Pharmacology and Toxicology

The Brody School of Medicine at East Carolina University

In Partial Fulfillment

of the Requirements for the Degree

Doctor of Philosophy in Pharmacology and Toxicology

By

Taylor Ann Mattox

February, 2014

DISCOVERY AND INVESTIGATION OF A NOVEL ROLE FOR MITOCHONDRIAL PROHIBITIN IN MITIGATING ACUTE HEART FAILURE IN ENDOTOXIC SHOCK

by

Taylor Ann Mattox

APPROVED BY:

DIRECTOR OF

DISSERTATION:_____

Ethan J. Anderson, PhD

COMMITTEE MEMBER: _____

Abdel A. Abdel-Rahman, PhD

COMMITTEE MEMBER: _____

Rukiyah Van Dross-Anderson, PhD

COMMITTEE MEMBER: _____

David Brown, PhD

COMMITTEE MEMBER: _____

Alan P. Kypson, MD

CHAIR OF THE DEPARTMENT

OF PHARMACOLOGY & TOXICOLOGY: _____

David Taylor, PhD

DEAN OF THE

GRADUATE SCHOOL: _____

Paul J. Gemperline, PhD

ACKNOWLEDGEMENTS

First and foremost I would like to thank God for lending me His strength to finish this process and blessing me with a wonderful support system. I would like to thank my family and friends for that support throughout the last five years. To my moms and dads (yes, all four), I would never have been able to achieve this goal without their constant love and backing. I want to thank them for teaching me that nothing is impossible once I set my mind to it. I want to thank them for their unending belief in me, even when they thought I would make a career as a professional student. I promised I will get a job now. I want to thank my wonderful siblings for putting up with me the last few years. Finally to my Toby, a simple thank you will not suffice. Without his stabilizing influence I would not have made it through this exciting and stressful time in my life.

I would like to thank all my fellow classmates for the fun and all the support, especially near the end. I would like to thank Dr. Carlyle Rogers for always being willing to listen to my experimental ideas and for making sure I had everything properly controlled. I cannot thank him enough for being the sounding board I always needed. I would like to thank Anusha Penumarti for always letting me complain and for making me smile! I wish you all the best in your future endeavors.

Additionally, I would like to thank all the faculty and staff of the Department of Pharmacology and Toxicology at the Brody School of Medicine. The support I have received from everyone during my time in the department has been immeasureable. I would like to extend a very special thank you to Kathleen Thayne for her technical expertise, advice and most importantly her friendship. I would also like to thank the members of my committee, Drs.

Abdel-Abdel Rahman, Rukiyah Van Dross-Anderson, David Brown, and Alan Kypson for their input and critical role in shaping my research. I would like to extend a special thank you to Dr. David Taylor; without his endless support and guidance, I would not have made it to the finish line.

Last but certainly not least, I would like to extend my deepest gratitude and appreciation to my dissertation advisor, Dr. Ethan Anderson for his instrumental and enthusiastic direction throughout the last five years. The support and encouragement he has given me has been invaluable as I matured as a scientist.

TABLE OF CONTENTS

LIST OF TABLES

LIST OF FIGURES

LIST OF SYMBOLS OR ABBREVIATIONS

ADP	adenosine diphosphate
Ap5a	P1, P5 Di(adenosine-5')Pentaphosphate
ARE	antioxidant response element
ATP	adenosine triphosphate
BAP37	B-cell receptor associated protein and prohibitin 2
CFU	colony forming units
CI	cardiac index
CLP	cecal ligation and puncture
DAMPs	damage-associated molecular patterns
DSS	dextran sodiun sulfate
EDTA	ethylenediaminetetraacetic acid
EF	ejection fraction
ELISA	enezyme-linked immunosorbent assay
eNOS	endothelial derived nitric oxidase synthase
ERK	extracellular signal-regulated kinase
FS	fractional shortening
GCLC	glutamate-cysteine ligase
GFP	green fluorescent protein
GPX	glutathione peroxidase
HDACs	histone deacetylases
HL1c	HL-1 cardiomyocytes
HO	heme oxygenase
HR	heart rate
HRP	horseradish peroxidase

IBD	inflammatory bowel disease
ICU	intensive care unit
IKK	IκB kinase complex
IL1β	interleukin 1 beta
IL6	interleukin 6
iNOS	inducible nitric oxide synthae
IP	intraperitoneal
IRAK	interleukin receptor-associated kinase
IV	intravenous
JAK	janus kinase
Keap1	kelch-like ECH-associated protein
Lamp2a	lysosome associated protein 2a
LC3	light chain 3
LD50	lethal dose 50
LDH	lactate dehydrogenase
LPS	lipopolysaccharide
LV	left ventricle
LVeDD	left ventricle end diastolic diameter
LVeSD	left ventricle end systolic diameter
mAAA	mitochondrial ATPase Associated with diverse cellular Activities
MAPK	mitogen-activated protein kinase
mATP	mitochondrial ATP generation
mCa^{2+}	mitochondrial calcium uptake
MCP	monocyte chemotactic protein

MEFs	mouse embryo fibroblasts
mH_2O_2	mitochondrial hydrogen peroxide emitting potential
MIM	mitochondrial inner membrane
mO_2	mitochondrial oxygen consumption
MODS	multiple organ dysfunction syndrome
MOM	mitochondrial outter membrane
MDF	myocardial depressant factor
mtDNA	mitochondrial DNA
NADP+	nicotinamide adenine dinucleotide phosphate
NFκB	nuclear factor kappa light chain-enhancer of activated B cells
NLRP3	NLR family, pyrin domain containing 3
nNOS	neuronal derived nitric oxide synthase
NO	nitric oxide
NQO1	NAD(P)H dehydrogenase quinone 1
Nrf2	nuclear factor (erythorid-derived 2) like2
Nrf2KO	Nrf2 knockout
$O_2^{\bullet-}$	superoxide
OPA1	optic atrophy 1
oPHB	overexpression of prohibitin
OxPhos	oxidative phosphorylation
P/M	pyruvate/malate
PAMPs	pathogen-associated molecular patterns
PC+M	pamitoyl carnitine + malate
PHB	prohibitin 1

PHB2	prohibitin 2
PI3K	phosphatidylinositol 3 kinase
PIP3	phosphatidylinositol 3,4,5-triphosphate
PKCδ	protein kinase C delta
PPAR	peroxisome proliferator-activated receptor
RCR	respiratory control ratio
RNS	reactive nitrogen species
ROS	reactive oxygen species
rPHB	recombinant prohibitin
RT	room temperature
S	succinate
SDS-PAGE	sodium dodecyl sulfate-polyacrylamide gel electrophoresis
SERCA	scaroplasmic/endoplasmic reticulum Ca-ATPase
siRNA	short interfereing RNA
SIRS	systemic inflammatory response syndrome
SOD	superoxide dismutase
SPFH	stomatin, prohibitin, flotillin, HflK/c
STAT	signal transducer and activators of transcription
SV	stroke volume
TBS-T	tris-buffered saline - 0.1% tween20
TCA	the citric acid cycle
TGFβ	transforming growth factor beta
TLR	toll-like receptor
TNFα	tumor necrosis factor alpha

TRX	thioredoxin (TxnRd) = thioredoxin reductase)
UCPs	uncoupling proteins
Vec	vector tranfected control cells
Veh	vehicle
WT	wild-type
$\Delta\psi_{mito}$	mitochondrial membrane potential

CHAPTER ONE – Introduction

1.1 Sepsis

Sepsis, the 10th leading cause of death in the United States, is a complex disorder with an estimated 750,000 cases annually resulting in 210,000 deaths (Angus et al., 2001; Melamed and Sorvillo, 2009; Angus and van der Poll, 2013). Medical care for patients suffering from sepsis and the diseases along its continuum (e.g. MODS) are estimated to be in excess of $17 billion in the United States each year (Coopersmith et al., 2012). The term sepsis dates back to Hippocrates who used it to describe how "flesh rots, swamps generate foul smells, and wounds fester" (Majno, 1991). In 1991, the American College of Chest Physicians and Society of Critical Care Medicine Consensus Conference was held to standardize the definition of sepsis and its sequelae. The consensus conference defined 'sepsis' as the systemic inflammatory response (SIRS to infection. The conference further defined 'severe sepsis' as sepsis complicated by organ failure, and 'septic shock' was defined as severe sepsis with refractory hypotension (Bone et al., 1992). Septic shock is the number one cause of MODS in intensive care units and is strongly correlated to mortality (Blanco et al., 2008). Additionally, MODS accounted for 43.1% of deaths in a retrospective study of septic patients, making it the leading cause of death associated with severe sepsis (Vincent et al., 2011). Sepsis is characterized by complex interactions between the infecting microorganism, the host immune system, inflammatory and coagulation responses (Hotchkiss and Karl, 2003). In spite of advances in our knowledge of the mechanisms underlying sepsis and improved treatments (Levy et al., 2010; Angus and van der Poll, 2013), the mortality rate has risen over the past several decades (Dombrovskiy et al., 2007) and is expected to continue rising as the US population ages (Melamed and Sorvillo, 2009).

Many mediators have been proposed to trigger sepsis. Much interest has fallen on products released from bacteria, including lipopolysaccharide (LPS) and lipoteichoic acid. LPS is a component of the outer wall of gram negative bacteria. LPS and endotoxin are used interchangeably throughout the literature. Both LPS and lipoteichoic acid are ligands from a subset of pattern recognition receptors known as the toll-like receptors (TLRs) (Erridge, 2010). In response to bacterial invasion LPS is released from gram negative bacteria to activate TLR4 on phagocytic cells, resulting in a robust release of proinflammatory cytokines thought to play a central role in the pathogenesis of sepsis-induced MODS (Clark and Coopersmith, 2007). Despite the well-characterized pathophysiology, most attempts at mitigating MODS with pharmacological interventions have failed. Recently, a clinical trial involving 1800 septic patients and the use of a TLR4 antagonist, eritoran, was discontinued due to the drug's inability to decrease 28-day mortality in patients with severe sepsis (Opal et al., 2013). Since the 1980s, approximately 60 phase two and phase three clinical trials have been conducted for pharmacological agents in the treatment of sepsis. In a 2013 publication, Mitchell Fink compiled a list of these clinical trials and reported that only a very small number of drug trials have resulted in improved survival, none of which have been remarkable (Fink, 2013). Clearly, gaps exist in current knowledge of the molecular mechanisms involved in the development of sepsis and MODS, and further investigation and data from preclinical studies involving animal models of sepsis are needed to address these knowledge gaps so that effective therapies can be developed.

1.1.1 Animal Models

Sepsis is a heterogeneous clinical condition, making it difficult to develop an experimental model to match the physiology of human sepsis. Sepsis and the conditions on its continuum are induced experimentally in a number of ways. As discussed above, knowledge obtained using animal models of sepsis has yielded misleading results. New approaches for animal models of sepsis are being investigated, but the most commonly used are intraperitoneal (IP) bolus of LPS, intravenous (IV) infusion of LPS and cecal ligation and puncture (CLP). Some lesser-used variations of the first two include cecal slurry and injection of bacteria. All models have their benefits and limitations.

Using LPS as an induction method leads to systemic activation of the innate immune system. At large doses, LPS can mimic some clinical characteristics of gram negative infection in humans including marked hypotension, cardiac impairment, increased circulating proinflammatory cytokines and lactic acidosis (Fink, 2013). This method of induction yields highly reproducible degrees of sepsis or acute septic shock in animals. The major drawback to this method is related to the varying degree of susceptibility of mice to the toxic effects of LPS. The dose required to kill half the mice (LD50) in a cohort at 24 hours was 24 mg/kg (Ramana et al., 2006). Fink relays that the dose used to investigate the response of healthy humans to LPS is between 2-4 ng/kg and this resulted in symptoms including fever and increased circulating proinflammatory cytokines (Barber et al., 1995; Suffredini et al., 1995; Fink, 2013). Furthermore, to induce severe illness in humans the dose is 1,000-10,000 fold lower than what is used in mice (Taveira da Silva et al., 1993). Other major confounding results include the ability of anti-inflammatory agents, such as tumor necrosis factor-alpha (TNFα) neutralizing

antibodies, to increase survival in animal models of LPS-induced sepsis but their failure in clinical trials. This could be due to underlying difference in gene expression responses to LPS between species (Seok et al., 2013).

CLP is considered the "gold standard" animal model of sepsis. CLP surgery includes ligation distal to the ileocecal valve and needle puncture of the ligated cecum which results in leakage of fecal matter into the peritoneum causing polymicrobial bacteremia and sepsis (Rittirsch et al., 2009). Clinical characteristics mimicked by CLP include multiple strains of bacteria in the bloodstream (Alexander et al., 1991), progressive systemic inflammatory response, severe hypotension and immunosuppression thought to be the result of lymphocyte apoptosis (Ayala and Chaudry, 1996; Hotchkiss and Karl, 2003). However, despite encompassing more clinical features of sepsis it is still missing some key features. The foremost limitation is that the surgery is not well standardized and if done incorrectly, can yield highly variable results. CLP fails to reproducibly induce acute kidney or lung injury (Kuhlmann et al., 1994; Yang and Hauptman, 1994). Another major drawback is that septic patients usually receive multiple forms of supportive care (e.g., antibiotics and fluid resuscitation), and while some of these are included in murine models, the more complex interventions are rarely used (Fink, 2013).

The lesser known and used animal models of sepsis are riddled with flaws, but have some benefit to certain lines of research. Using an injection of bacteria does not mimic clinical characteristics of sepsis, however, it is helpful to study to mechanisms of host response to infectious pathogens. The method of cecal slurry induction, a process by which mice are injected with a slurry containing feces and saline, yields a high degree of variability due to

inaccurate calculations of colony forming units (CFU) as well as varying infectious agents (Jon et al., 2005).

1.1.2 Cardiac dysfunction in sepsis

Impairment of cardiac contractility and function has been suggested to be an initial and key component of clinical sepsis and the development of MODS (Sharma, 2007; Flierl et al., 2008; Werdan et al., 2009). The first evidence for cardiac dysfunction in septic patients with adequate fluid resuscitation was reported by Calvin and colleagues in 1981. Using radionuclide cineangiography this group demonstrated decreased ejection fraction (EF) and increased end-diastolic volume index in patients suffering from severe sepsis (Calvin et al., 1981). Echocardiographic studies have demonstrated impaired left ventricle (LV) systolic and diastolic dysfunction in septic patients (Poelaert et al., 1997). Much work has been done to delineate the mechanism by which cardiac dysfunction occurs during sepsis. Despite this, the pathophysiology of this condition remains elusive and is likely multifactorial. Decreased contractility and impaired myocardial compliance have been demonstrated across various experimental models of sepsis including cell culture (Ren et al., 2002), isolated heart studies (McDonough et al., 1998; Merx et al., 2004) , and *in vivo* models (Natanson et al., 1986; Ramana et al., 2006). Other mechanisms implicated in the pathophysiology of cardiac dysfunction in sepsis include inflammatory signaling (Liu and Malik, 2006; Ding et al., 2009; Fallach et al., 2010; Zou et al., 2010), mitochondrial dysfunction (Crouser, 2004; Lancel et al., 2005; Crouser et al., 2008; Exline and Crouser, 2008), cellular damage and death (Hassoun et al., 2008; Celes et al., 2010; Kao et al., 2010), and autonomic deregulation (Werdan et al., 2009; Wondergem et al., 2010). The development of sepsis-induced cardiac dysfunction is directly correlated to worse

outcomes in patients. Patients that develop sepsis-induced cardiac dysfunction have a 50% higher mortality rate than patients that do not development this condition (Merx and Weber, 2007).

1.1.3 Mitochondrial dysfunction in sepsis

Mitochondria are a network of interconnected structures that are constantly remodeling through dynamic processes known as fission and fusion. Depending on cell type and energy demand, mitochondria adjust shape and distribution (McBride et al., 2006; Cerveny et al., 2007). Mitochondria are responsible for supplying the cell with energy through the conversion of food to adenosine triphosphate (ATP). The chemiosmotic theory, originally proposed in 1961 by Mitchell (Mitchell, 1961), states that mitochondria pump protons out of the mitochondrial matrix to create a proton motive force. Mitochondria utilize this electrochemical gradient to free energy needed for the F_1F_o-ATPase to phosphorylate ADP to ATP. Mitochondrial membrane potential ($\Delta\psi_{mito}$) comprises a major portion of the proton motive force. While this is the most well described function of the mitochondria, evidence over the past two decades suggests mitochondria are directly involved in cell signaling (Li et al., 1999) and facilitate other cellular processes including proliferation, calcium homeostasis (Marhl et al., 1998) and cell death (Marchetti et al., 1996). Mitochondrial dysfunction ca and its sequelae n be characterized by 1) loss of mitochondrial respiratory capacity, 2) mutated or decreased mitochondrial DNA, 3) elevated reactive oxygen/nitrogen species generation (ROS/RNS) and/or 4) altered $\Delta\psi_{mito}$. The end result of this dysfunction usually culminates in reduced ATP generation and cell death if the dysfunction is not reversed. The emerging importance of mitochondria has led to its association with the pathogenesis of many human diseases, including mitochondrial disorders (Shoffner et

al., 1989; Wallace et al., 1989; Zheng et al., 1989), diabetes (Poulton et al., 1995; Maechler and Wollheim, 2001), cardiac dysfunction (Lesnefsky et al., 2001), sepsis (Chopra et al., 2011; Garrabou et al., 2012) and numerous neurological disorders (Petrozzi et al., 2007).

The importance of mitochondrial dysfunction in sepsis-induced MODS, particularly in the heart, is widely accepted and has been clearly demonstrated in experimental models (Brealey et al., 2004; Larche et al., 2006; Hassoun et al., 2008; Lowes et al., 2008; Chopra et al., 2011; Lowes et al., 2013). Clinically, mitochondrial dysfunction has been linked to both severity and outcome in septic patients (Brealey et al., 2002). In 2007, Rudiger and colleagues published a detailed review of the mechanisms implicated in the development of sepsis-induced mitochondrial dysfunction and subsequent cardiac dysfunction (Rudiger and Singer, 2007). To summarize, the proposed mechanisms include ultrastructural mitochondrial damage (Schumer et al., 1971; Cowley et al., 1979; Hersch et al., 1990), reduced mitochondrial oxygen consumption (Schumer et al., 1971), decreased activity of enzyme complexes central to the function of the electron transport chain (Suliman et al., 2004; Tavener et al., 2004), the inhibitory effects of RNS and ROS on oxidative phosphorylation and ATP production (Brealey et al., 2002; Suliman et al., 2004), and increased expression of uncoupling proteins (UCPs), which could reduce $\Delta\psi_{mito}$ and ATP synthesis (Echtay et al., 2002; Roshon et al., 2003). Recent strategies for novel therapies have focused on the mitochondria. L-carnitine supplementation has been used as a mitochondrial therapy in many diseases associated with oxidative stress, including sepsis, type 2 diabetes (Makowski et al., 2009) and organ dysfunction. An IP bolus of L-carnitine was shown to decreased circulating levels of TNFα, IL1β and IL6 (importance of these cytokines is discussed below) in a rat model of sepsis (Winter et al., 1995). In an earlier study using a bacterial infusion of *Escherichia coli* in rats, oral administration of L-carnitine prior to the

infusion increased survival rates in the rats (Takeyama et al., 1989). Succinate supplementation has been another mitochondrial therapy explored in sepsis. During sepsis, it has been commonly reported that complex I function is decreased, while complex II function (i.e. succinate dehydrogenase activity) is largely untouched (Brealey et al., 2002; Brealey et al., 2004). Protti and colleagues showed in 2007, that following induction of sepsis via cecal slurry, mitochondrial oxygen consumption in the soleus muscle with complex I substrates, glutamate and malate, was severely depressed. With the addition of complex II substrate, succinate respiration increased by 39% compared to only a 10% increase in sham animals (Protti et al., 2007). Accordingly, an infusion of succinate preserved liver ATP content and improved lactate clearance in a rat model of sepsis (Malaisse et al., 1997). In the more clinically based CLP sepsis model, succinate infusion increased the survival time of rats (Ferreira et al., 2000).

In addition to targeting mitochondria substrates as a potential therapy for sepsis, studies have also looked at mitochondrial antioxidants and scavengers. As explained earlier in this section, mitochondria are a major source of intracellular ROS and RNS. In a healthy individual it is estimated that 2-4% of electrons leak from the electron transport chain. Under normal physiological conditions the mitochondria have a defense system in place to combat excess ROS and RNS, which include glutathione, manganese superoxide dismutase (SOD), and the peroxiredoxins. During sepsis the levels of mitochondrial-derived RNS and ROS increase, thus the balance between pro-oxidants and antioxidants is shifted toward oxidative stress through the depletion of the antioxidant systems and overproduction of ROS/RNS (Svistunenko et al., 2006; Doise et al., 2008). However, the use of antioxidant-based therapies in the treatment of intensive care unit (ICU) patients with sepsis have yielded no conclusive beneficial results (Mishra, 2007). More recently, experimental studies have focused on the role of mitochondrial-targeted

antioxidants including MitoE (mitochondrial targeted vitamin E) and MitoQ as well as the mitochondrial specific ROS scavenger mitoTempol. MitoE has been shown to improve total antioxidant capacity and decrease H_2O_2 generation in cardiac mitochondria when compared to treatment with vitamin E and vehicle in septic rats (Zang et al., 2012). The same group went on to show that MitoE treatment decreased lipid and protein oxidation, preserved $\Delta\psi_{mito}$ and recovered respiratory function. Both vitamin E and MitoE suppressed peripheral and myocardial proinflammatory cytokine production, however, MitoE elicited a stronger inhibitory response (Zang et al., 2012). Similar results have been published with the use of MitoQ (Lowes et al., 2008; Supinski et al., 2009; Lowes et al., 2013) and mitoTempol (Zacharowski et al., 2000; Mariappan et al., 2007). Thus, mitochondrial-targeted antioxidants remain a promising therapeutic avenue in sepsis and MODS, although much investigation is still needed to validate and understand the mechanisms by which mitochondrial dysfunction and oxidative stress are involved in the pathophysiology of this condition.

1.2 Important signaling pathways in sepsis

Multiple intracellular signaling pathways have been investigated in sepsis, all in varying cell types. These pathways include kinase/phosphatase signaling, transcription factor activation/inhibition and immune modulation. All are thought to contribute in part to MODS and death in sepsis. As described previously, these intracellular events are initiated by the interaction of microbial products with pattern recognition receptors such at TLRs. Subsequent activation of kinases leads to enhanced transcription of inflammatory mediators resulting in local and systemic release of these inflammatory mediators. Once in circulation, the inflammatory mediators have the ability to interact with membrane bound receptors, which activate feed-forward intracellular

pathways resulting in an increase in their production. Kinases central to this process are p38 and extracellular signal regulated kinase (ERK) 1/2 (Guha et al., 2001; Kyriakis and Avruch, 2012).

1.2.1 NFκB signaling

As a central mediator in the inflammatory response to sepsis and perhaps one of the most well characterized signaling pathways, nuclear factor (NF)-κB (Guha and Mackman, 2001; Kyriakis and Avruch, 2012) is a transcriptional regulator of many cytokines, chemokines, adhesion molecules, and enzymes (Abraham, 2003). The family of NFκB transcription factors function as hetero- or homo- dimers involving p65 (RelA), p50, RelB, c-Rel, and p52. The classic transcriptionally active form is a heterodimer of p65 and p50. Under basal conditions these transcription factors are found bound to their inhibitory protein, IκB which blocks the nuclear localization signal in the cytoplasm of cells (Verma et al., 1995; Ghosh and Karin, 2002; Karin and Lin, 2002). NFκB is central to the production of proinflammatory mediators following the engagement of TLRs by microbial products, such as LPS. LPS binding to TLR4 results in the activation of kinases including IL1 receptor-associated kinase (IRAK)-1 and IRAK-4, while signaling through the TLRs and receptors result in the activation of p38, and Akt (O'Neill, 2002; Medvedev et al., 2003). These kinases in turn activate the IκB kinase complex (IKK), which is comprised of two kinases (IKKα and IKKβ) and a regulatory subunit (IKKγ). The IKK complex phosphorylates IκB on serine residues 32 and 36 resulting in ubiquitination and subsequent degradation (Israël, 2010). Following phosphorylation, the NFκB dimer is released from IκB and accumulates in the nucleus where it enhances transcription of genes including TNFα, IL1β, IL6, and inducible nitric oxide synthase (iNOS). Secreted TNFα and

IL1β can in turn activate their respective membrane-bound receptors, resulting in a feed-forward loop and potentiating the activation of NFκB (Figure 1.1). (Parrillo et al., 1990).

1.2.2 STAT3 signaling

Generally, cytokine receptors lack intrinsic tyrosine kinase activity, requiring association with receptor associated kinases in order to propagate signal transduction. The Janus kinases (JAKs) are associated with many cytokine receptors and can fulfill the functions described above (Ihle, 1995). Cytokine binding results in dimerization of the receptor, which allows JAKs to phosphorylate one another while concurrently phosphorylating the receptor. The phosphorylated cytokine receptor then binds signal transducers and activators of transcription (STATs) transcription factors. Once bound the STATs are phosphorylated by JAK, this releases them from receptor binding to allow for dimerization. Following dimerization STATs are translocated to the nucleus (Scott et al., 2002) (Figure 1.2). STAT3 regulates the gene transcription of the potent anti-inflammatory cytokine IL10 and LPS administration in macrophage specific STAT3 knockout circulating cytokines mice resulted in elevated levels of TNFα, IL1β, IL6 and interferon-γ. These STAT3-/- mice were particularly susceptible to LPS-induced sepsis, with increased production of inflammatory cytokines. Together these data suggests that STAT3 is central to suppressing cytokine secretion likely through the anti-inflammatory action of IL10 (Takeda et al., 1999).

1.2.3 Nrf2 signaling

Nuclear factor (erythorid-derived 2)-like 2 (Nrf2) is a transcription factor that binds to the antioxidant response element (ARE) regulating the basal and inducible expression of a battery of antioxidant genes including glutamate-cysteine ligase (GCLC), NAD(P)H dehydrogenase

quinone 1 (NQO1), glutathione peroxidase 1 (Gpx1), glutathione peroxidase 4 (Gpx4), and thioredoxin reductase 2 (Trx2), heme-oxygenase 1 (HO1) and catalase (Venugopal and Jaiswal, 1996). Nrf2 is a basic leucine zipper transcription factor with redox sensitivity. In the absence of stimuli, nuclear levels of Nrf2 are low due to Nrf2 binding to its cytosolic inhibitor kelch-like ECH-associated protein 1 (Keap1). Discovered in 1999 as a binding protein anchoring Nrf2 in the cytoplasm, Keap1 serves as the oxidative stress sensor which is central to Nrf2 activation (Itoh et al., 1999). In response to inflammatory or oxidative stimuli, four cysteine residues on the Keap1 protein sense oxidative stress either via adduct formation with electrophiles, or via disulfide bond formation and subsequent structural changes in the protein, thus releasing Nrf2 and allowing it to accumulate in nuclear compartments (Dinkova-Kostova et al., 2002) (Figure 1.3). Evidence has implicated Nrf2 as a critical mediator of the innate immune response and central to survival in experimental models of sepsis. In 2006, Thimmulappa and colleagues showed that Nrf2 knock-out (Nrf2KO) mice were more sensitive to a lethal dose of LPS. 1.5 mg/mouse of LPS resulted in morality of 100% of Nrf2KO mice in less than 48 hours compared to 20% mortality in age-matched wild-type (WT) mice (Thimmulappa et al., 2006). More recently, work from the same group showed that myeloid cell-specific deletion of Keap1 resulted in enhanced Nrf2 activity in macrophages and neutrophils. Enhanced Nrf2 activity resulted in decreased circulating level of IL6, TNFα, monocyte chemotactic protein 1 (MCP1), and IL10 and improved survival in a CLP model of sepsis (Kong et al., 2011).

1.2.4 Autophagy signaling

Autophagy is recognized as a non-apoptotic, non-necrotic form of cell death which is independent of caspase activity and is characterized by the formation of autophagosome that

engulf cellular components or in some cases whole cellular compartments (Clarke, 1990). However, it is heavily debated whether autophagy is a primary cause of cell death or a mechanism by which the cell tries to rescue itself from an insult. During this highly-conserved process, redundant and/or dysfunctional proteins, even whole organelles such as mitochondria are sequestered in a double membrane autophagosome and delivered to lysosomes for degradation and recycling. The signaling involved in autophagy is complex and regulated by a family of proteins known as autophagy-regulated genes. Briefly, induction of autophagy happens when ULK1-Atg13-FIP200-Atg101 kinase complex activates autophagic signaling via mTor signaling (Xie and Klionsky, 2007). Following induction, an omegasome, which was given its name because it looks like the Greek letter omega, is formed from endoplasmic reticulum as the precursor to the autophagosome. Two ubiquitin-like modifications to Atg12 and light chain 3 (LC3) are essential for proper membrane elongation and ultimately autophagosome formation. In a process known as selective or chaperone-mediated autophagy, p62/SQSTM1 binds to proteins and these ubiquitylated proteins form aggregates that are sequestered into autophagosomes. Accumulation of p62-positive aggregates are a sign of impaired autophagy. Lysosome associated protein 2a (Lamp2a), is a lysosomal membrane associated protein that recognizes proteins tagged for selective autophagy. Upon proper formation, the outer membrane of the autophagosome fuses with a lysosome to form an autolysosome. Inside the autolysosome, lysosomal hydralases begin degrading the contents (Tanida, 2011). Classical autophagy can degrade proteins, lipids, or organelles. In contrast, selective or chaperone-mediated autophagy only degrades protein (Figure 1.4). It has been suggested that autophagy is involved in the regulation of inflammation, however, the mechanisms underlying the regulation are poorly understood (Ohsumi, 2001; Levine and Deretic, 2007; Mizushima et al., 2008). Studies have

shown that mitochondrial dysfunction and increased ROS/RNS production trigger the induction of autophagy (Ding et al., 2010). In 2011, a study found that autophagy was impaired in CLP-induced mice by showing increased autophagasome production but few autolysosomes. This was associated with decreased cardiac performance. When rapamycin was given to the animals to induce completion of autophagy, cardiac performance and ATP content were restored in the CLP model of sepsis (Hsieh et al., 2011). A 2008 study by Saitoh and colleagues found that autophagy related 16-like-1 (Atg16L1) deficiency in cells results in the loss of LC3 conjugation which causes impaired autophagasome formation and reduced autophagy-driven degradation of protein. In macrophages stimulated with LPS, Atg16L1 deficiency caused excessive release of IL1β and IL18 (Saitoh et al., 2008).

1.3 Prohibitin

Prohibitin (PHB) is an essential highly conserved ~32kDa protein that is present in the genome of all eukaryotes sequenced to date. PHB belongs to the stomatin/prohibitin/flotillin/ HflK/C (SPFH) domain containing superfamily of proteins. PHB is closely related to B-cell receptor associated protein 37 (BAP-37), also known as prohibitin 2 (PHB2). Functional redundancy of PHB and its isoform PHB2 is not likely, as at least one gene of each isoform is found in all genomes sequenced (Coates et al., 1997). Structurally, PHB contains an N-terminal transmembrane spanning domain, which consists of a hydrophobic membrane-anchoring alpha helix. This region is known as the SPFH domain, and is the common characteristic of all SPFH superfamily proteins (Winter et al., 2007). The C-terminus is a coiled-coil structure of alpha helices. Also at the C-terminus a leucine/isoleucine rich motif is present and serves as a nuclear export sequence (Winter et al., 2007) (Figure 1.5). Predominantly, PHB has been found to

anchor in the inner mitochondrial membrane (Ikonen et al., 1995; Coates et al., 1997; Berger and Yaffe, 1998; Artal-Sanz et al., 2003), where it forms a large complex with PHB2 (Nijtmans et al., 2000; Artal-Sanz et al., 2003; Tatsuta et al., 2005). This membrane bound complex is composed of multiple PHB and PHB2 subunits. Co-immunoprecipitation experiments have confirmed assembly of PHB and PHB2 subunits in human fibroblasts (P.J.Coates et al., 2001). Deletion of one PHB gene leads to loss of both PHB proteins, however, this has not lead to evidence of transcriptional co-regulation, instead suggests degradation in the absence of the assembly partner (Berger and Yaffe, 1998; Artal-Sanz et al., 2003; Katsumi et al., 2006; Merkwirth and Langer, 2009). Interestingly, IL6 has been shown to increase PHB protein abundance, mRNA expression and induce PHB promoter activity in intestinal epithelial cells. An IL6 response element site identified in the PHB promoter was demonstrated to be critical for basal promoter activity and promoter responsiveness to IL6. Additional work showed that a STAT3 antibody supershifted nuclear protein binding to the IL6 response element on the PHB promoter and short interference RNA (siRNA) to STAT3 attenuated IL6 induced increases in PHB expression, suggesting that STAT3 regulates PHB activity via IL6 (Theiss et al., 2007b). Further work in cardiomyocytes found that IL6 preconditioning improved cell viability following exposure to H_2O_2. Proteomic analysis found that IL6 preconditioning resulted in increased PHB expression and when PHB was knocked down using siRNA the protective effect of IL6 preconditioning was lost. Use of tyrosine kinase inhibitor AG490 decreased STAT3 phosphorylation and PHB expression resulting in further weakened the protective effects of IL6 preconditioning (Jia et al., 2012). Collectively, these results suggest that PHB may be under transcriptional regulation of IL6 induced STAT3 activation. In addition to mitochondrial localization, PHB has been shown to localize to the cell surface (Sharma and Qadri, 2004;

Yurugi et al., 2012), and the nucleus (Wang et al., 2002a; Fusaro et al., 2003; Gamble et al., 2004; Rastogi et al., 2006; Sripathi et al., 2011) in various cell types. PHB has been shown to be essential for embryonic development in mice (Park et al., 2005; He et al., 2008; Merkwirth et al., 2008) and *C. elegans* (Artal-Sanz et al., 2003).

As its name indicates, PHB was originally identified as a tumor suppressor in liver tissue (McClung et al., 1989), however, this function was later attributed to the 3'untranslated region of PHB gene which encodes a functional RNA that halts cell cycle transition between the G1 and S phases (Manjeshwar et al., 2003; Manjeshwar et al., 2004). The well-characterized function of PHB is as a chaperone and scaffold protein in the mitochondria (Figure 1.5) allowing for proper stabilization of mitochondrial proteins (Coates et al., 1997; Nijtmans et al., 2000; Nijtmans et al., 2002). Studies have also provided evidence suggesting a wide variety of roles for PHB including transcriptional regulation (Wang et al., 2002a; Fusaro et al., 2003), a cell-surface binding protein actively involved in signal transduction (Rajalingam and Rudel, 2005; Rajalingam et al., 2005; Yurugi et al., 2012), a secreted protein found in circulation (Mengwasser et al., 2004; Wang et al., 2004; Mishra et al., 2007; Kang et al., 2008), a regulator of autophagy (Kathiria et al., 2012a) and apoptosis (Liu et al., 2009; Lee et al., 2010), as well as a mediator of inflammatory (Sharma and Qadri, 2004; Theiss et al., 2009a; Theiss et al., 2011) and oxidative signaling (Theiss et al., 2007a; Theiss et al., 2009b; Lee et al., 2010; Theiss et al., 2011; Kathiria et al., 2013). Recent data have implicated PHB as a functional player in the pathogenesis of various disease states including inflammatory bowel disease (Kathiria et al., 2012b; Kathiria et al., 2013), insulin resistant/type 2 diabetes (Vessal et al., 2006; Lee et al., 2010) and obesity (Kolonin et al., 2004; Hossen et al., 2010), and a diverse range of cancers (Sato et al., 1993; Tsai et al., 2006; Wu et al., 2007; Gregory-Bass et al., 2008; Kang et al., 2008; Ren et al., 2010). Underlying factors, which

are common for all these diseases include mitochondrial dysfunction, oxidative stress and inflammation. This diversity in roles that have been shown for PHB has been suggested to have a direct correlation to the complexity of PHB's post-translational modifications. PHBs have several tyrosine and serine phosphorylation sites as well as *O*-Glc*N*Ac modifications, palmitoylations, transamidations and tyrosine nitrosylations (Mishra et al., 2010). The profound effects these modifications have on PHB activity will be discussed below.

1.3.1 Role of PHB in the mitochondria

As discussed above, PHB is localized to the mitochondria in most cells types studied to date. Accordingly, the majority of recent studies into the function of PHB have focused on its role in maintaining normal mitochondrial structure and function. Artal-Sanz and colleagues were first to show, in 2003, that loss of PHB had a severe effect on mitochondrial morphology. The study found that mitochondria in muscle cells with depleted PHB appear fragmented and disorganized (Artal-Sanz et al., 2003). Similar results were found in studies with mouse embryo fibroblasts (MEFs) (Merkwirth et al., 2008) and HeLa cells (Katsumi et al., 2006). A potential mechanism explaining the destabilization of mitochondria structure when the prohibitins are depleted was proposed by Merkwirth and colleagues in 2008. Using conditional gene targeting, PHB2 was depleted in mice and OPA1 destabilization followed (Merkwirth et al., 2008). OPA1, optic atrophy 1, is found on the mitochondrial inner membrane where it serves as an essential mediator of mitochondrial fusion and proper cristae formation. The mitochondrial fragmentation and disorganization found in PHB2-depleted MEFs bears a striking similarity to the mitochondrial morphology seen in OPA1 down-regulation (Griparic et al., 2004). Evidence also suggests a role for PHB in the assembly and stability of proteins associated with oxidative

phosphorylation (OxPhos) (Nijtmans et al., 2000; Nijtmans et al., 2002). However, it is unclear if there is a direct interaction with the PHB complex and OxPhos protein complexes. Some evidence suggests that the PHB complex is associated with complex IV in yeast (Nijtmans et al., 2000) and complex I in mammals (Taylor et al., 2003; Bourges et al., 2004). Instability of mitochondrial-en8coded subunits of the electron transport chain has been shown in yeast cells lacking PHB (Steglich et al., 1999) and conversely, overexpression of the PHB complex in yeast results in stabilization of the same subunits (Nijtmans et al., 2000). It has been suggested that PHBs protect newly imported proteins by preventing their degradation by mitochondrial ATPase Associated with diverse cellular Activities (m-AAA) protease (Steglich et al., 1999), while also promoting mitochondrial protein synthesis and maintaining the organization and copy number of mitochondrial DNA. Loss of PHB genes resulted in reduced $\Delta\psi_{mito}$ in yeast (Coates et al., 1997; Christof et al., 2009) while knockdown of PHB in endothelial cells resulted in mitochondrial membrane depolarization due to reduced complex I activity (Schleicher et al., 2008). Taken together, the evidence shows that depletion of PHB results in altered mitochondrial morphology and function, suggesting that PHB plays a critical role in maintaining proper mitochondrial homeostasis.

1.3.2 Physiological role of PHB outside the mitochondria

Cancer is one of the most common pathological settings in which PHB has been investigated. In addition to the functions described above, PHB has also been shown to interact with p53 in the nucleus of cancer cells. p53 is a transcription factor that regulates genes responsible for tumor suppression, cell cycle, apoptosis, genomic stability and angiogenesis (Fusaro et al., 2003). Data suggests that Skp2B, an ubiquitin ligase complex found in high

abundance in breast cancer, promotes the degradation of PHB and PHB2 which in turn causes the attenuation of p53 activity (Chander et al., 2010), thereby promoting the survival of cancer cells. In addition to p53, PHB1 has been shown to regulate retinoblastoma tumor suppressor protein (Rb), p107 and p130 (two members of the Rb super family). The Rb super family suppresses growth via inhibition of E3F-mediated transcription. PHB represses E2F gene transcription through its interaction with Rb, histone deacetylases (HDACs) and nucleosomes-remodeling proteins Brg-1 and Brm (Wang et al., 1999a; Wang et al., 1999b; Wang et al., 2002a; Wang et al., 2002b) resulting in cell cycle arrest in cancer cells (Wang et al., 1999a; Wang et al., 1999b). Interestingly, PHB has also been linked to pro-tumorigenic activity as well. Both PHBs have been implicated in the growth, resistance to chemotherapy, and metastasis through activation of the Ras-C-Raf-MEK-ERK pathway, altered transforming growth factor β (TGFβ) signaling and transcriptional regulation. In response to insulin, PHB is phosphorylated at tyrosine 114 (Tyr114) which facilitates binding of Shp1, a phosphatase that facilitates Akt and enhances insulin signaling (Ande et al., 2009a). PHB has also been shown to interact with phosphatidylinositol 3, 4, 5-triphosphate (PIP3). Overexpression of PHB was found in attenuate insulin signaling downstream of phosphatidylinositol 3 (PI3) kinase and interestingly, Akt phosphorylation of PHB on threonine 258 (Thr258) prevents the interaction between PHB and PIP3 and enhanced insulin signaling (Ande and Mishra, 2009). Phosphorylation of Thr258 on PHB is also necessary for the activation of oncogene serine/threonine-protein kinase (C-Raf or Raf-1) in response to Ras (rat sarcoma) (Chiu et al., 2013). The activation of C-Raf by Ras requires the heterodimerazation of phosphor-PHB1 (Thr528) with C-Raf (Rajalingam et al., 2005). On the surface of cancer cells phosphor-PHB1(Thr258) activates PI3K/Akt and C-Raf/ ERK pathways to result in the promotion of proliferation and metastasis (Chiu et al., 2013).

Evidence indicates that PHB may have a role in the biphasic response TGFβ exhibits in cancer cells (Zhu et al., 2010). TGFβ serves as a tumor suppressor early in tumorigenesis, although in the late stage it promotes tumor progression. By binding to its receptor, TGFβ triggers the C-Raf/ERK and Smad 2/3 pathways, prompting opposite effects. ERK activation leads to protein kinase C δ (PKCδ) activation, which phosphorylates PHB1 leading to cell survival and invasion. Activation of Smad signaling upregulates proteins associated with inhibition of PKCδ, resulting in reduced PHB phosphorylation and promoting apoptosis (Zhu et al., 2010). A growing body of work indicates that PHB overexpression on the surface of cancer cells may be conferring cell resistance to paclitaxel, doxorubicin and etoposides (Patel et al., 2010). It is likely that much of the opposing results surrounding the role of PHB in tumorigenesis can be explained by sub-cellular localization. Similarly, cellular localization of PHB has been shown to affect cellular apoptosis (Rastogi et al., 2006). While many studies of PHB in cancer have explored expression level, few have reported on the sub-cellular distribution.

In addition to cancer, several studies *in vivo* and *in vitro* have suggested a role for PHB in the alleviation of inflammation in intestinal epithelial cells and promotion of cell survival in a setting of inflammatory or oxidative stress. Oxidative stress is a major contributor to the etiology of many inflammatory diseases. In response to bacterial, fungal, or other antigen, activation of membrane-bound NADPH oxidase in immune cells such as macrophages and neutrophils results in the release of ROS, specifically superoxide ($O_2^{\bullet -}$) and H_2O_2. Similarly, increased expression of iNOS results in excessive production and release of NO. Crohn's disease and ulcerative colitis, two common subsets of inflammatory bowel disease, are characterized by increased ROS, decreased antioxidant capacity and increased NO generation in the intestinal mucosa (Rachmilewitz et al., 1995; McKenzie et al., 1996). Decreased mRNA

levels and expression of PHB were shown in experimental models (Yeo et al., 2006; Theiss et al., 2007a) of IBD and in humans (Hsieh et al., 2006). Overproduction and stimulation of TNFα in the inflamed colon was shown to drive PHB1 expression down (Theiss et al., 2009a). The decrease in PHB expression resulted in increased ROS signaling, autophagy, and excessive inflammation in patients with irritable bowel disease (IBD) (Kathiria et al., 2012a). Extensive work has been done to explore the impact of PHB in IBD. In a transgenic mouse, overexpressing PHB specifically in intestinal epithelial cells caused significantly less NFκB activation and signaling in response to TNFα exposure. Investigation into the mechanism by which PHB mediated this inhibition of NFκB activity demonstrated that PHB decreased the nuclear accumulation of NFκB by down-regulating expression of importin α3, a protein involved in NFκB nuclear import (Theiss et al., 2009a). Using the same transgenic mouse, PHB overexpression resulted in attenuated oxidative stress and reduced susceptibility to the development of colitis. This effect was mediated by an increase in Nrf2-mediated gene transcription (Theiss et al., 2009b). The evidence for PHB as a therapeutic target in the treatment of IBD was strengthened using enema administration of recombinant adenovirus or nanoparticle-based delivery of PHB. Both delivery methods increased PHB expression in intestinal epithelial cells, resulting in decreased sensitivity to dextran sodium sulfate (DSS) induced colitis demonstrated by an attenuated body weight loss, clinical score, proinflammatory cytokine production, histological score and protein carbonyl content when compared to mice without increase PHB expression (Theiss et al., 2011).

PHBs have also been implicated in other models of inflammatory disease. *Salmonella typhi* is the causative agent of typhoid. PHB binds to *S.typhi* antigen to inhibit the inflammatory response caused by this infectious agent. This inhibition is mediated through the downregulation

of mitogen-activated protein kinase (MAPK) signaling (Sharma and Qadri, 2004). More recently, PHB repressed PITX1 when it accumulated in the nucleus of osteoarthritic chondrocytes. PITX1, is a transcription factor involved in osteoarthritis, a well-characterized inflammatory disease. PHB binds to a distal E2F1 transcription factor site in the promoter region on *PITX1,* where it suppressed mRNA level and expression of PITX1 (Picard et al., 2013). In B lymphocytes, PHB and PHB2 were found to bind CD86 following CD40 engagement. Association of CD86 and PHB1/2 elicited an immune response by inducing phosphorylation of IκB, phospholipase Cγ2, and protein kinase Cα/β(II) yielding increased nuclear accumulation of p65 and enhance transcription of Oct-2 and IgG1 (Lucas et al., 2013). Additionally, PHB1/2 can be found on the surface of activated T cells, where they are co-localized with CD3 and contribute to the activation of T cells through ERK signaling (Yurugi et al., 2012). Interestingly, PHB is found embedded in lipid droplets in human serum where it interacts with complement protein C3 to induce an innate immune response (Mishra et al., 2007). Elevated circulating levels of PHB and PHB2 have been found in patients with cancer (Mengwasser et al., 2004).

In 2009 Ande and Mishra demonstrated the importance of PHB in insulin signaling and adipose differentiation (Ande et al., 2009a; Ande and Mishra, 2009). As discussed previously, the insulin receptor directly phosphorylates PHB to promote insulin signaling and Akt phosphorylation, while PHB phosphorylation by Akt mediates the opposite effect. But phosphorylation is not the only post-translation modification that affects PHB in response to insulin. *O*-linked β-N-acetylglucosamine conjugated PHB is found in myoblasts in response to insulin or high glucose. This conjugation has been implicated in insulin resistance (Ande et al., 2009b; Gu et al., 2011). Vessal et al. in 2006 provided evidence that PHB may be involved in lipid accumulation by demonstrating in adipocytes that PHB inhibited pyruvate carboxylase and

decreased insulin-stimulated oxidation of glucose and fatty acid (Mahmood et al., 2006). Upregulation of PHB1 in response to insulin and a peroxisome proliferator-activated receptor γ (PPARγ) agonist was demonstrated in preadipocytes and enhanced expression of PHB was sufficient to induce adiopgenesis (Ande et al., 2012).

Collectively, the pleiotropic effects of PHB make this protein an appealing therapeutic target for cancer, metabolic diseases, neurodegenerative disease and inflammatory diseases. Over the last 10 years, PHBs have been found to interact with 60 other proteins resulting in the regulation and modification of a diverse set of cellular events. Clearly much more research into this fascinating protein is necessary. Specifically, more investigation is needed into the intracellular (and extracellular) localization and translocation of PHB in response to various stimuli, as location seems to be an important factor in determining PHB function. This dissertation seeks to address the hypothesis that PHB mitigates the cardiac response to sepsis through preservation of mitochondrial function and integrity while also suppressing proinflammatory signaling and oxidative stress. Using a comprehensive approach, we have investigated the intra- and extra-cellular translocation of PHB in response to a severe inflammatory stress, the role of PHB in inflammatory stress-induced mitochondrial dysfunction and subsequent cell death, and the potential for PHB to serve as a signal transducer blunting the NFκB-driven inflammatory response.

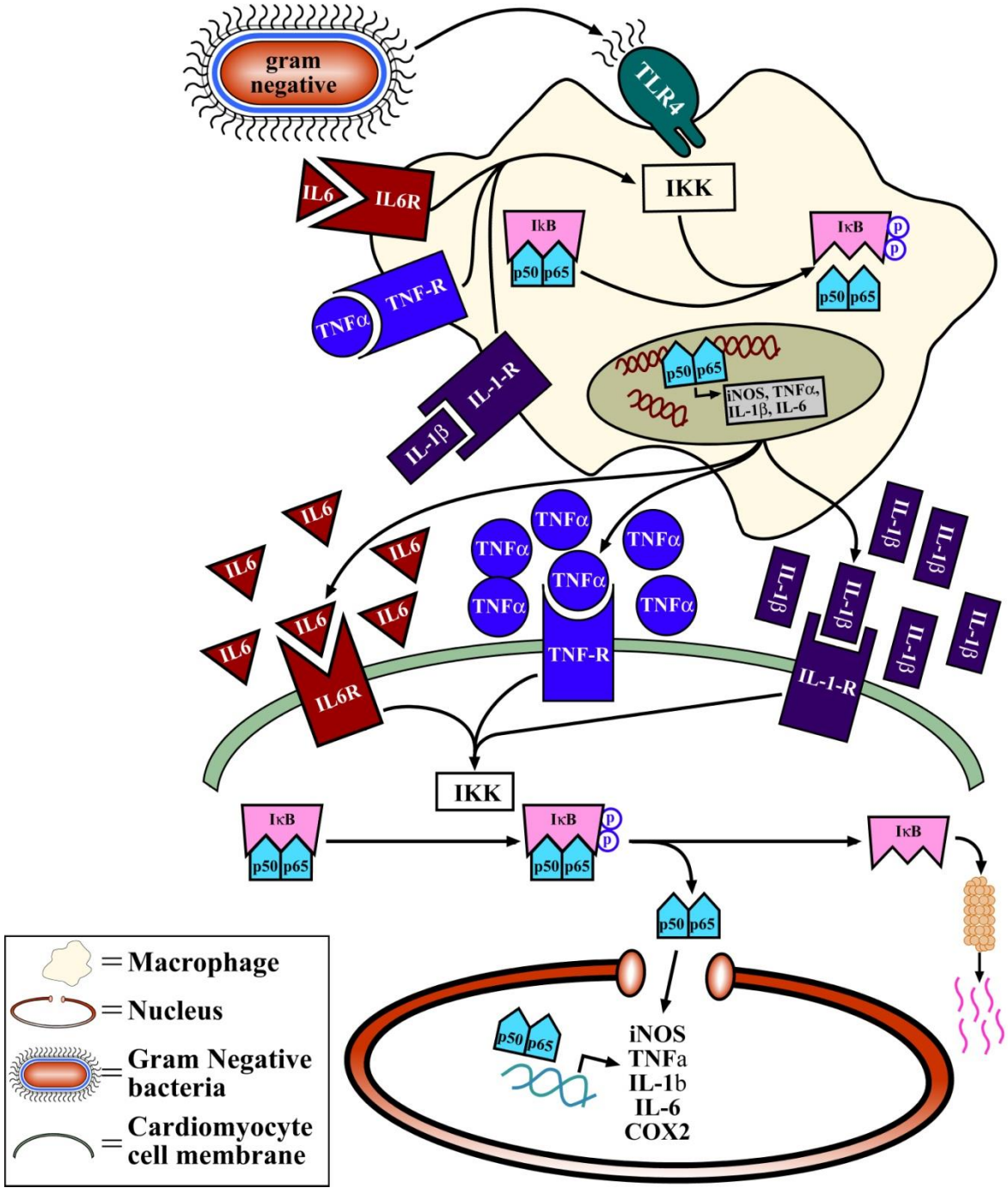
gram negative
TLR4
IKK
IL6
IL6R
IkB
p50
p65
IκB
P
TNF-R
TNFα
IL-1-R
IL-1β
iNOS, TNFα, IL-1β, IL-6
IKK
iNOS
TNFa
IL-1b
IL-6
COX2
= Macrophage
= Nucleus
= Gram Negative bacteria
= Cardiomyocyte cell membrane

Figure 1.1 LPS mediated NFκB feed-forward signaling.

Schematic representation of LPS induced NFκB signaling. Upon binding to the TLR4 receptor on macrophages, LPS stimulates the activation of a series of kinases resulting in activation of the IKK complex and phosphorylation of IκB. Following phosphorylation, IκB releases the NFκB dimer which allows it to translocate to the nucleus where it initiates the transcription of TNFα, IL1β, IL6, iNOS, etc. The cytokines are then released into circulation where they are free to bind and activate their respective receptors on the surface of surrounding cells (ie. cardiomyocytes) or on the surface of the macrophage. Cytokine binding promotes activation of NFκB and initiation of transcription. See section 1.2.1 for a detailed description of NFκB signaling.

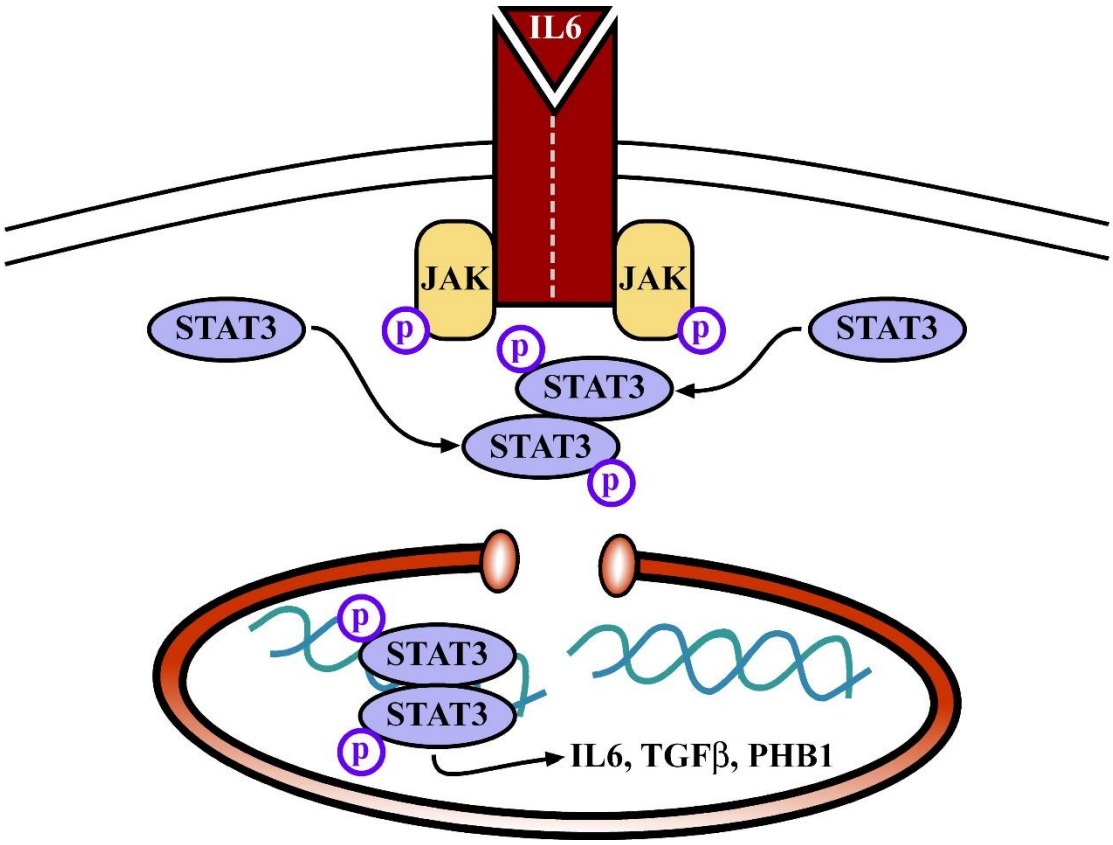
IL6
JAK
JAK
STAT3
STAT3
STAT3
STAT3
STAT3
STAT3
IL6, TGFβ, PHB1

Figure 1.2 IL6 activation of the JAK/STAT pathway.

Schematic representation of IL6-induced activation of the JAK/STAT pathway. Cytokine receptors lack intrinsic tyrosine kinase activity, requiring association with receptor associated kinases in order to propagate signal transduction. Following IL6 binding the IL6 receptor induces phosphorylation of JAK, which in turn phosphorylate STAT3. Phosphorylated STAT3 dimerizes and translocates to the nucleus, where they bind the STAT3 binding element to initiate transcription. See section 1.2.2 for detailed description of JAK/STAT signaling.

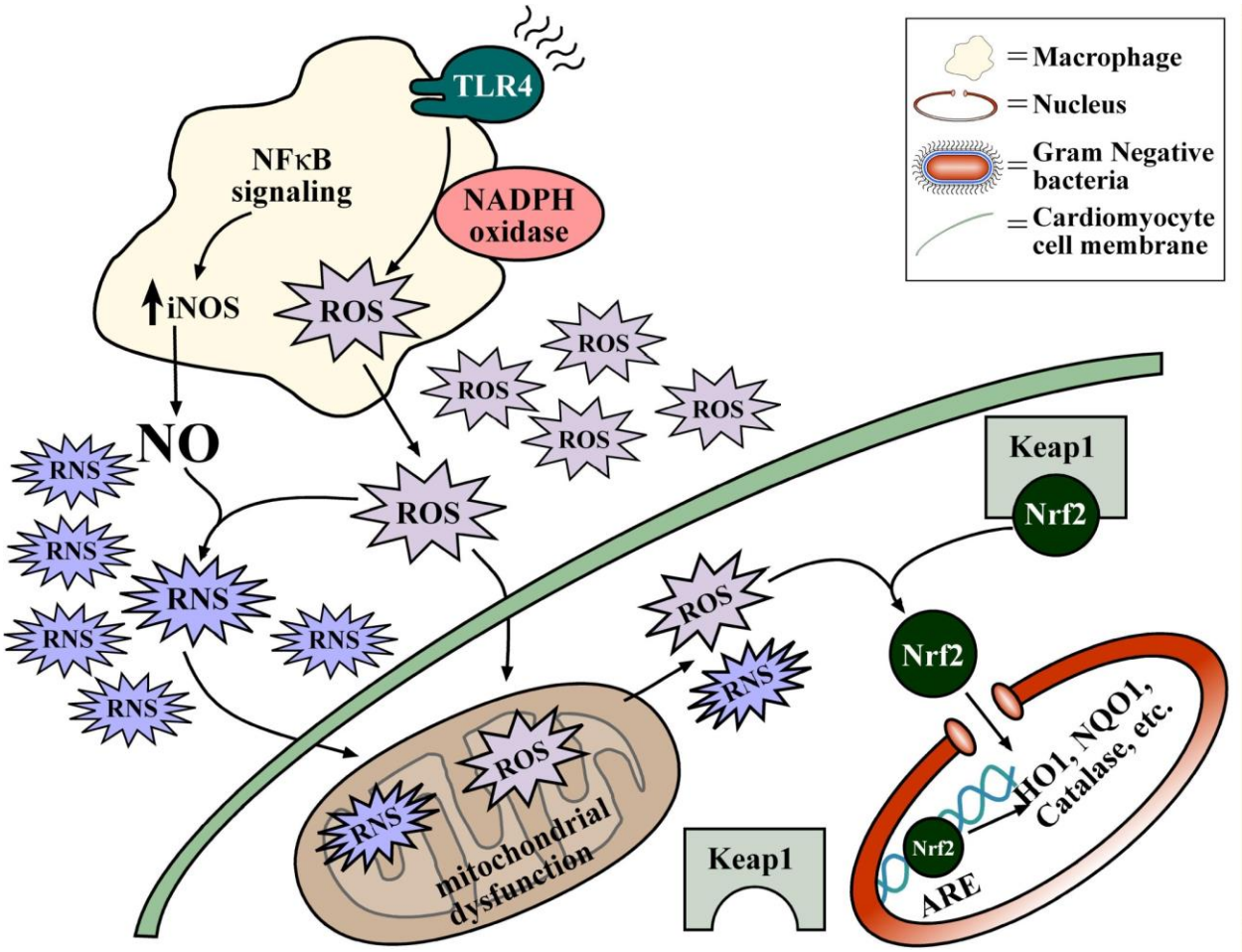
= Macrophage
= Nucleus
= Gram Negative bacteria
= Cardiomyocyte cell membrane
TLR4
NFκB signaling
NADPH oxidase
iNOS
ROS
NO
RNS
Keap1
Nrf2
mitochondrial dysfunction
HO1, NQO1, Catalase, etc.
ARE

Figure 1.3 LPS-mediated activation of Nrf2.

Schematic representation of LPS mediated Nrf2 activation. LPS binding to TLR4 activates NADPH oxidases on the surface of macrophages to produce ROS. NFκB activation drives an increase in iNOS expression resulting in increased RNS. Together these intermediates modify critical thiol residues on KEAP1 release Nrf2 allowing it to translocate to the nucleus. Once in the nucleus it can interact with small Maf and bind to the antioxidant response element (ARE). See section 1.2.3 for more detail.

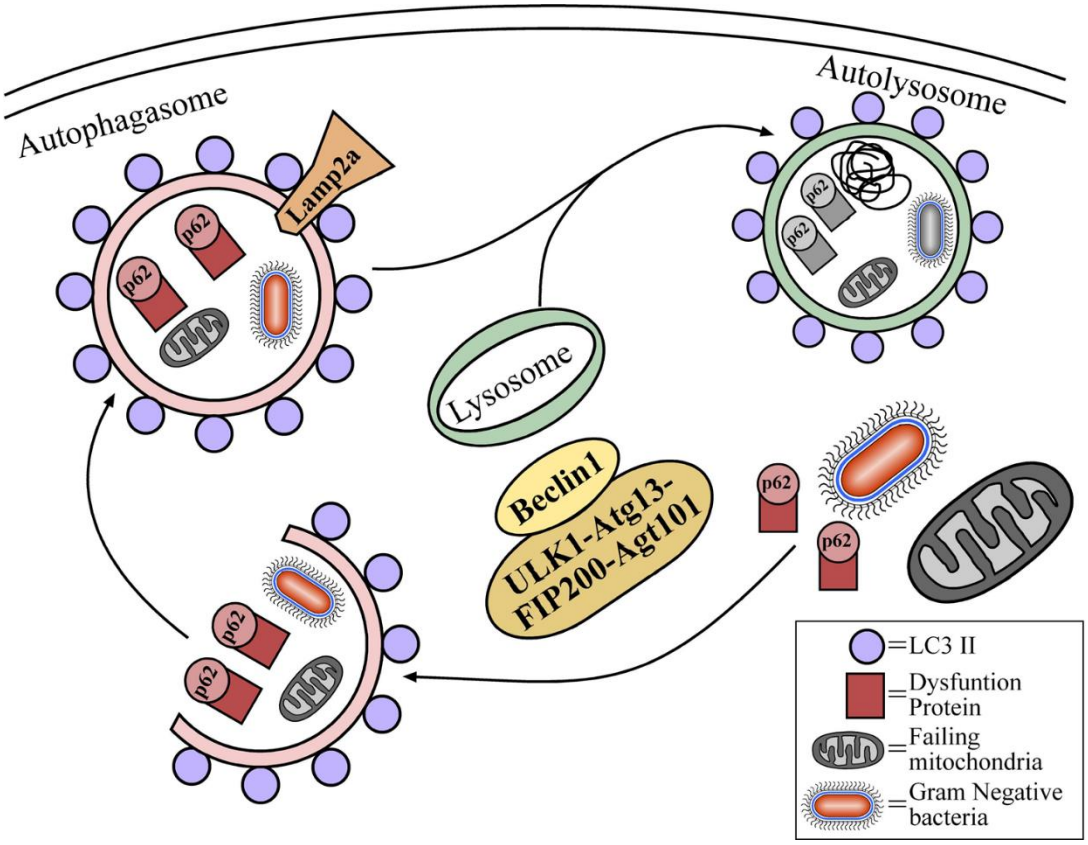
Autophagasome
Lamp2a
p62
p62
Autolysosome
p62
p62
Lysosome
Beclin1
ULK1-Atg13-
FIP200-Agt101
p62
p62
p62
p62
=LC3 II
=Dysfuntion Protein
=Failing mitochondria
=Gram Negative bacteria

Figure 1.4 Schematic representation of autophagy.

Schematic representation of autophagy. Autophagy is characterized by rearrangement of subcellular membranes to sequester dysfunctional or redundant proteins, organelles and infectious agents for delivery to the lysosome to be degraded and recycled. See section 1.2.4 for more detailed explanation.

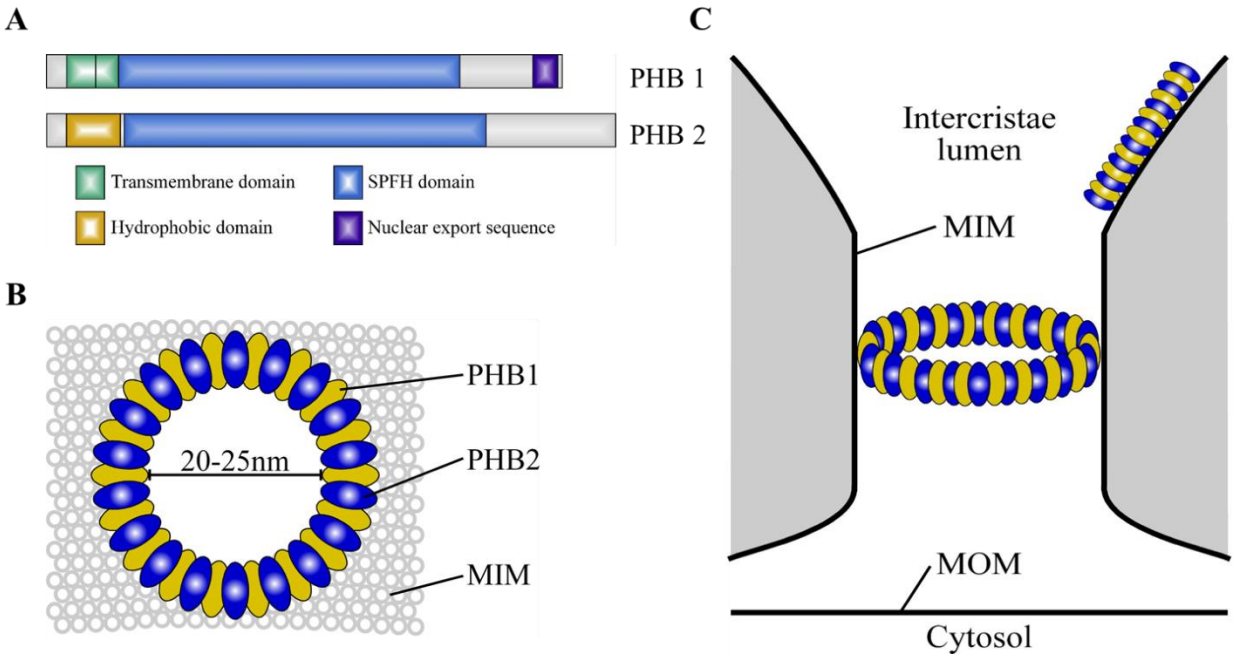
A
PHB 1
PHB 2
Transmembrane domain
SPFH domain
Hydrophobic domain
Nuclear export sequence
B
PHB1
20-25nm
PHB2
MIM
C
Intercristae
lumen
MIM
MOM
Cytosol

Figure 1.5 PHB ring complex in the mitochondrial inner membrane.

A, Doman structures of mammalian prohibitins. Green box indicates the transmembrane spanning domain of PHB and the gold box indicates the hydrophobic domain of PHB2, these regions anchor PHB and PHB2 into the mitochondrial inner membrane (MIM). The blue boxes represent the SPFH domain and the violet the nuclear export signal on PHB1. B, PHB and PHB2 subunits form a multimeric ring complex in the MIM. Single-particle electron micrograph confirms this ring structure (Osman et al., 2009b). Additionally, it has been suggested that the PHB ring complex could assemble perpendicular to the axis of cristae tubules (C), to help with proper cristae formation (Merkwirth et al., 2008; Merkwirth and Langer, 2009).

CHAPTER TWO - Materials and Methods

2.1 Animals

Male Sprague-Dawley rats (Charles River Laboratory Wilmington, MA) weighing between 275-300 grams (9-11 weeks old) were used in all animal studies in Chapter three. Male C57 Black/6 mice (Charles River Laboratory Wilmington, MA) weighing between 20-25 grams (8-10 weeks old) were used in all animal studies in Chapter four. Animals were housed in temperature and light-controlled conditions with free access to food and water. All experiments were conducted with approval from the Institutional Animal Care and Use Committee at East Carolina University.

2.1.1 Induction of sepsis and delivery of recombinant prohibitin (rPHB)

Sepsis was induced in rats and mice with an IP injection of LPS purified from *Escherichia coli* (Sigma-Aldrich, St. Louis, MO) mixed in 5% Dextrose-H_2O at various concentrations [rats – 0.5 and 7.5 mg/kg and mice 4 and 12 mg/kg]. Vehicle-treated animals received an injection of 5% Dextrose-H_2O (Vehicle, Veh). Following the LPS-injection all animals were monitored every 4 hours. Purified rPHB (Origene, Rockville, MD) was diluted in saline immediately prior to injection. Mice received an IP injection of rPHB to achieve a final circulating volume of 200ng/mL 2, 8, 14 hours following the induction of sepsis. This concentration of rPHB was estimated by assuming a mouse blood volume/mass ratio of 58.5 ml/kg (NC3Rs). Vehicle and LPS-treated groups received IP injections at equal volumes of saline. Table 2.1 shows the treatment groups used in the animal experiments and figure 2.1 depicts the time course for the animal experiments.

2.1.2 Echocardiography

Direct cardiac function measurements were obtained using the Visualsonics Vevo 2100 (Toronto, Ontario, Canada). Both rats and mice were kept under controlled anesthesia using vaporized isoflurane (2-3% isoflurane in oxygen at a flow rate of 100 mL/min). Echocardiography was recorded at baseline, 4, and 24 hours in the rat model and at baseline, 4, 8, and 14 hours in the mouse model. Images were analyzed using Vevo®2100 1.3.0 software.

2.1.3 Preparation and permeabilization of cardiac fibers

This technique has been described by our group (Fisher-Wellman et al., 2013) and others (Saks et al., 1998) in detail. Following exsanguination under anesthesia the heart was removed, briefly rinsed in saline to remove excess blood and dried. A portion of the left ventricle (LV) near the apex was removed from the heart for mitochondrial experiments. This LV muscle samples were placed in ice-cold (4◦C) Buffer X containing (mM): 7.23 K2EGTA, 2.77 CaK2EGTA, 20 imidazole, 20 taurine, 5.7 ATP, 14.3 phosphocreatine, 6.56 MgCl2.6H2O and 50Mes (pH 7.1, 295 mosmol l−1). Fat and connective tissue were removed from muscle samples under a dissecting microscope and small bundles of fibers were prepared (>1mg wet weight per fibers bundle). Fibers bundles were treated with 50 μg ml^{-1} saponin for 30 min as previously described (Anderson and Neufer, 2006). Following permeabilization, myofiber bundles were washed in ice-cold Buffer Z containing (mM): 110 K-Mes, 35 KCl, 1 EGTA, 5 K2HPO2, 3 MgCl2.6H2O and 5mgml−1 bovine serum albumin (BSA; pH 7.4, 295 mosmol l−1) and remained in Buffer Z on a rotator at 4◦C until analysis (<4 h). We have observed that permeabilized myofibers bundles exhibit a very strong Ca2+-independent contraction that is temperature sensitive and can occur even at 4◦C (Perry et al., 2011); therefore, 20 μM blebbistatin was added to the wash buffer, in addition to the respiration medium during

experiments, to prevent contraction as previously described. Following permeabilization and washing in Buffer Z, all mitochondrial function measurements in this study were performed in exactly the same order from one animal to another and among groups, to minimize the potential influence that the timing and duration of washing may have on the end-points measured.

2.2 Cell Culture

HL-1 cardiomyocyte (HL1c) cells were used in this study. HL1c are an immortalized atrial cardiomyocyte cell line (Claycomb et al., 1998; White and Claycomb, 2003; White et al., 2004), a kind gift from Dr. WC Claycomb (Louisiana State University Medical Centre, LA). Cells were cultured in Claycomb media (Sigma-Aldrich, St. Louis, MO) supplemented with 10% fetal bovine serum, 4mM L-glutamine, 10μM norepinephrine and MycoZap™Plus-CL (Lonza, Walkersville, MD) and maintained at 37°C and 5% CO_2. In all experiments where TNFα and IL1β were used in this study, the concentration was 3 and 100 (ng/mL) respectively (0.17nM TNFα and 5.71nM IL1β). These dosages were determined using a modified dose-response curve (Figure 3.8), where this dosage, when compared to control, showed an increase in nuclear localization of p65. For PHB exposure, cells were incubated with recombinant Flag-tagged PHB (6.25uM or 200ng/mL, dose chosen based Figure 3.14) or transfected with a pCMV6-AC-GFP vector (Origene, Rocksville, MD) containing a human clone of PHB or a GFP positive scrambled vector (see 2.2.1 below).

2.2.1 Cell transfection

For over-expression of PHB, we used a *PrecisionShuttle™ Vector System* (Origene, Rockville, MD) with a pCMV6-AV vector, which is a mammalian expression vector, containing the human PHB gene encoded in-frame with a green fluorescent protein (GFP) sequence on the

C-terminal end. The transfection was performed at 75-80% of cell confluency. Five micrograms of PHB-GFP or control vector (Vec) and 4µL of Lipofectamine Reagent (Life Technologies, Grand Island, NY) were mixed carefully in unsupplemented Claycocmb medium. Following thorough mixing by pipetting, the mixture was incubated at room temperature (RT) for 30 minutes. The tranfection mix, containing either PHB-GFP or control vector was then applied to the cells and cultured for 24 hours. For the ARE reporter assay, we used a *Lenti ARE reporter (GFP)* System (SABiosciences, Valencia CA) which is a preparation of VSV-g pseudotype lentivirus particles with minimal CMV promoter and tandem repeats of the ARE transcriptional response element controlling the expression of GFP. This system allows us to monitor transient pathway regulation. The transfection process was similar to the one previously described in this section. Cells were transfected at 85-90% confluency. One microgram of ARE-GFP and 1uL of Lipofectamine Reagent (Life Technologies, Grand Island, NY) were mixed carefully in unsupplemented Claycocmb medium. Following thorough mixing by pipetting, the mixture was incubated at room temperature (RT) for 30 minutes. The tranfection mix was then applied to the cells and cultured for 24 hours.

2.2.2. Preparation of HL1c for assessment of mitochondrial function.

HL1c were lifted from culture flasks with 0.05% Trypsin-Ethylenediaminetetraacetic acid (EDTA) and counted using the Vi-Cell SGL (Beckman Coulter). The protocol for permeabilization was adapted from Boyle *et. al* (Boyle et al., 2012). Briefly, 2.0 million cells (for mitochondrial O_2 consumption) and 1.0 million cells (for mitochondrial H_2O_2 and Ca^{2+} uptake) cells were centrifuged at 500xg for 5 minutes at room temperature. Cells used for mitochondrial O_2 consumption were resuspended in room temperature MiRO5.1 (respiration

buffer: 110mM Sucrose, 60mM K-MES, 20mM HEPES, 20mM Taurine, 10mM KH_2PO_4, 3mM $MgCl_2 \cdot 6H_2O$, 1mM EGTA and 2.5g/L BSA [pH=7.4 with KOH]) while cells for mitochondrial H_2O_2 and Ca^{2+} uptake were resuspended in room temperature buffer Z-lite (150mM K-MES, 30mM KCL, 10mM KH_2PO_4, 5mM $MgCl_2 \cdot 6H_2O$, 1mM EGTA and 0.5mg/L BSA [pH=7.4]). Cells are permeabilized using 3.0 µg/million cells of digitonin (Sigma-Aldrich, St. Louis, MO) in final resuspension before functional assessment.

2.2.3 Subcellular Fractionation

Nuclear extract preparations were performed using fresh portions of cardiac tissue immediately after dissection and HL1c lifted using 0.05% trypsin/EDTA, according to the method described by (Deryckere and Gannon, 1994). Briefly, after removal of connective tissue, the fresh myocardial tissue was placed in ice-cold hypotonic buffer (10 mM HEPES, pH 7.5; 40 mM NaF; 10 µM Na_2MoO_4; 0.1 mM EDTA, 1 mM β-glycerophosphate; 1 mM Na_3VO_4, and protease inhibitor cocktail (Sigma-Aldrich, St Louis, MO) and transferred to the laboratory. Tissue was then minced very fine, placed back into ice-cold hypotonic buffer, pulverized in a dounce homogenizer for 10-12 strokes, and incubated on ice for 15 minutes. The sample was then centrifuged at 300xg for 10 minutes and supernatant retained as a cytosolic fraction. Pellet was then resuspended in ice-cold hypotonic buffer and again incubated for 15 minutes on ice. Nonidet P-40 was added at 0.1X the sample volume and centrifuged at 14,000Xg for 30 seconds. This supernatant was also retained as the cytosolic fraction, and pellet was resuspended in nuclear extraction buffer (10 mM HEPES, pH 7.9; 0.1 mM EDTA; 3 mM $MgCl_2$; 420 mM $NaCl_2$; 10% glycerol (v/v)), vortexed at full speed for 30 seconds and then incubated for 15

minutes at 4°C with rocking. This step was repeated. The sample was then centrifuged at 14,000Xg for 10 minutes at 4°C, and the supernatant retained as the nuclear fraction.

2.3 Measurement of Mitochondrial Function

All experimental were performed at 30ºC and in Buffer Z. mO_2 consumption was measured using the O_2K Oxygraph system (Oroboros Instruments, Austria) in buffer Z containing 20mM creatine monohydrate (Sigma-Aldrich, St. Louis, MO). Substrates and respiratory inhibitors were provided as indicated in the figure legends. Measurements of mitochondrial ATP generation were obtained using a custom tandem oxi-fluorometer approach developed and validated in our laboratory (Anderson et al., 2011), by coupling ATP hydrolysis to NADPH release and autofluorescence (Figure 2.2). To maintain coupling of ATP hydrolysis to NADPH release, 2.5 U/mL of glucose-6-phosphate dehydrogenase (Roche, Indianapolis IN) 2.5 U/mL yeast hexokinase (Roche, Indianapolis IN), 5mM nicotinamide adenine dinucleotide phosphate (NADP+) (Sigma-Aldrich, St. Louis, MO), and 5mM D-glucose (Sigma-Aldrich, St. Louis, MO) were added to the assay media. P1,P5-Di(Adenosine-5′)Pentaphosphate (Ap5A) (Sigma-Aldrich, St. Louis, MO) was added to inhibit adenylate kinase and ensure that ATP production being measured by the system was solely from the mitochondria. Mitochondrial H_2O_2 and Ca^{2+} uptake studies were done using a spectrofluorometer (Photon Technology Instruments, Birmingham, NJ). All experiments were performed at 30°C. Mitochondrial H_2O_2 studies were performed in the presence of 125μM ADP, 5mM glucose and 1 unit/ml hexokinase to keep the mitochondria in a permanent submaximal phosphorylating state. For mitochondrial H_2O_2 measurements, buffer z-lite contained 10μM Amplex Red, 3 unit/ml horseradish peroxidase, 25 units/mL superoxide dismutase (SOD), 5mM pyruvate, 2mM malate and 5mM succinate, and the

H_2O_2 emission rate was calculated as outlined previously. For Ca^{2+} uptake measurements, buffer Z-lite contained 1μM Calcium Green 5-N, 5mM pyruvate, 2mM malate, 5mM succinate. At the start of the Ca^{2+} uptake studies 1.5μM thapsigargin was added to inhibit the sarcoplasmic/endoplasmic reticulum Ca^{2+} -ATPase (SERCA) and 10μM EGTA, to chelate any remaining Ca^{2+}. Pulses of 30μmol Ca^{2+} ($CaCl_2$) were added sequentially and Ca^{2+} uptake was followed until the mitochondrial permeability transition pore opening, as described previously (Anderson et al., 2011). At the conclusion of the experiment, a 1mM bolus of $CaCl_2$ was added to saturate the probe. Using the known Kd for Calcium Green 5-N and the F_{min} and F_{max} established during each experiment, changes in free calcium were calculated using the equations described by Tsien (Tsien, 1988).

2.4 Myocardial Protein Extraction

For whole tissue protein preparation, myocardial samples frozen in liquid N2 were homogenized in ice-cold 10x (w/v) of TEE Buffer (10mM Tris-base; 1mM EDTA and 1mM EGTA pH 7.4) containing 0.5% Triton X-100 and protease inhibitor cocktail (Sigma-Aldrich, St. Louis, MO), using a glass grinder (Kimble Chase, Vineland, NJ). After 5 minute incubation on ice, homogenates were spun at 10,000 rpm for 10 minutes to pellet debris, and supernatants were retained for protein analysis.

2.5 Serum PHB Enzyme-linked immunosorbent assay

Blood was drawn from the tail vein of the rats at baseline (time 0), and 4 and 12 hours following the induction of sepsis with LPS. At the 24 hour time point, blood was collected by cardiac puncture. In the mouse studies, blood was collected at 4 and 16 hours by cardiac puncture. The blood was centrifuged at 500xg for 5 minutes to separate the serum. Serum was

removed and flash frozen in liquid nitrogen and stored at -80°C until the time of analysis. The absolute amount PHB in circulation determined by a quantitative ELISA approach developed in our lab. A standard curve of PHB was first established using purified recombinant PHB (Origene, Rockville, MD). Standards and undiluted serum samples were added to an Immunolon-coated 96-well assay plate (Fisher Scientific). Samples were incubated overnight at 4°C, and subsequently washed with PBS+0.05% Tween-20 and blocked for 2 hours with with 10% fetal bovine serum (Sigma-Aldrich, St. Louis, MO) diluted in PBS Samples were then incubated with anti-PHB antibody (1:200 in PBS+0.05% BSA, Abcam) for 2 hours at 37°C. Samples were washed with PBS+0.05% Tween-20 and incubated with secondary antibody for 2 hours at room temperature (goat anti-rabbit HRP, Bio-Rad). Following this incubation, samples were washed as before and incubated with TMBZ for 20 minutes at room temperature. Reaction was quenched with 1M sulfuric acid, and the absorbance of the samples at 450 nm was determined. Total quantities of serum PHB in each group was determined using standard curve of rPHB, and expressed in absolute amount as ng/mL.

2.6 Immunocytochemistry

HL1c were grown in glass bottom 6-well plates (MatTek Corporation). Where appropriate, 50nM MitoTracker® Red CMXRos was incubated on the cells for 15 minutes at 37°C after which the cells were washed twice in sterile PBS. Using 3.7% para-formaldehyde, cells were fixed. Fixative was washed off with PBS. Cells were permeabilized using 0.1% Triton X-100 and blocked using 5% goat serum. Cells were incubated with primary antibodies as indicated throughout (antibody information can be found in Table 2.3) overnight at 4°C. Cells were washed and incubated with secondary antibodies as indicated throughout (see Table 2.3 for

antibody information) for 1 hour at room temperature. Cell were washed with PBS and incubated with Draq5 (Cell Signaling Technology, Danvers, MA) for 5 minutes. Cell microscopy was carried out with a Carl Zeiss LSM 510 using a 63X magnification.

Measurements of mitochondrial ROS production using MitoSox™Red were carried out in live cells. Cells were exposed to a cocktail of 3/100 (ng/mL) TNFα/IL1β for 24 hours. Following treatment the cells were incubated with 2μM MitoSox™Red in buffer containing Ca and Mg for 10 minutes. Cell were then washed with PBS and imaged with a Nikon Eclipse Ti microscope using 20X magnification

Measurements of ARE-driven GFP fluorescence were carried out in live cells. Transfected cells were exposed to PBS as a vehicle control, 20uM sulforphane (Sigma-Aldrich, St. Louis, MO), a cocktail of 3/100 (ng/mL) TNFα/IL1β only, rPHB (200ng/mL) only or a combination of rPHB and TNFα/IL1β (both applied at time 0 and rPHB added 12 hours after TNFα/IL1β) for 24 hours. Following treatment cells were washed with PBS and imaged using with a Nikon Eclipse Ti microscope using 20X magnification.

2.7 Cytotoxicity

Cell death was assessed 24 hours after the inflammatory insult using a commercially available lactate dehydrogenase (LDH) assay kit (Abcam, Cambridge, MA). Briefly, HL1c were grown to 85% confluency in normal growth media. Upon reaching 85% confluency, HL1c were incubated in phenol-red free Opti-MEM media and treated with 3.0 ng/mL TNFα and 100 ng/mL IL1β. Following treatment, 100μL of medium was removed to an optically clear 96-well plate. LDH Reaction Mix was added to each well and color development was monitored for 20-30 minutes. Absorbance was measured at 450nm.

2.8 Real-time quantitative PCR

For mRNA extraction, cardiac samples frozen in liquid N_2 and HL1c were homogenized using a Pro Scientific Pro200 tissue homogenizer in 350µL and 600µL respectively and then subjected to a brief proteinase K treatment (55°C for 10 min). Total mRNA was then extracted in RNeasy columns according to the manufacturer's instructions (Qiagen, Inc., Valencia, CA, USA). Reverse transcription and relative changes in mRNA of all redox- and anti-inflammatory target genes were determined by fluorescence-based real-time PCR using SsoAdvanced SYBR Green Supermix (BioRad Laboratories, Hercules, CA, USA). The primer pairs used in these experiments are listed in Table 2.2, along with their respective source. Data were analyzed by the ΔΔCt (threshold cycle) method using Bio-Rad CFX Manager software and mRNA levels were normalized to β-Actin and 18S under various conditions.

2.9 Western Blot Analysis

Proteins were separated based on molecular weight using sodium dodecyl sulfate polyacrylamide gel electrophoresis (SDS-PAGE). Following electrophoresis, proteins were transferred to Immobilon FL PVDF (Milipore, Billerica, MA) membrane using a semi-dry blot apparatus (Trans-Blot SD; Bio-Rad Laboratories, Hercules, CA). After transfer, membranes were blocked using 5% non-fat dry milk in tris-buffered saline with 0.1% Tween-20 (TBS-T) for at least 1 hour at room temperature, to prevent nonspecific antibody binding. Membranes were washed with TBS-T three times for 10 minutes and incubated overnight at 4°C with primary antibodies. The following day, membranes were washed with TBS-T three times for 15 minutes to remove any unbound primary antibody. Following washing, membranes were incubated with secondary antibodies for 1 hour at room temperature. Before imaging, membranes were washed

three times for 10 minutes. Protein-antibody complexes were imaged using Odyssey® CLx (Li-Cor; Lincoln, NE). Various proteins were probed for using specific antibodies, a list can be found in table 2.3. The densitometric analysis of immunoblots was performed using ImageJ software (National Institutes of Health).

2.10 Macrophage Activation

RAW 264.7cells, an immortalized murine macrophage-like cell line, were cultured in DMEM medium (Life Technologies, Grand Island, NY) supplemented with 10% FBS, 100U/mL penicillin and 100µg/mL streptomycin and maintained at 37°C with 5% CO_2. To explore the effect of PHB on macrophage activation, RAW264.7 cells were stimulated with 10µg/mL purified from *Escherichia coli* (Sigma-Aldrich, St. Louis, MO). Upon reaching 90% confluence, cells were lifted using 0.05% trypsin/EDTA and counted using a Vi-Cell SGL (Beckman Coulter, Brea CA). Following counting, cells were centrifuged and resuspended to a concentration of $1x10^6$ cells/mL in media. In a 96-well plate, 50µL of cell suspension was added to all sample wells containing 50µL of media for a total volume in the well of 100µl. 96-well plates were incubated for 2 hours at 37°C with 5% CO_2 to allow cells to adhere. At least three wells received no cells and served as blanks. Following time for adherence, media was removed and fresh was added as indicated in the table below. Table 2.4 shows the different experimental conditions. Cells were stimulated with LPS for 17-20 hours.

Blood collected from mice at four and 16 hours following the administrations of LPS was centrifuged to separate the plasma. Plasma was flash frozen in liquid nitrogen and stored at -80°C until use in the cytokine multiplex.

2.10.1 Macrophage Nitrite Secretion

The nitrite secretion assay was adapted from the Griess Reagent Kit for Nitrite Determination (Life Technologies, Grand Island, NY). This method utilizes the Griess diazotization reaction (Figure 2.3) to determine the amount of nitrite formed following spontaneous oxidation of NO. Breifly, $NaNO_2$ was used to create a standard curve at the concentrations listed in table 2.5. The Griess reagent is comprised of equal parts 1.0% sulfanilamide (0.025g into 2500µL) and 0.1% naphtylethyenediamine dihydrochloride in 2.5% H_3PO_4 (0.0025g into 2500µL of 2.5% H_3PO_4) and was prepared fresh daily. 50µL of media was removed from each well of the 96-well plate containing the RAW 264.7 macrophages and added to a fresh 96-well plate. An equal volume of Griess reagent was added and mixed using a pipette. The plate was protected from light and color development was monitored. Plate was read at 548 nm within 30 minutes.

2.10.2 Macrophage Reactive Oxygen Species (ROS) Secretion

The ROS secretion assay was adapted from the Amplex Red Hydrogen Peroxide/Peroxidase Assay Kit (Life Technologies, Grand Island, NY). In the presence of horseradish peroxidase (HRP), Amplex® Red reagent, reacts with H_2O_2 to produce resorufin (ex/em 571/585nm), the fluorescent product. SOD was added to ensure all superoxide molecules were converted to H_2O_2. Briefly, H_2O_2 was used for production of the standard curve at the following concentrations, 0, 0.5, 1, 2, 4 and 8 µM. Working concentrations of HRP, SOD, and Amplex® Red were prepared daily. Equal volumes of the HRP, SOD, and Amplex® Red mixture and media from macrophages stimulated with LPS for 17-20 hours were added to a fresh

96-well plate to a total volume of 100µL. The plate was protected from light and color development was monitored. Plate was read at 560 nm within 30 minutes.

2.10.3 Cytokine Multiplex

The concentrations of circulating serum cytokines IL6 and TNFα were determined following the manufacture protocol provided with the Q-plex Array™ Mouse IR (Quansys Biosciences, Logan, Utah). Briefly, antigen standards and serum from animals was incubated in the wells of a manufacturer provided 96-well plate for two hours at 400 RPM at room temperature. After washing, a proprietary Detection Mix was incubated for an additional two hours, followed by washing. The plate was then protected from light and incubated for 30 minutes with DyLight® IR Dye. After washing, the plate was rinsed with Stabilizing Solution and allowed to dry at room temperature, protected from light. Prior to imaging, the bottom of the plate was wiped down with 70% ethanol. The plate was imaged using a LI-COR® Odyssey-CLx®, and densitometry was performed using ImageJ software (National Institutes of Health).

2.11 Statistical Analysis

Statistical analysis was performed with PRISM (GraphPad Software, San Diego, CA). All data are expressed as means ± standard error of the mean (SEM) unless otherwise noted. Differences were determined by one-way ANOVA, followed Newman-Keuls multiple comparisons test. A two-way ANOVA was used to determine difference in all echocardiography data. In all cases, a *P* value of less than 0.05 was used to indicate statistical significance between groups.

Table 2.1 Experimental groups used in animal experiments.

Group	Species	rPHB (ng/mL)	5%Dextrose H_2O (µL)	LPS (mg/kg)
Vechicle	Rat	--	550	--
	Mouse	--	250	--
rPHB	Mouse LD	200	250	--
	Mouse HD	200	250	--
LPS	Rat LD	--	550	0.5
	Rat HD	--	550	7.5
	Mouse LD	--	250	4
	Mouse HD	--	250	12
rPHB + LPS	Mouse LD	200	250	4
	Mouse HD	200	250	12

A. *In vivo r*at time course

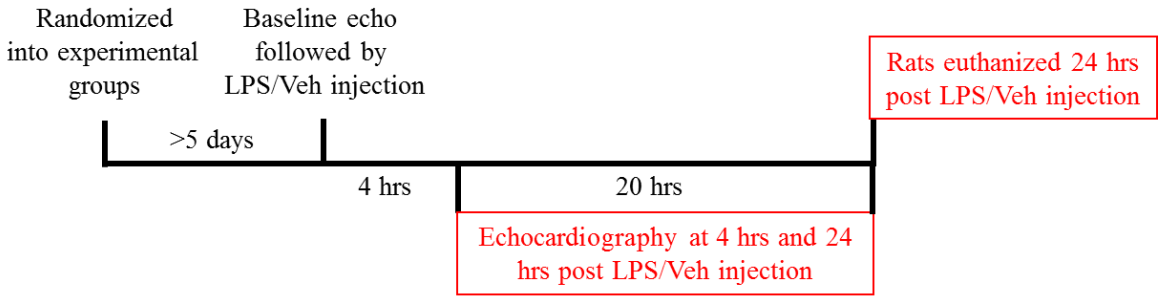

B. *In vivo* mouse time course

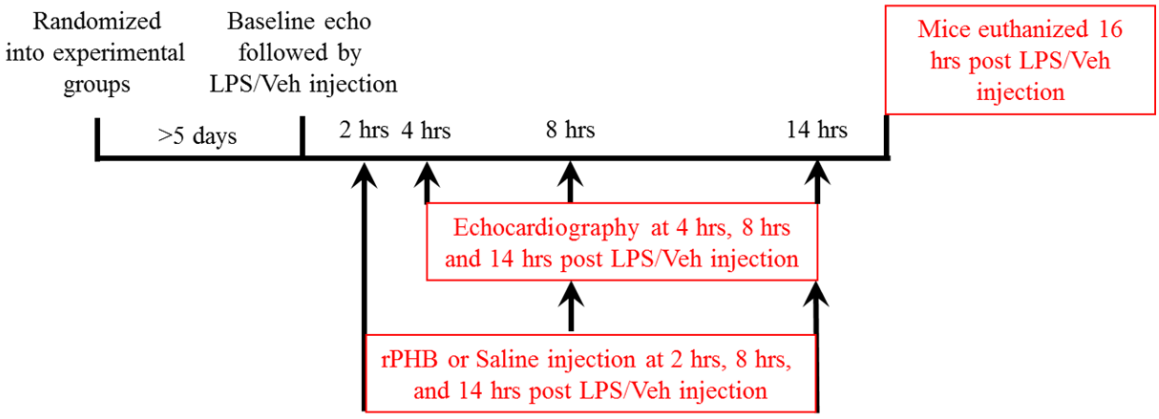

Figure 2.1 Schematic overview of experimental time courses.

A, The 24 hour time course of LPS-induced sepsis in rats. B, The 16 hour time course of LPS-induced sepsis in mice.

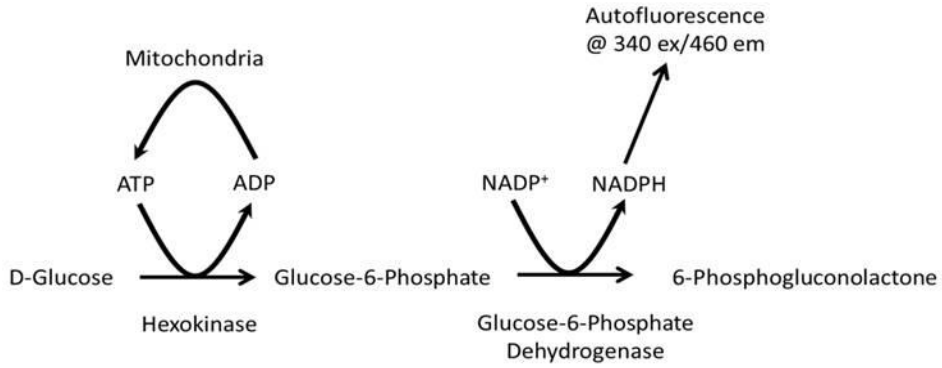
Autofluorescence
@ 340 ex/460 em
Mitochondria
ATP
ADP
NADP+
NADPH
D-Glucose
Glucose-6-Phosphate
6-Phosphogluconolactone
Hexokinase
Glucose-6-Phosphate
Dehydrogenase

Figure 2.2 Enzyme coupling of ATP hydrolysis to NADPH release

Saturating the system with glucose, hexokinase, $NADP^+$ and glucose-6-phosphate dehydrogenase ensures that upon its production ATP will be used to convert glucose to glucose-6-phosphate by hexokinase yielding ADP. In the presence of $NADP^+$, glucose-6-phosphate is converted to 6-phosphogluconolactone by glucose-6-phosphate dehydrogenase to yield NADPH which autofluoresces at 340 ex/460 em.

Table 2.2 List of PCR primers

Primers	Sequence (5'→3')	Reference
Prohibitin 1 Mouse		
Forward	GCATTGGCGAGGACTATGAT	(Theiss et al., 2009b)
Reverse	CTCTGTGAGGTCATCGCTCA	
Nrf2 Mouse		
Forward	CTACTCGTGTGGGACAGCAA	(Theiss et al., 2009b)
Reverse	AGCAGACTCCAGGTCTTCCA	
TNFα Mouse		
Forward	ACTCAACAAACTGCCCTTCTGAG	(Niu et al., 2007)
Reverse	TTACAGCTGGTTTCGATCCATTT	
IL1β Mouse		
Forward	TGTGGCTGTGGAGAAGCTGT	(Niu et al., 2007)
Reverse	CAGCTCATATGGGTCCGAGA	
IL6 Mouse		
Forward	CACGGCCTTCCCTACTTCAC	(Niu et al.,

Reverse	TGCAAGTGCATCATCGTTGT	2007)
iNOS Mouse		
Forward	CCCTTCCGAAGTTTCTGGCAGCAGC	(Heo et al., 2010)
Reverse	CCCTTCCGAAGTTTCTGGCAGCAGC	
COX2 Mouse		
Forward	CACTACATCCTGACCCACTT	(Heo et al., 2010)
Reverse	ATGCTCCTGCTTGAGTATGT	
CRP Mouse		
Forward	AGCCTCTCTCATGCTTTTGG	(Paul et al., 2004)
Reverse	TGTCTCTTGGTGGCATACGA	
NRF1 Mouse		
Forward	TGGAGGAGCACGGAGTGA	(Ding et al., 2007)
Reverse	CAGCCAGATGGGCAGTTA	
PGC1α Mouse		
Forward	GGAGCCGTGACCACTGACA	Ding et al., 2007)
Reverse	TGGTTTGCTGCATGGTTCTG	

Tfam Mouse		
Forward	CATTTATGTATCTGAAAGCTTCC	(Thundathil et al., 2005)
Reverse	CTCTTCCCAAGACTTCATTTC	
Gpx1 Mouse		
Forward	CTCACCCGCTCTTTACCTTCCT	(Gosbell et al., 2006)
Reverse	ACACCGGAGACCAAATGATGTACT	
Gpx4 Mouse		
Forward	TGAGGCAAAACTGACGTAAACTACA	(Gosbell et al., 2006)
Reverse	GCTCCTGCCTCCCAAACTG	
Trx2 Mouse		
Forward	CAGCCTCTGGCACATTTCCT	(Gosbell et al., 2006)
Reverse	GTTCGGCTTCTGGTTTCCTTT	
NQO1 Mouse		
Forward	CCATTCTGAAAGGCTGGTTTG	(Zhu et al., 2008)
Reverse	CTAGCTTTGATCTGGTTGTC	
HO1 Mouse		

Forward	GCCTTGAAGGAGGCCACCAA	(Zhu et al., 2008)
Reverse	CCTCAAACAGCTCAATGTTG	
GCLC Mouse		
Forward	GGAGGCTACTTCTGTACTA	(Zhu et al., 2008)
Reverse	CGATGGTCAGGTCGATGTCATT	
GSTA1 Mouse		
Forward	CCGTGCTTCACTACTTCAAT	(Zhu et al., 2008)
Reverse	GCATCCATGGGAGGCTTTCT	
GR Mouse		
Forward	TGCCTGCTCTGGGCCATT	(Zhu et al., 2008)
Reverse	CTCCTCTGAAGAGGTAGGAT	
Catalase Mouse		
Forward	GACATGGTCTGGGACTTCTG	(Zhu et al., 2008)
Reverse	GTAGGGACAGTTCACAGGTA	
Prohibitin 1 Rat		
Forward	TGGCGTTAGCGGTTACAGGAG	(Zhu et al.,

Reverse	GAGGATGCGTAGTGTGATGTTGAC	2008)
TNFα Rat		
Forward	GCCTCTTCTCATTCCTGC	(Pan et al., 2011)
Reverse	CTTCTCCTCCTTGTTGGG	
IL1β Rat		
Forward	GCTAGGGAGCCCCCTTGTCGAG	(Pan et al., 2011)
Reverse	AGGCAGGGAGGGAAACACACGTT	
IL6 Rat		
Forward	TCCGCAAGAGACTTCCAGCCAG	(Pan et al., 2011)
Reverse	TGTGAAGTAGGGAAGGCAGTGGC	
LC3b		
Forward	CGATACAAGGGGGAGAAGCA	(Raffaello et al., 2010)
Reverse	ACTTCGGAGATGGGAGTGGA	
Beclin-1		
Forward	TGAATGAGGATGACAGTGAGCA	(Raffaello et al., 2010)
Reverse	CACCTGGTCTCCACACTCTTG	

Lamp2a		
Forward	TGGCTAATGGCTCAGCTTTC	(Raffaello et al., 2010)
Reverse	ATGGGCACAAGGAGTTGTC	
p62		
Forward	GGAGGAGCTCGAGCCATGGCGTTCACGGTGAA	(Perera et al., 2011)
Reverse	TATTATTTTTGGATCCTTCAATGGTGGAGGGTG TTCG	

Table 2.3 Primary and Secondary Antibodies

Antibody	Concentration	Vendor (Cat. No)
Prohibitin 1	1:1000 (WB) 1:10 (ICC)	Abcam (ab28172)
Prohibitin 2	1µg/mL	Millipore (AB10198)
COX-IV	1µg/mL	Abcam (ab14744)
Alpha-Tubulin	1:5000	Abcam (7291)
TATA Binding Protein	1:2000	Abcam (ab818)
Beta-Actin	1:250	Abcam (ab8226)
NFκB-p65	1µg/mL	Abcam (ab16502)
Draq5®	1:1000 (ICC)	Cell Signaling (4084)
iNOS	1:500	Cell Signaling (2977)
Nrf2	1:1000	Abcam (ab62352)
DYKDDDDK Epitope Tag (Flag Epitope)	1:1000	Novus Biologicals (NBP1-06712)
FITC- Goat Anti Rat	1:50	Jackson ImmunoResearch Laboratories (112-095-003)

FITC-Donkey Anti Rabbit	1:50	Jackson ImmunoResearch Laboratories (711-095-152)
FITC-Donkey Anti Mouse	1:50	Jackson ImmunoResearch Laboratories (715-095-150)
HRP-Goat Anti Rabbit	1:7500	Bio-Rad (170-651)
Goat Anti-Rabbit IgG, DyLight™ 680 Conjugated	1:17000	Thermo Scientific (35568)
Goat Anti-Mouse IgG, DyLight™ 800 Conjugated	1:17,000	Thermo Scientific (35521)
Donkey Anti-Rabbit IRDye® 680	1:30,000	Li-Cor (926-32223)
Donkey Anti-Mouse IRDye® 800CW	1:30,000	Li-Cor (926-32212)
Goat Anti-Rat IRDye® 800CW	1:30,000	Li-Cor (926-32219)

Table 2.4 Experimental Conditions for Macrophage Activation

	Medium (µl)	rPHB (ng/mL)	LPS (µg/mL)
Blank	100	--	--
Negative Control	100	--	--
Positive Control	99	--	10
rPHB Control	99	200	--
Sample A	98	200	10
Sample B	98	200 (10 hours after insult)	10

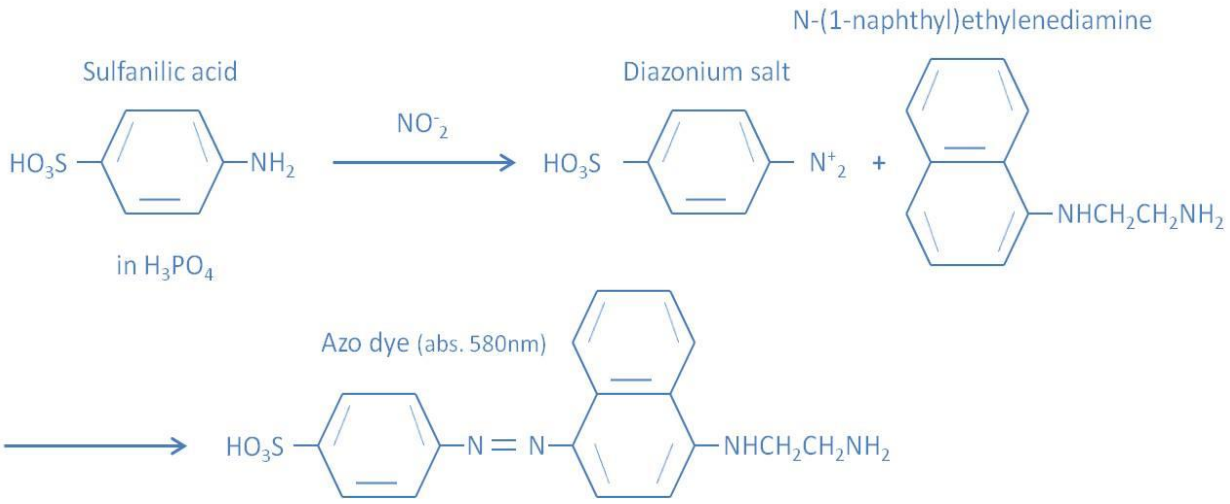
N-(1-naphthyl)ethylenediamine
Sulfanilic acid
Diazonium salt
NO^-_2
HO_3S
NH_2
HO_3S
N^+_2
+
$NHCH_2CH_2NH_2$
in H_3PO_4
Azo dye (abs. 580nm)
HO_3S
N = N
$NHCH_2CH_2NH_2$

Figure 2.3 The Griess diazotization reaction: Nitrite determination

NO is a short-lived molecular mediator of a number of physiological processes including vasodilation, reduced cardiac contractility, inflammation, immunity, and thrombosis. NO is rapidly converted to nitrate (NO_3^-) and nitrite (NO_2^-) in cells, making it hard to determine levels of NO in physiological systems. The Griess diazotization reaction allows for the detection of NO_2^-. When sulphanilic acid is added to a solution containing NO_2^- a diazonium salt is formed. In the presence of an azo dye, a pink color develops which can be measured spectrophotometrically at 548nm. The combination of sulphanilic acid and the azo dye are the commercially available "Griess Reagent."

Table 2.5 Nitrite secretion assay standards

0 µg/mL	0 nM
2.5 µg/mL	36 nM
5.0 µg/mL	72 nM
10 µg/mL	145 nM
20 µg/mL	290 nM
40 µg/mL	580 nM

CHAPTER THREE – Prohibitin coordinates an anti-inflammatory/antioxidant feedback loop from mitochondria to nucleus during inflammatory stress

Research over the last 10 years has linked PHB to a myriad of pleiotropic effects in numerous cell types, resulting in its becoming a therapeutic target for cancer, inflammatory diseases, type-2 diabetes and neurodegenerative diseases. Despite its promise, little is known and much more research needs to be done on this protein. Specifically, many questions remain concerning PHB's intra- and extracellular localization and translocation in response to various stimuli, as location appears to be critical to determining PHB's function. This section of the dissertation will outline preliminary *in vivo* work that established changes in expression and localization of PHB in response to LPS. Here, we addressed the hypothesis that overexpression of PHB, would result in increased cell viability in response to hyper-inflammatory stress (i.e. TNFα/IL1β exposure) by preserving mitochondrial function and suppressing oxidative stress.

3.1 Study Design

Male Sprague-Dawley rats (Charles River Laboratory Wilmington, MA) weighing between 275-300 grams (9-11 weeks old) were used in this study. Animals' ages and weights can be found in Table 3.1. Once assigned, rats were given a minimum of five days to acclimate to the animal facility. A schematic representation of the experimental timeline can be found in figure 3.1 As described in detail in chapter two and in Figure 2.1, rats were randomized into one of four experimental groups: 1) Vehicle (Veh) – 550 µL IP injection of 5% dexterous water, 2) Low-dose 24 hours (LD24) LPS – IP injection of 0.5 mg/kg LPS in 550 µL of 5% dexterous water 3) High-dose 24 (HD24) LPS – IP injection of 7.5mg/kg LPS in 550 µL of 5% dexterous water and 4) Low-dose 4 (LD4) LPS – IP injection of 0.5 mg/kg LPS in 550 µL of 5% dexterous

water. Rats in groups one through three were euthanized 24 hours after the IP injection of LPS or vehicle (Veh). Rats in group four were euthanized four hours after the IP injection of LPS.

HL1 cardiomyocytes (HL1c) were obtained from Dr. William Claycomb. Cells were exposed to 3.0 ng/mL TNFα in combination with 100 ng/mL IL1β for various times to explore PHB expression and localization. Transient transfection with PHB-GFP (oPHB) and incubation with rPHB were utilized in HL1c to investigate mitochondrial function, oxidative stress, cytokine production and cytotoxicity following TNFα/IL1β exposure.

3.2 Validation of LPS-mediated experimental models of sepsis.

Four hours following the administration of LPS the animals were more lethargic, exhibited marked piloerection and appeared to have halted grooming behaviors. Additionally, LPS treated animals labored to breathe and frequently their eyes became encrusted. In order to verify that the doses of LPS were inducing a sepsis-like inflammatory response we examined NFκB transactivation in LV tissue. We found that LPS caused a dose and time-dependent increase in NFκB activation. LD4 LPS and HD24 LPS elicited a significant increase in NFκB activation, however the effect was gone in the LD24 LPS group (Figure 3.2A). In addition, we investigated the mRNA levels of target genes under regulation of NFκB in LV tissue. TNFα, IL1β and IL6 are cytokines released from macrophages in response to LPS activation of TLR4 receptors. These cytokines then act on their respective receptors on other cell types (ie. cardiomyocytes) to activate NFκB and enhance their own transcription, resulting in a feed-forward regulatory cycle that perpetuates itself (i.e. so-called "cytokine storm") (Figure 1.1). Both LD24 LPS and HD24 LPS induced an increase in TNFα and IL1β gene expression while LD4 LPS increased the mRNA level of all three cytokines relative to Veh (Figure 3.2B)

3.2.1 Endotoxin-mediated sepsis induces myocardial impairment

Cardiac function was monitored using a noninvasive transthoracic echocardiography in rats under anesthesia. Echocardiography was obtained at baseline, 4 hours and 24 hours after the injection of Veh or LPS. LPS administration resulted in a decrease in wall thickening at 4 hours in both LD24 LPS and HD24 LPS, which remained significantly decreased at 24 hours in HD24 LPS. The decrease in wall thickening corresponded to increased left ventricular end-systolic diameter (LVeSD) at 4 hours in both dose groups and significantly decreased left ventricular end-diastolic diameter (LVeDD) at 4 hours in the high dose group and 24 hours in both dose groups (Table 3.1). There were no significant differences in the baselines of LPS injected and Veh injected animals. Using the dimensional measurements, parameters of cardiac function were calculated. Veh injected animals had no significant changes in heart rate (HR), stroke volume (SV), fractional shortening (FS), ejection fraction (EF) or cardiac index (CI) across the time points. As expected, HR significantly increased in the HD24 LPS group, 19.4 ±11% and 18.8 ± 7% and 13.5 ± 6% and 15.1 ± 6% in the LD24 LPS group at 4 and 24 hours, respectively (Table 3.1). Additionally EF, which is the percentage of blood pumped out of the heart with each cardiac cycle, was significantly reduced by 21.3 ± 6% and 12.0 ± 7% in HD24 LPS animals at 4 and 24 hours, respectively and 22.2 ± 8% in LD24 LPS animals at 4 hours (Figure 3.3A). FS, an index used to calculate contractile function of the heart, is the ratio of LVeDD to LVeSD. In a pattern similar to EF, FS was reduced by 29.7 ± 9% and 20.0 ± 10% in HD24 LPS animals at 4 and 24 hours, respectively and 32.7 ± 9% in LD24 LPS animals at 4 hours (Figure 3.3B). CI is a hemodynamic measurement that related cardiac output to bodyweight, resulting in a measure of cardiac performance relative to the size of the animal. CI was reduced at four hours in HD24 LPS and LD24 LPS animals. The reduction in CI was sustained in the HD24 LPS

animals, but returned to baseline in the LD24 LPS animals (Figure 3.3C). Representative m-mode echocardiographic traces comparing a Veh and HD24 LPS animal four hours following LPS administration shows a substantial decrease in cardiac contractility (Figure 3.4)

3.2.2 Endotoxin-mediated sepsis induces mitochondrial dysfunction

As a common feature of severe sepsis, mitochondrial dysfunction (reviewed in (Exline and Crouser, 2008; Harrois et al., 2009; Galley, 2011)), has been linked to both severity and outcome (Brealey et al., 2002; Garrabou et al., 2012) of the disease in patients. Using permeabilized LV muscle fibers we examined mitochondrial respiration supported by the tricarboxylic acid (TCA) cycle and fatty-acid substrates. Shown in Figure 3.5 is a representative overlap of ADP-stimulated O_2 consumption in permeabilized LV muscle fibers from a Veh animal (red) and a HD24LPS animal (green) in response to substrates from the TCA cycle. Permeabilized fibers in the absence of substrate (deFB) were added to respiration medium in the presence of 20 mM creatine (in order to saturate creatine kinase). The chamber was hyperoxygenated to an O_2 tension of ~400 nmol/mL and respiratory substrates were added as indicated.

There were no differences in basal mitochondrial O_2 respiration (mO_2) supported by carbohydrate-based complex I substrates, pyruvate and malate (P/M), suggesting there was no difference in mitochondrial content between the LV fiber bundles (Figure 3.6A). Additionally, there was no difference in the respiratory control ratio (RCR), a measure of mitochondrial coupling, between groups (Figure 3.6B). LPS caused a significant reduction in ADP-stimulated state-3 mO_2 supported by P/M (P/M_{ADP}) in HD24 LPS animals and trended towards a decrease in LD24 LPS animals (P=0.0514) (Figure 3.6A). When succinate (S) is added, driving maximal mO_2 through both complex I and II ($P/M+S_{ADP}$), the LPS-mediated reduction in ADP-stimulated

respiration was sustained (Figure 3.6A). Complex II-only mO_2 was assessed using rotenone to inhibit complex I. In line with the literature on mitochondrial dysfunction in sepsis (Brealey et al., 2002; Protti et al., 2007), we found no differences in complex II (S_{ADP}) stimulated mO_2 (Figure 3.6A). This suggests that complex I is responsible for LPS-induced decreases in mitochondrial O_2 consumption. There was no difference between the LD4 LPS and Veh animals. LPS did not cause any change in basal fatty–acid respiration driven by pamitoyl-carnitine + malate (PC+M). However, ADP-stimulated mO_2 supported by PC+M ($PC+M_{ADP}$) was reduced in all animals exposed to LPS (Figure 3.6C).

Sepsis is associated with the development of oxidative stress. ROS/RNS from the mitochondria are important for the host response to infection (Fang, 2004), however, in excess they also exacerbate organ injury (Crimi et al., 2006). Thus we sought to determine if mitochondrial ROS emission (mH_2O_2) was elevated in rats in response to LPS. Mitochondrial H_2O_2 emission was measured under continuous submaximal phosphorylating state, in the presence of glucose, hexokinase and ADP, to more closely model physiological conditions. In the presence of P/M, HD24 LPS rats had a significant increase in mH_2O_2 (Figure 3.6D). Upon addition of S, all LPS treated groups demonstrated an increase mH_2O_2. .

3.3 LPS induces changes in cardiac PHB expression and localization *in vivo*

Recent evidence suggesting a protective role for PHB in oxidative stress (Liu et al., 2009; Lee et al., 2010) and inflammation (Theiss et al., 2009a) led us to investigate cardiac PHB during sepsis. Figure 3.7 A & C show representative western blots of whole heart homogenate and nuclear protein analyzed for both PHB and β-Actin or TATA, respectively. PHB protein levels significantly decreased ($p<0.05$) in whole hearts of both LD24 LPS (-50%) and HD24 LPS (-

75%) animals compared to Veh (Figure 3.7B). Under normal physiological conditions, PHB is localized to the mitochondria. Interestingly, in both LD24LPS and HD24LPS, nuclear expression of PHB increased ($p<0.05$) ~140% and ~290% (Figure 3.7 D), respectively with no significant change in mitochondrial PHB expression.

PHB has been reported to be released from adipocytes into circulation embedded in lipid droplets (Brasaemle et al., 2004), and has also been reported to be detectable in the serum of cancer patients (Mengwasser et al., 2004), leading us to investigate PHB levels in circulation during sepsis. Blood was drawn from the tail vein of rats in each experimental group during the time-points shown in Figure 3.1. To our surprise, serum levels of PHB spiked ~2 and 3-fold as early as four hours following the induction of sepsis in LD24 LPS and HD24 LPS, respectively. Serum levels remained significantly ($p<0.05$) elevated at 12 hours in both dose groups and at 24 hours in the HD24 LPS animals (Figure 3.8).

3.4 Development and characterization of *in vitro* model of severe inflammatory stress

As discussed in detail in section 1.1 and 1.2.1, LPS acts on TLRs in immune cells to trigger the release of proinflammatory cytokines. These proinflammatory cytokines then act on their respective receptors on the same immune cells or surrounding cells to activate a feed forward mechanism through activation of NFκB. TNFα and IL1β, two proinflammatory cytokines released in response to LPS, are known to act synergistically (Kuldo et al., 2005) on NFκB activation. We examined p65 nuclear translocation and gene expression of NFκB target genes in response to increasing doses of a cocktail of TNFα and IL1β. Doses ranging from 0.003 ng/mL TNFα and 0.1 ng/mL IL1β to 3.0 ng/mL TNFα and 100 ng/mL IL1β were incubated with HL1c for four hours. Following exposure, we performed subcellular fractionation to isolate the

cytosol, mitochondria and nuclear compartments, in addition to isolating RNA. We observed that TNFα/IL1β cocktail dose-dependently increased the amount of nuclear p65 (Figure 3.9). Additionally, we also examined the mRNA expression of four target genes under regulation of NFκB: TNFα, IL1β, IL6 and iNOS. Similarly to the p65 nuclear translocation data, increasing concentrations of TNFα/IL1β caused an increase in the gene expression of all four target genes compared to Veh-treated cells (Figure 3.10 A-D). These experiments validated using 3.0 ng/mL TNFα and 100 ng/mL IL1β as cytokine cocktail in all subsequent in vitro experiments.

3.5 *In vitro* localization of endogenous PHB

PHB1 subcellular translocation in response to TNFα/IL1β was examined using immunocytochemistry in HL1c. Organelles and endogenous PHB were visualized using Draq5 (nuclear DNA shown in blue, 650/680nm ex/em), MitoTracker® Red CMXRos (mitochondria shown in red, 579/599nm ex/em) and FITC (PHB, shown in green, 492/520nm ex/em). Changes in localization were quantified using Pearson's coefficient, which measures the overlapping pixels from different fluorescent channels. Confluent HLlc were treated with a cocktail of 3.0 ng/mL TNFα and 100 ng/mL IL1β for 24 hours. Figure 3.11 shows representative confocal images following various treatments. HL1c exposed to TNFα/IL1β showed a significant increase in nuclear localization of PHB, whereas untreated cells showed mitochondrial localization of PHB (Figure 3.12). To examine the trigger of PHB translocation HL1c were pretreated with 400nM MitoQ, a mitochondrial specific antioxidant, and 10 μM MnTMPyP, a cytosolic-specific ROS scavenger. MitoQ attenuated the translocation induced by TNFα/IL1β, while MnTMPyP had no effect (Figure 3.12). To investigate whether PHB translocation was dependent on specific mitochondrial complex inhibition, we stressed the cells with other stimuli including,

rotenone (a mitochondrial complex 1 inhibitor), oligomycin (an inhibitor of mitochondrial F_0F_1-ATPase), p-trifluoromethoxy carbonyl cyanide phenyl hydrazine (FCCP, a potent mitochondrial uncoupler that depolarizes mitochondrial membranes). Rotenone, which blocks electron flow through NADH dehydrogenase (complex 1) has been shown to increase mitochondrial ROS and induce apoptosis (Li et al., 2003). HL1c were treated with 1μM rotenone for 4 hours yielding a slight but significant increase in nuclear PHB (Figure 3.12). Treatment for 4 hours with 1 μg/mL oligomycin resulted massive loss of cell viability. Concurrently, oligomycin treatment caused a significant increase in nuclear PHB (Figure 3.12). FCCP, uncouples the components of the electron from the F_0F_1-ATPase, driving maximal respiration while depolarizing the MIM. FCCP treatment (1 μM for 3 hours) yielded a modest but significant increase in PHB nuclear localization (Figure 3.12). Collectively, these results suggest that mitochondrial-derived ROS and mitochondrial membrane depolarization are important mediators of PHB nuclear translocation. Recent reports have shown that exogenously added PHB can be taken up by cultured cells and regulate metabolism in adipocytes (Vessal et al., 2006), as well as protect against oxidative stress in pancreatic β cells (Lee et al., 2010).

3.6 Overexpression of PHB in HL1c preserves mitochondrial function during severe inflammatory stress

As a common feature of severe sepsis, mitochondrial dysfunction (Harrois et al., 2009) (Galley, 2011), has been linked to both severity and outcome (Garrabou et al., 2012) (Brealey et al., 2002). PHB has been shown to protect mitochondrial ATP generation in pancreatic β-cells exposed to H_2O_2 (Lee et al., 2010), leading us to examine the impact of PHB on mitochondrial function in an *in vitro* model of sepsis. TNFα/IL1β exposure disrupted mitochondrial function

similar to what was seen in rat heart following LPS challenge (Figure 3.13a and 3.5a). Using a custom tandem oxi-fluorometer approach developed and validated in our laboratory (Anderson et al., 2011) mitochondrial ATP production and O2 consumption were measured simultaneously in the presence of P/M (5mM/2mM), ADP_{sub} (200μM), ADP_{max} (1mM) and S (5mM). Vector-transfected HL1c (Vec) treated with 3/100 (ng/mL) TNFα/IL1β for 24 hours had decreased ($p<0.05$) ADP-stimulated mO_2 and ATP generation (Figure 3.13 A and B). Together these findings resulted in a decreased ($p<0.05$) P:O ratio, which is a measure of the efficiency of the OxPHOS (Figure 3.13C). When PHB was overexpressed in HL1c (oPHB) treated with 3/100 (ng/mL) TNFα/IL1β for 24 hours, mitochondrial function was completely unchanged compared to Vec cells.

Additional measurements of mitochondrial function yielded similar results. Under ADP-stimulated conditions supported by P/M and S, mH_2O_2 from Vec cells treated with TNFα/IL1β doubled ($p<0.05$) in comparison to untreated Vec cells. This increase in TNFα/IL1β-mediated mH2O2 was completely blocked with oPHB (Figure 3.13D). We investigated the mitochondrial permeability transition pore sensitivity to Ca^{2+} by determining the mitochondrial retention capacity for Ca^{2+} (mCa^{2+}). Consistent with the mH_2O_2 and OxPHOS function data, mCa^{2+} was reduced by ~60% ($p<0.05$) in Vec cells treated for 24 hours with 3/100 (ng/mL) TNFα/IL1β when compared to untreated Vec cells. PHB overexpression prevented the TNFα/IL1β – mediated decrease in mCa^{2+}. (Figure 3.13E).

3.7 PHB mediates mRNA expression of NFκB and Nrf2 target genes during severe inflammatory stress

NFκB's dichotomous actions have been highly debated over the past decade. Prolonged activation and signaling through NFκB has been suggested to be detrimental in the heart by eliciting production of an elaborate network of cytokines including TNFα, IL1β, and IL6 (Bonfoco et al., 1995; Hamid et al., 2011). Recent reports have suggested that PHB may inhibit NFκB activation in colonic epithelial cells (Theiss et al., 2009a; Theiss et al., 2011). Here, we investigated the impact of rPHB on the expression of NFκB target genes in an *in vitro* model of sepsis in order to determine optimal dose of rPHB for future studies. Not surprisingly, exposure of HL1c to 3/100 (ng/mL) TNFα/Il1β for four hours resulted in a dramatic increase ($p<0.05$) in NFκB target genes, TNFα, IL1β, IL6, and iNOS. In contrast, prior incubation with a range of rPHB doses for 16 hours prior attenuated the cytokine-mediated increase in NFκB target genes, with the greatest response coming with the 200 ng/mL rPHB dose. (Figure 3.14 A-D).

We repeated the above experiment using 200 ng/mL rPHB and with oPHB to investigate the potential for PHB to inhibit NFκB activated target gene expression. oPHB and rPHB treatment in the absence of TNFα/Ilβ had no effect on NFκB target gene expression. However, following incubation with the inflammatory cocktail for three hours, both oPHB and rPHB treatment completely abolished the TNFα/IL1β driven increases in TNFα, IL1β, IL6, and iNOS gene expression (Figure 3.15 A-D).

We next sought to determine if PHB could up-regulate the Antioxidant Response Element (ARE) signaling pathway in HL1c. Theiss *et al* provided evidence that PHB may affect the Nrf2 pathway (Theiss et al., 2009b). Nrf2 is a transcription factor that regulates the oxidant response by causing increased expression of a myriad of antioxidant enzymes including

glutamate-cysteine ligase (GCLC), NAD(P)H, quinine oxioreducttase 1 (NQO1), glutathione peroxidase 1 (Gpx1), glutathione peroxidase 4 (Gpx4), and thioredoxin reductase 2 (Trx2). Using cells transfected with an ARE-GFP construct rPHB treatment caused a dramatic increase in GFP fluorescence in presence and absence of inflammatory stimuli (Figure 3.16B). Interestingly, incubation with rPHB resulted in an increase ($p<0.05$) in all Nrf2 target genes, in the presence or absence of inflammatory stress while oPHB only increased GCLC and NQO1 gene expression (Figure 3.17).

3.8 rPHB prevents LPS-induced macrophage activation

Macrophages play a central role in the response of the innate immune system to infection. Following activation, macrophages secrete proinflammatory cytokines, prostaglandins, NO and ROS all of which can propagate the feed-forward regulatory cycle. We therefore investigated whether rPHB treatment would prevent NO and ROS generation in LPS-activated RAW 264.7 macrophages. As expected LPS caused a dramatic increase in both nitrite and ROS levels. Remarkably, both concomitant and post-endotoxin treatment with rPHB abolished the LPS-induced increase in nitrite (Figure 3.18A) and ROS secretion (Figure 3.18B).

3.9 PHB protects against mitochondrial oxidative stress and cytotoxicity during severe inflammatory stress

Mitochondria are a major source of intracellular ROS, generated as a result of leakage of unpaired electrons from complexes I and III of the electron transport chain. During sepsis the balance between pro-oxidants and antioxidants favors a state of oxidative stress, resulting in overproduction of ROS, depletion of antioxidant systems, cellular damage and cell death (Svistunenko et al., 2006; Vanasco et al., 2008). We sought to determine if the NFκB inhibition

and Nrf2 activation induced by rPHB or oPHB would result in reduced oxidative stress using immunocytochemsitry and MitoSox™Red (510/580 nm ex/em). Figure 3.19A shows representative images of MitoSox™Red staining in HL1c. As expected, TNFα/IL1β treatment caused a significant ($p<0.05$) increase in MitoSox™Red fluorescence (Figure 3.19B). In contrast, oPHB prevented the TNFα/IL1β-mediated increase in MitoSox fluorescence. In addition, incubation for 16 hours with rPHB blunted the TNFα/IL1β-mediated increase in ($p<0.05$) MitoSox™Red fluorescence when compared to untreated Vec cells

Dysfunctional mitochondria can be fatal to the cell through programmed breakdown of the cell into apoptotic bodies or ATP depletion, which promotes necrotic cell death (Vanasco et al., 2008). During either necrotic or apoptotic cell death LDH is lost to the culture media following loss of plasma membrane integrity and therefore can be used as an early indicator of cytotoxicity. We used LDH release to determine if PHB could confer cytoprotection during cytokine toxicity. Exposure of Vec cells to 3/100 (ng/mL) TNFα/IL1β for 24 hours caused a ~40% increase ($p<0.05$) in cell death. This increase was completely abolished with oPHB or incubation of rPHB 16 hours prior to the start of treatment (Figure 3.20). Interestingly, incubation of rPHB six hours following the beginning of the treatment substantially attenuated ($p<0.05$) cytotoxicity as well, implicating a potential 'rescue' effect of PHB in this context (Figure 3.19).

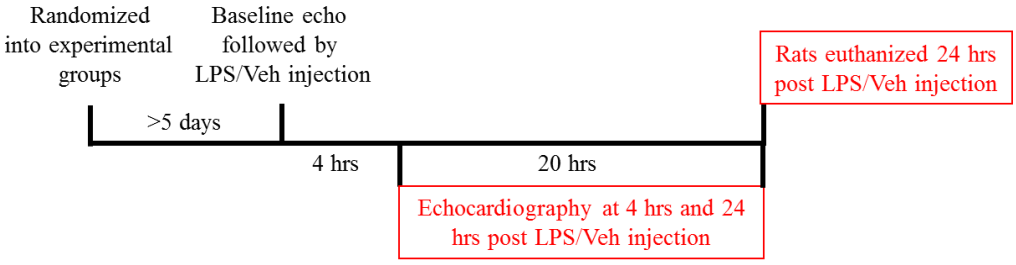
Randomized into experimental groups
Baseline echo followed by LPS/Veh injection
Rats euthanized 24 hrs post LPS/Veh injection
>5 days
4 hrs
20 hrs
Echocardiography at 4 hrs and 24 hrs post LPS/Veh injection

Figure 3.1 Schematic representation of the study design.

24 hour time-course of sepsis in rats.

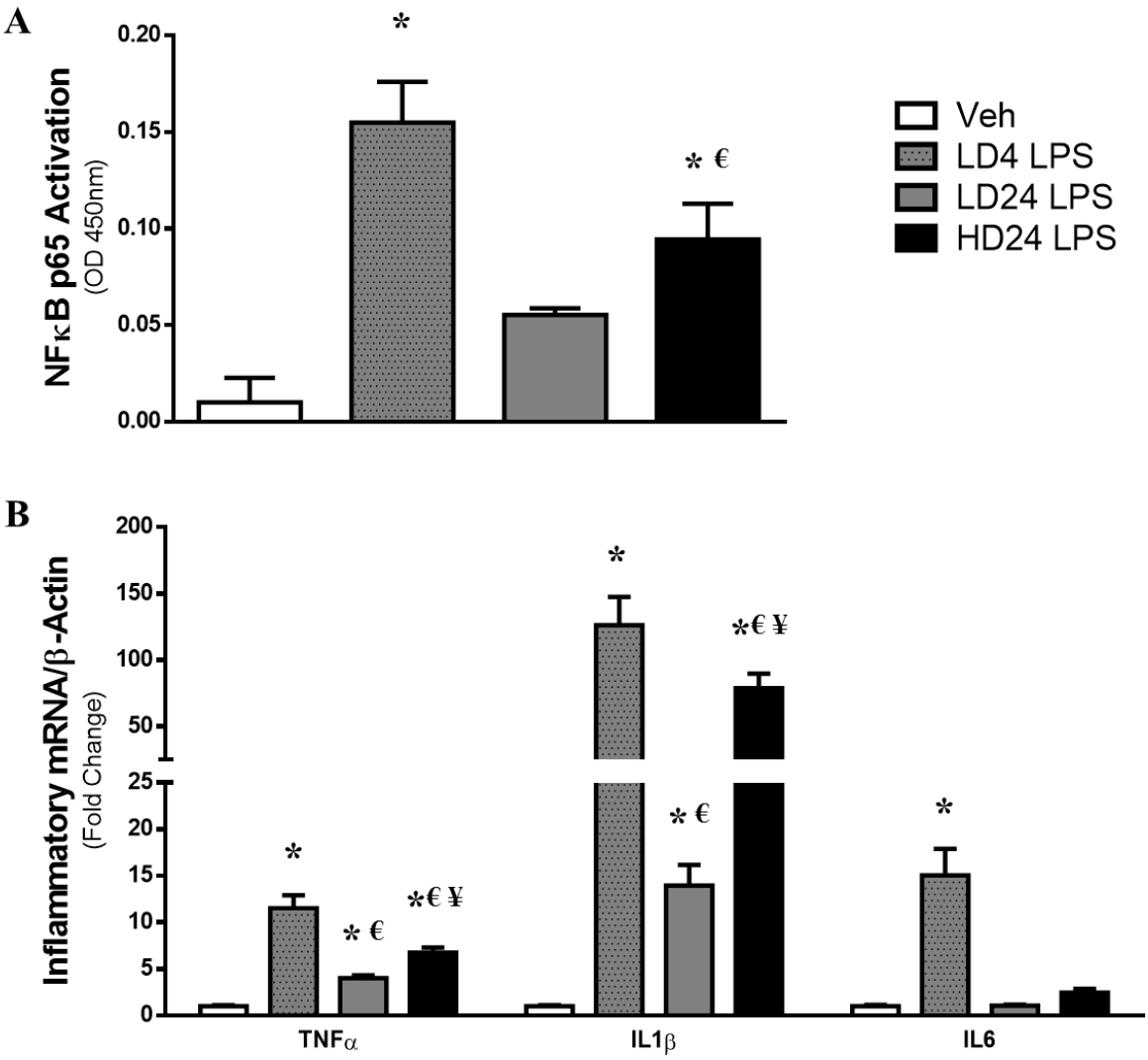
A
NFκB p65 Activation
(OD 450nm)
0.20
0.15
0.10
0.05
0.00
*
* €
Veh
LD4 LPS
LD24 LPS
HD24 LPS
B
Inflammatory mRNA/β-Actin
(Fold Change)
200
150
100
50
25
20
15
10
5
0
*
* €
*€ ¥
*
* €
*€ ¥
*
TNFα
IL1β
IL6

Figure 3.2 LPS-induces rapid time and does-dependent inflammatory response.

A, Quantified level of NFκB transactivation in the nuclear compartment of LV myofibers. LPS induced a rapid, time and dose-dependent increase in NFκB activation. B. Gene expression of targets under regulation of NFκB. LPS induced a rapid, time and dose-dependent increase in gene expression of targets known to be under direct regulation of NFκB. Data are represented as means ± SEM, N=3-6, * P<0.05 vs. Veh, € P<0.05 vs. LD4LPS, ¥ P<0.05 vs. LD24LPS

	Veh	0.5 mg/kg LPS			7.5 mg/kg LPS		
Age (weeks)	12.3 ± 2.2	10.5 ± 1.2			14.1 ± 1.0		
Body Weight (g)	322.3 ± 45.2	342.6 ± 29.3			314.3 ± 26.1		
		Baseline	**4 hour**	**24 hour**	**Baseline**	**4 hour**	**24 hour**
Left Ventricular Systolic Diameter (mm)	3.47 ± 0.8	3.83 ± 0.4	4.68 ± 0.8 *	3.43 ± 0.6	3.36 ± 0.5	3.97 ± 0.6*	3.55 ± 0.8
Left Ventricular Diastolic Diameter (mm)	7.66 ± 0.9	7.89 ± 0.8	7.38 ± 0.7	7.00 ± 0.7 *	7.43 ± 0.5	6.46 ± 0.6*	6.32 ± 1.0*
Heart Rate (bpm)	330.73 ± 38.9	375.32 ± 24.6	375.32 ± 18.6*	375.32 ± 21.4*	343.42 ± 46.4	394.75 ± 37.9*	393.07 ± 22.3*
Stroke Volume (uL)	264.12 ± 62.0	274.55 ± 59.9	186.45 ± 29.6*	208.55 ± 45.3*	245.95 ± 29.8	144.59 ± 28.7*	152.26 ± 45.6*
Wall Thickening (%)	75.05 ± 27.1	66.98 ± 22.7	28.95 ± 14.6 *	61.91 ± 15.7	75.47 ± 21.9	28.97 ± 14.3*	48.00 ± 12.7*

Table 3.1 *In vivo* cardiovascular changes induced by LPS

Echocardiography was preformed on rats under ansthesia before (baseline), 4 and 24 hours following administration of LPS. Two-way repeated measures (RM) ANOVA was found to be statistically significant. Data shown are mean ± SEM from M-mode images, N=3-6, * $P<0.05$ vs. Veh.

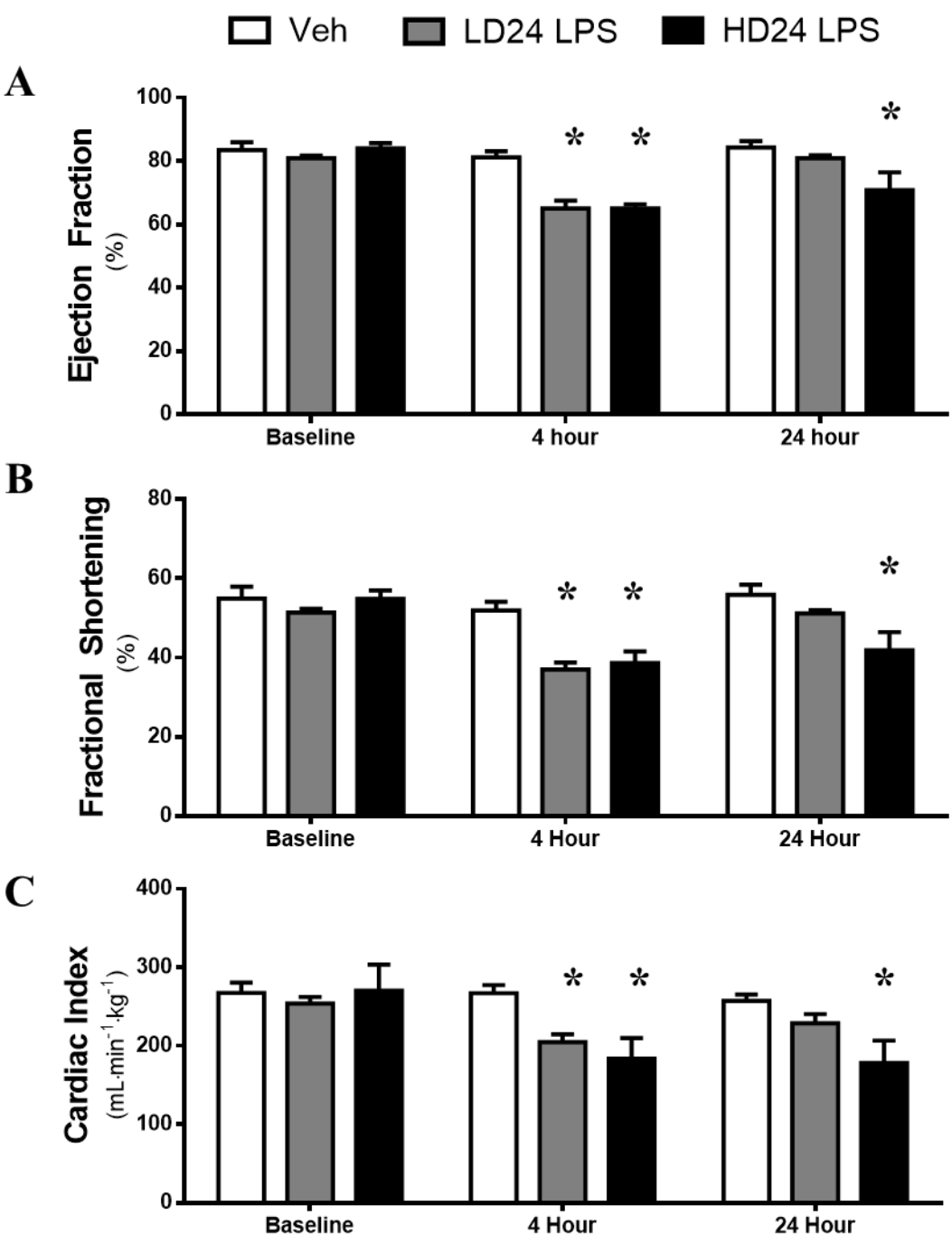
Veh
LD24 LPS
HD24 LPS
A
Ejection Fraction (%)
100
80
60
40
20
0
*
*
*
Baseline
4 hour
24 hour
B
Fractional Shortening (%)
80
60
40
20
0
*
*
*
Baseline
4 Hour
24 Hour
C
Cardiac Index (mL·min⁻¹·kg⁻¹)
400
300
200
100
0
*
*
*
Baseline
4 Hour
24 Hour

Figure 3.3 Effect of LPS administration of cardiovascular function *in vivo*

LPS-mediates a rapid reduction in ejection fraction (A), fractional shortening (B), and cardiac index (C) in anesthetized rats. Two-way repeated measures (RM) ANOVA was found to be statistically significant. Data shown are mean ± SEM from M-mode images, N=3-6, * $P<0.05$ vs. Veh

A

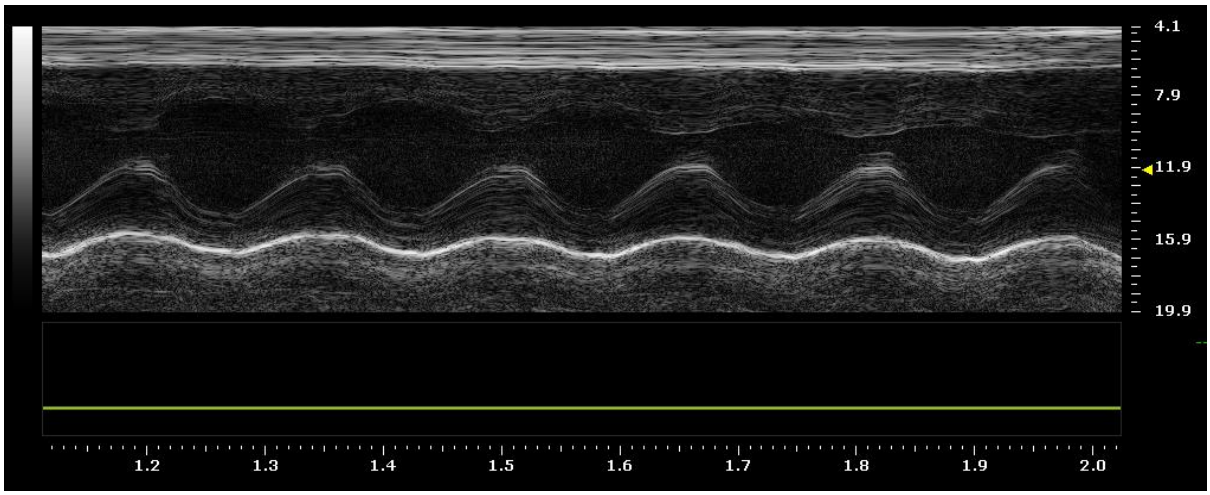
4.1
7.9
11.9
15.9
19.9
1.2
1.3
1.4
1.5
1.6
1.7
1.8
1.9
2.0

B

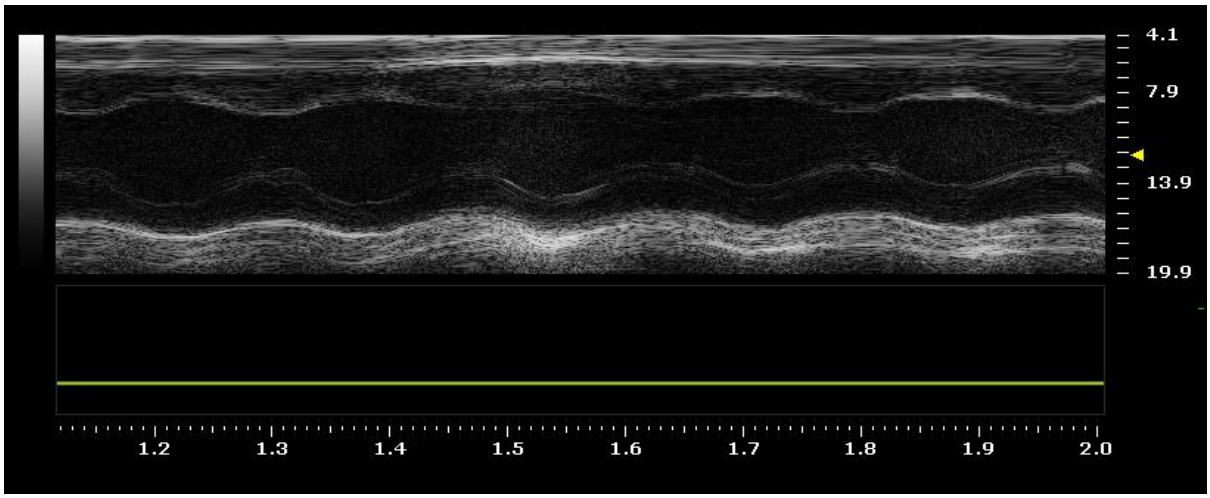
4.1
7.9
13.9
19.9
1.2
1.3
1.4
1.5
1.6
1.7
1.8
1.9
2.0

Figure 3.4 Representative M-mode echocardiography traces.

Representative m-mode echocardiography traces obtained using a Visualsonics Vevo 2100 ultrasound machine of a Veh (A) animal and a HD24LPS (B) animal four hours following the administration of LPS or Veh.

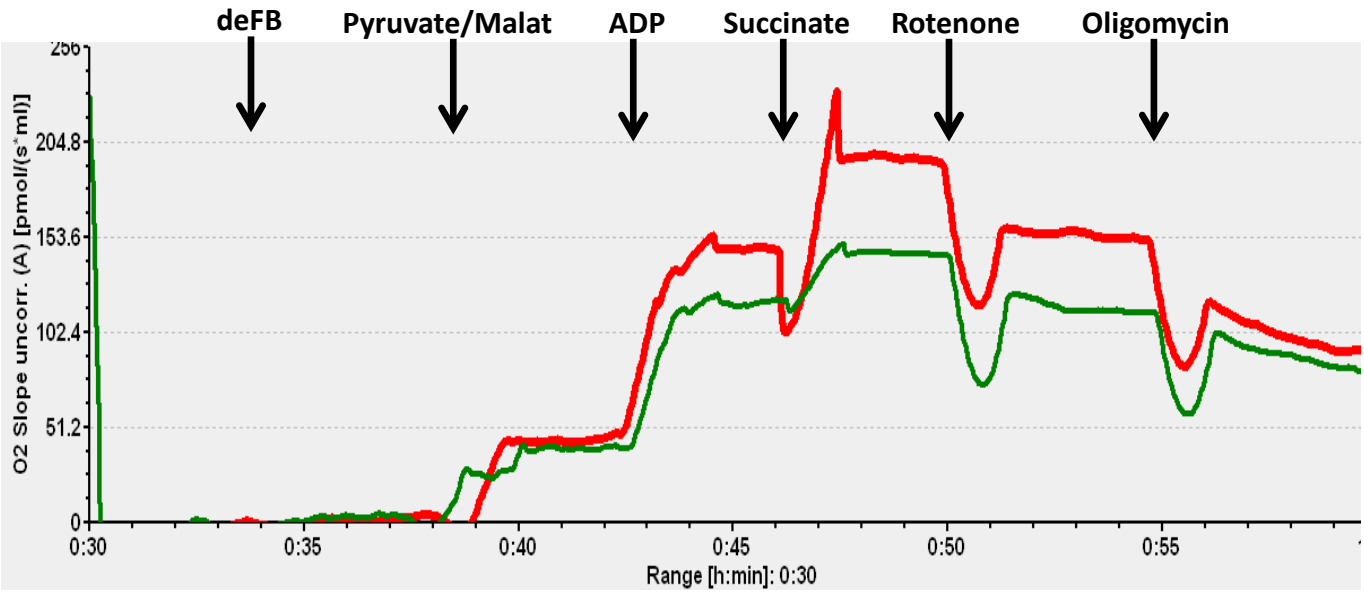
deFB
Pyruvate/Malat
ADP
Succinate
Rotenone
Oligomycin
O2 Slope uncorr. (A) [pmol/(s*ml)]
266
204.8
153.6
102.4
51.2
0
0:30
0:35
0:40
0:45
0:50
0:55
Range [h:min]: 0:30

Figure 3.5 Overlay of representative mO_2 traces

Representative raw trace of the rate of ADP-stimulated O_2 consumption over-laid to highlight the LPS-mediated decrease in mO_2 consumption in permeabilized LV myofibers from a Veh animal (red) and a HD24LPS animal (green) in response to substrates from the TCA cycle.

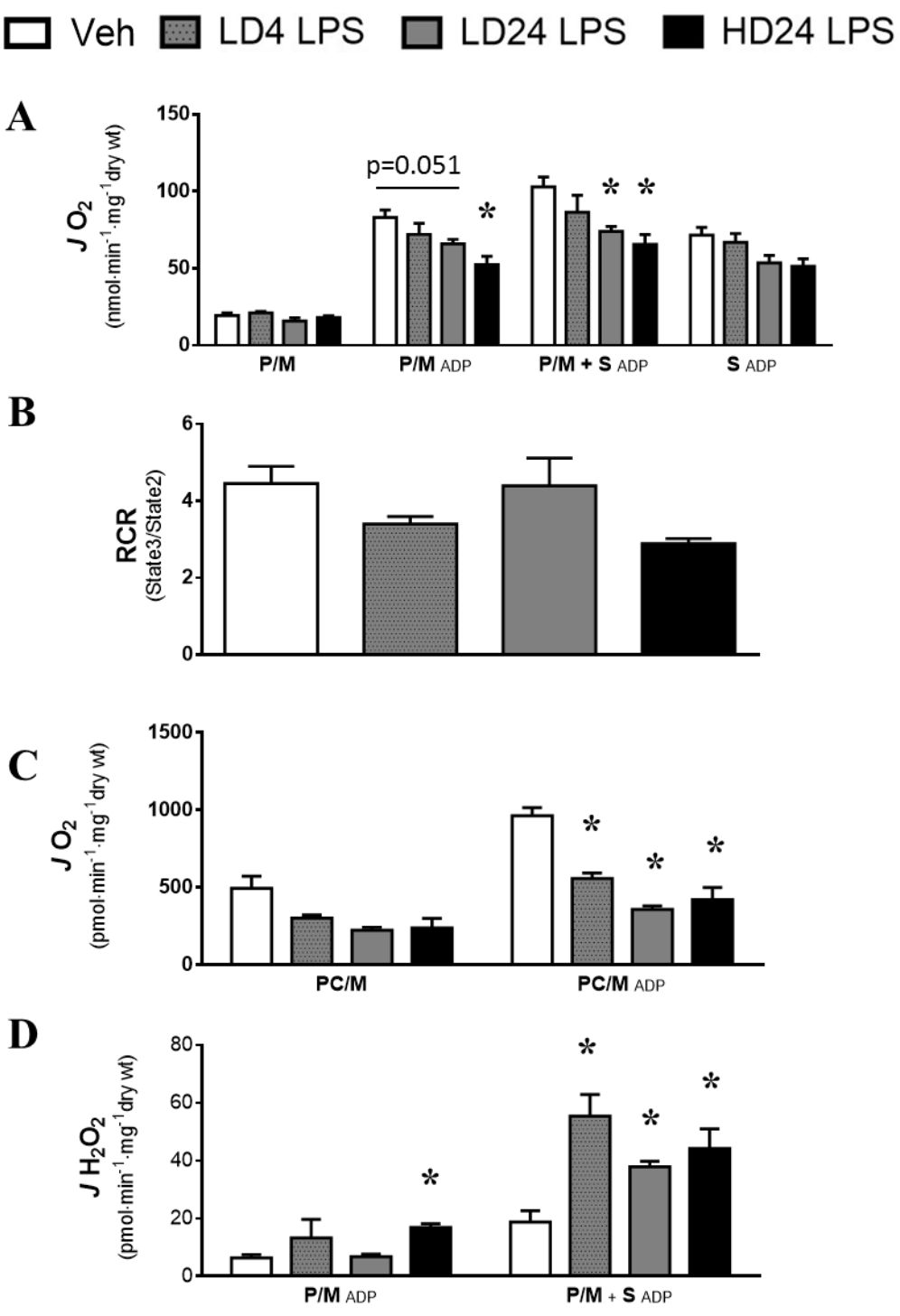
Veh
LD4 LPS
LD24 LPS
HD24 LPS
A
$J\,O_2$ (nmol·min^{-1}·mg^{-1}dry wt)
150
100
50
0
p=0.051
*
* *
P/M
P/M ADP
P/M + S ADP
S ADP
B
RCR (State3/State2)
6
4
2
0
C
$J\,O_2$ (pmol·min^{-1}·mg^{-1}dry wt)
1500
1000
500
0
*
*
*
PC/M
PC/M ADP
D
$J\,H_2O_2$ (pmol·min^{-1}·mg^{-1}dry wt)
80
60
40
20
0
*
*
*
*
P/M ADP
P/M + S ADP

Figure 3.6 LPS-mediates complex specific mitochondrial dysfunction

A, Quantified rates of pyruvate-supported respiration in permeabilized LV myofibers from Veh and LPS exposed rats. LPS administration decreased complex I driven mO_2. B, Calculated RCR shows no difference in mitochondrial coupling. C, Quantified rates of fatty-acid supported mO_2. D, Quantified rates of mitochondrial oxidant emitting potential during respiration supported by carbohydrate-based substrates. Data are expressed as means ± SEM, n=3=6, * $P<0.05$ vs. Veh

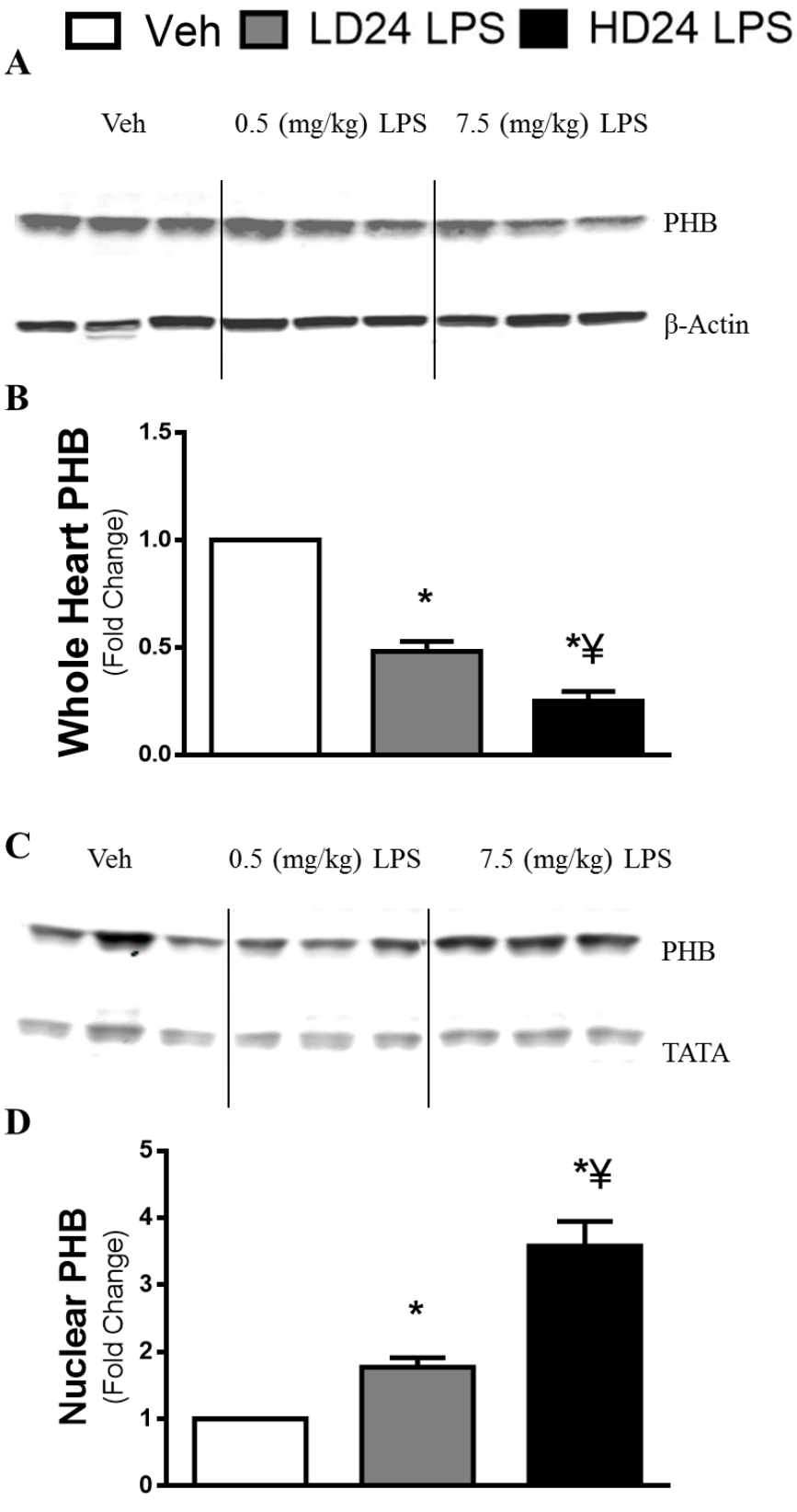
Veh
LD24 LPS
HD24 LPS
A
Veh
0.5 (mg/kg) LPS
7.5 (mg/kg) LPS
PHB
β-Actin
B
Whole Heart PHB
(Fold Change)
1.5
1.0
0.5
0.0
*
*¥
C
Veh
0.5 (mg/kg) LPS
7.5 (mg/kg) LPS
PHB
TATA
D
Nuclear PHB
(Fold Change)
5
4
3
2
1
0
*
*¥

Figure 3.7 LPS alters PHB expression and localization in LV muscle

Representative immunoblot (A) and fold-change quantified using relative density (B) of whole heart PHB expression normalized to β-Actin expression. Representative immunoblot (C) and fold-change quantified using relative density (D) of nuclear PHB expression normalized to TATA expression. Data are expressed as means ± SEM, n=3=6, * P<0.05 vs. Veh, ¥ P<0.05 vs. LD24LPS

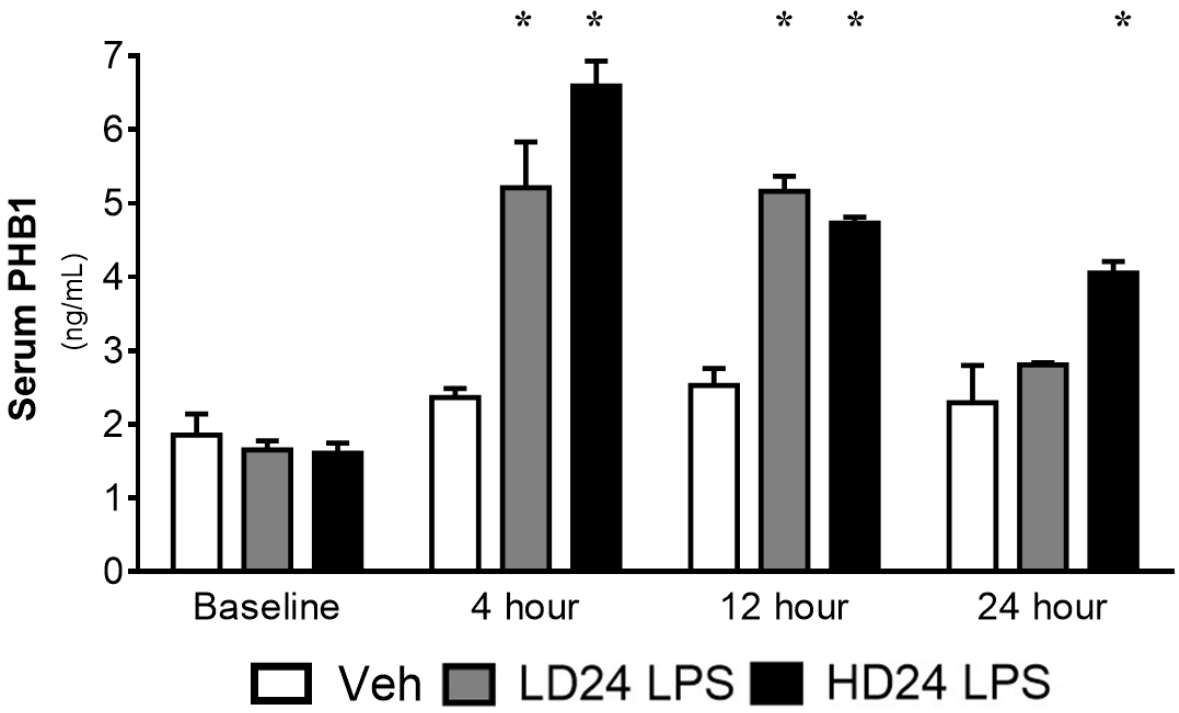
Serum PHB1
(ng/mL)
0
1
2
3
4
5
6
7
* * * * *
Baseline
4 hour
12 hour
24 hour
Veh
LD24 LPS
HD24 LPS

Figure 3.8 Effect of LPS administration on circulating levels of PHB

LPS administration caused a spike in circulating PHB expression. Two-way repeated measures (RM) ANOVA was found to be statistically significant. Data are expressed as means ± SEM, n=3=6, * $P<0.05$ vs. Veh

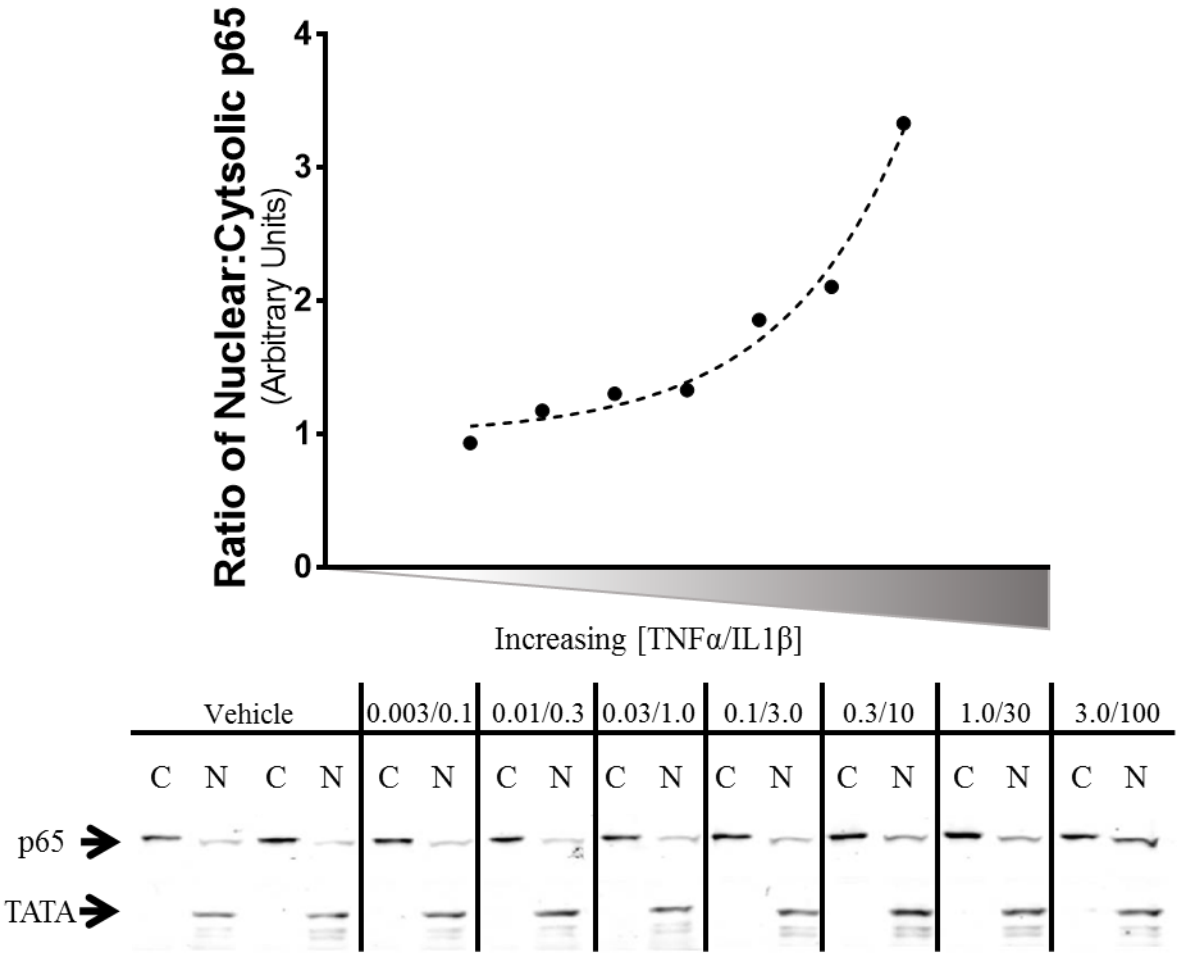
Ratio of Nuclear:Cytsolic p65
(Arbitrary Units)
4
3
2
1
0
Increasing [TNFα/IL1β]
Vehicle
0.003/0.1
0.01/0.3
0.03/1.0
0.1/3.0
0.3/10
1.0/30
3.0/100
C N C N C N C N C N C N C N C N C N
p65
TATA

Figure 3.9 TNFα/IL1β induced dose-dependent nuclear translocation of p65.

Ratio of the relative density of nuclear p65 to cytosolic 65 following exposure of HL1c to increasing concentration of a TNFα/IL1β cocktail for four hours. Increasing the dose of TNFα/IL1β resulted in a greater portion of nuclear p65. Data are expressed as means. These results are a composite of repeated experiments with each cytokine dose.

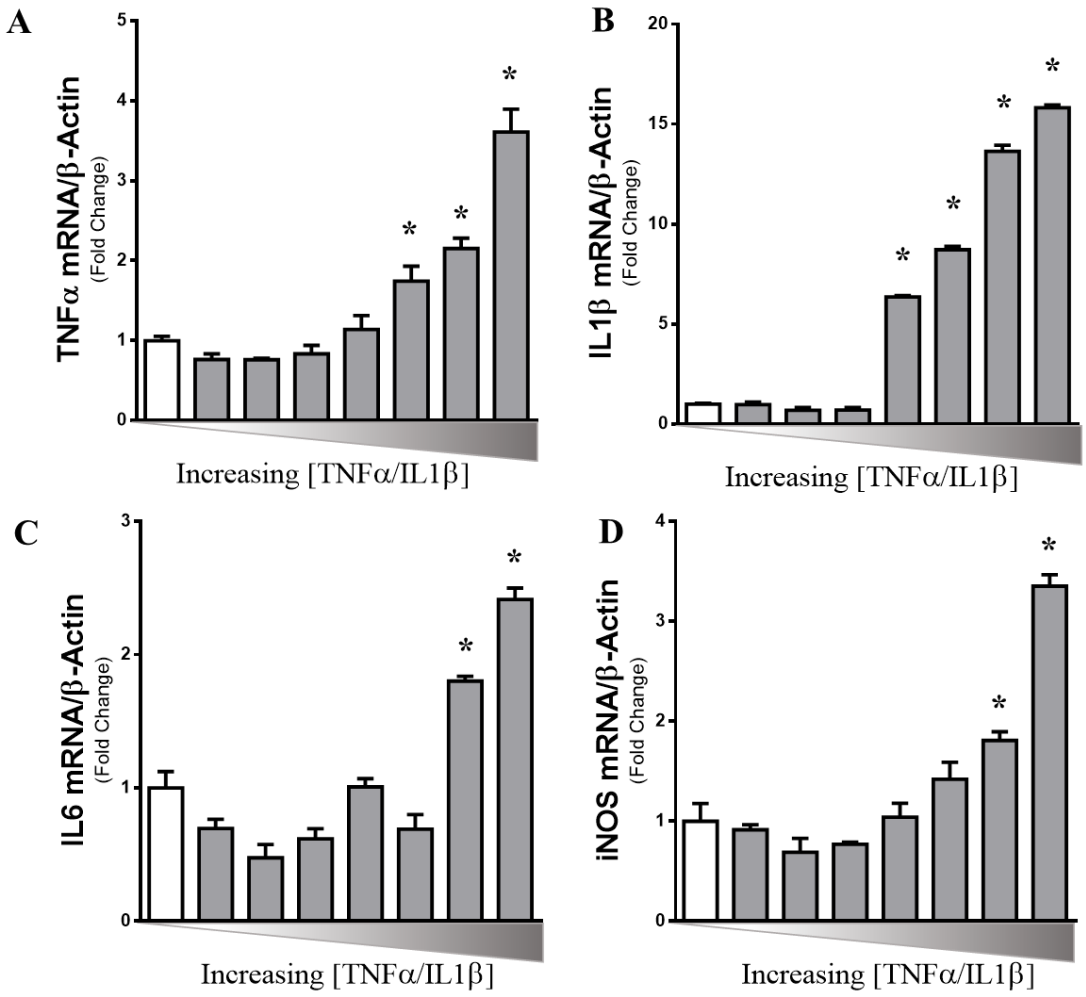
A
TNFα mRNA/β-Actin
(Fold Change)
Increasing [TNFα/IL1β]
B
IL1β mRNA/β-Actin
(Fold Change)
Increasing [TNFα/IL1β]
C
IL6 mRNA/β-Actin
(Fold Change)
Increasing [TNFα/IL1β]
D
iNOS mRNA/β-Actin
(Fold Change)
Increasing [TNFα/IL1β]

Figure 3.10 TNFα/IL1β induced increased transcription of NFκB target genes.

Real-time PCR analysis of targets downstream of NFκB activation in response to increasing doses of TNFα/IL1β. Increasing the dose of TNFα/IL1β resulted in increased gene expression of targets down stream of NFκB. The doses of TNFα and IL1β were 0.003/0.1, 0.01/0.3, 0.03/1.0, 0.1/3.0, 0.3/10, 1.0/30, 3.0/100 ng/mL. Data are expressed at means ± SEM, n=3, *P<0.05 vs. Veh.

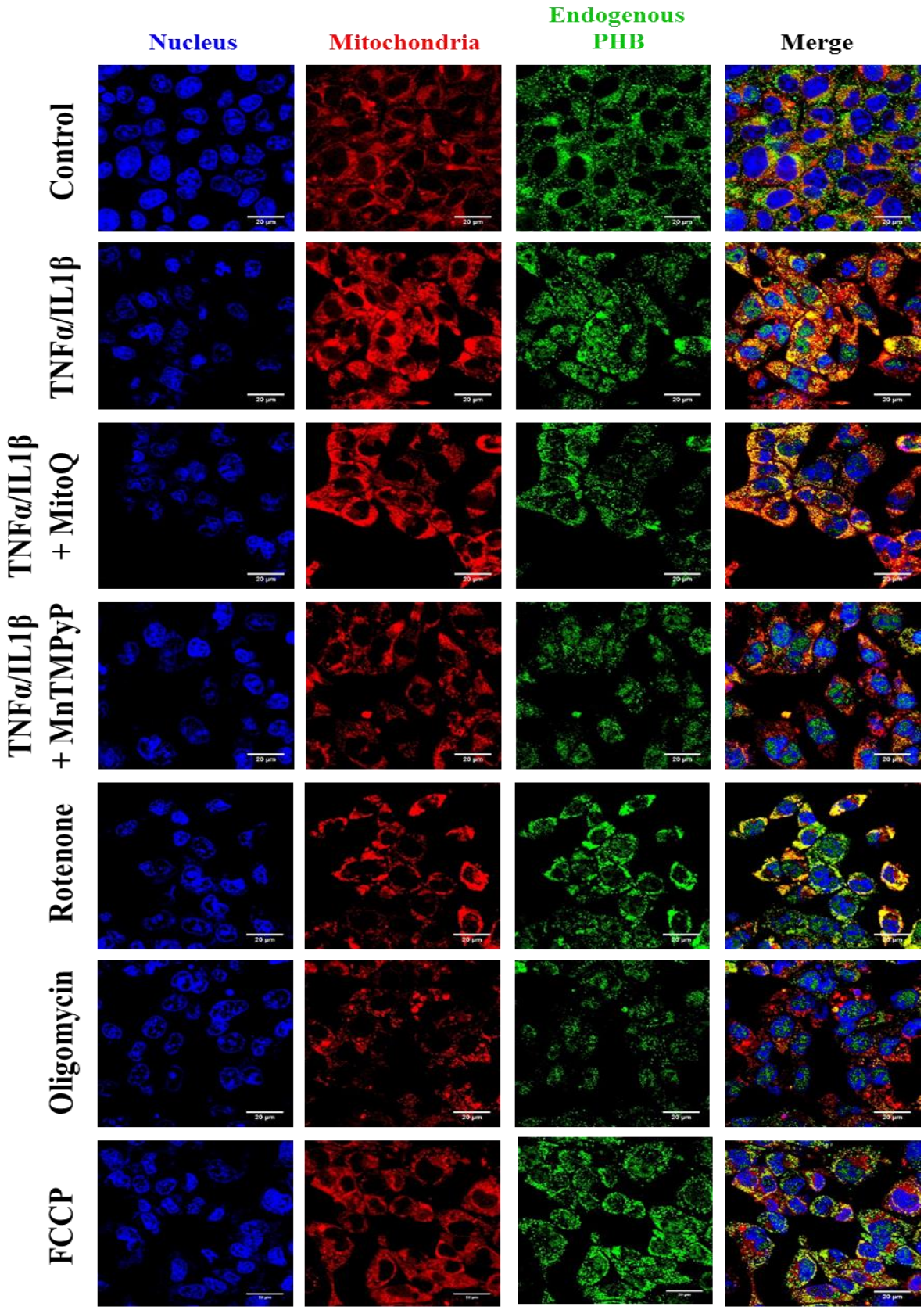
Nucleus
Mitochondria
Endogenous PHB
Merge
Control
TNFα/IL1β
TNFα/IL1β + MitoQ
TNFα/IL1β + MnTMPyP
Rotenone
Oligomycin
FCCP

Figure 3.11 Triggers of PHB nuclear translocation.

Representative confocal images demonstrating endogenous PHB localization in response to various stimuli. Draq5, blue nuclear stain, MitoTracker Red CMX, red mitochondrial stain, FITC, green endogenous PHB. 60X magnification, scale bars are 20μm.

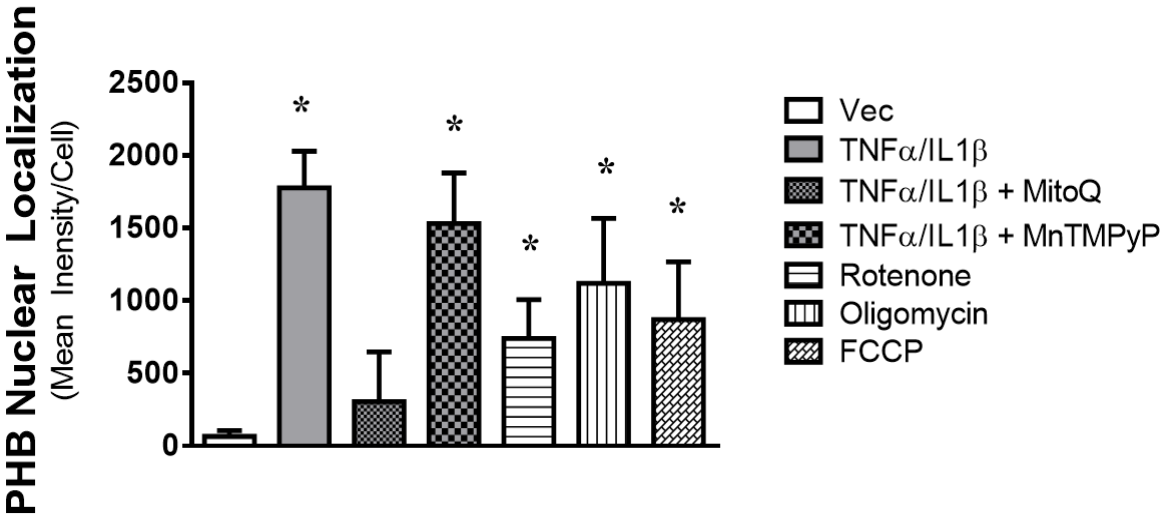
PHB Nuclear Localization
(Mean Inensity/Cell)
2500
2000
1500
1000
500
0
*
*
*
*
*
Vec
TNFα/IL1β
TNFα/IL1β + MitoQ
TNFα/IL1β + MnTMPyP
Rotenone
Oligomycin
FCCP

Figure 3.12 Fraction of nuclear localized PHB.

Quantified fraction of nuclear PHB localization using mean intensity per cell. Mitochondrial derived ROS and MIM depolarization appear to be a trigger for PHB nuclear translocation. Data are expressed at means ± SEM. N=25-30, *P<0.05 vs. Vec

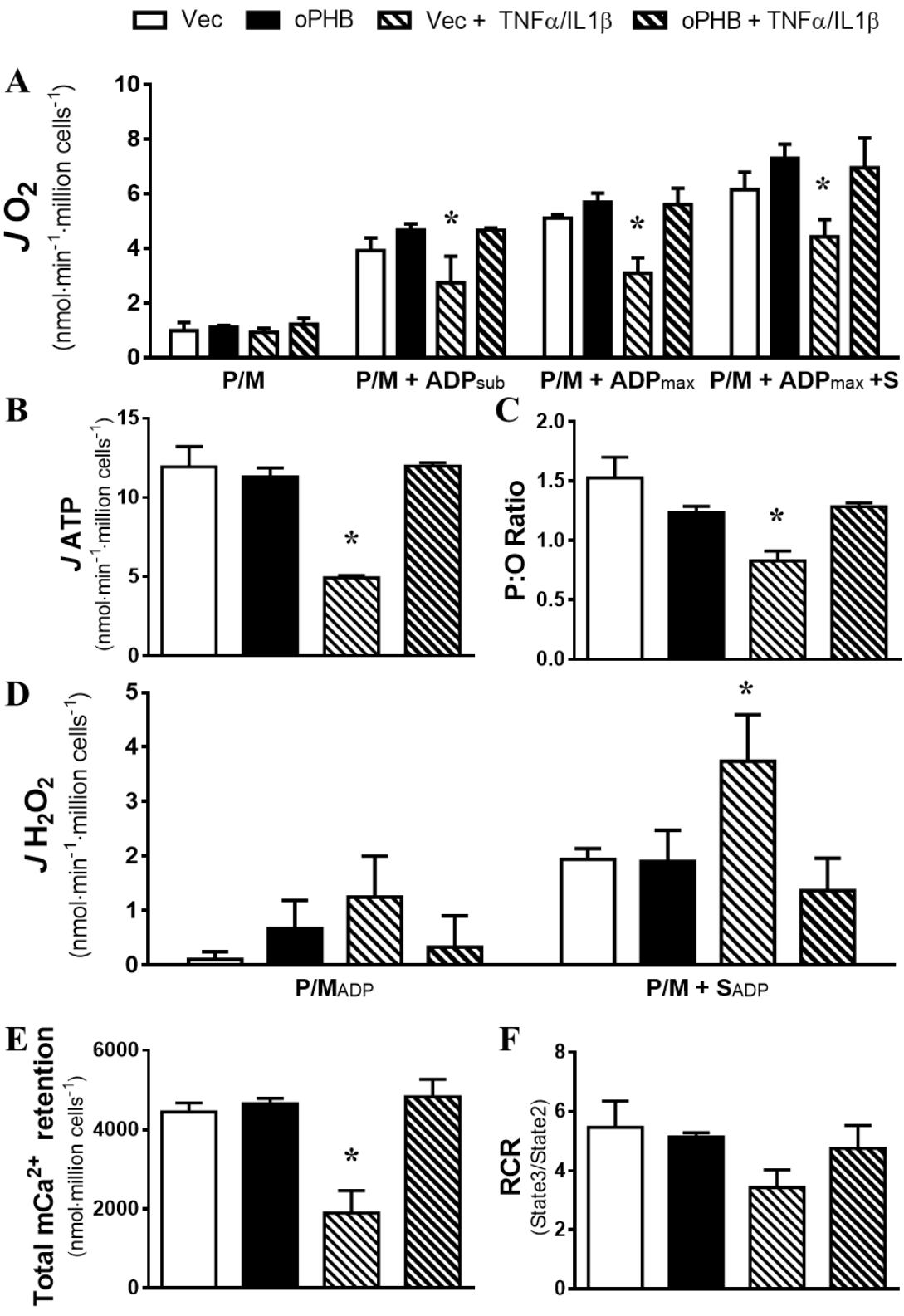
Vec
oPHB
Vec + TNFα/IL1β
oPHB + TNFα/IL1β
A
J O2
(nmol·min-1·million cells-1)
P/M
P/M + ADPsub
P/M + ADPmax
P/M + ADPmax +S
B
J ATP
(nmol·min-1·million cells-1)
C
P:O Ratio
D
J H2O2
(nmol·min-1·million cells-1)
P/MADP
P/M + SADP
E
Total mCa2+ retention
(nmol·million cells-1)
F
RCR
(State3/State2)

Figure 3.13 oPHB preserves mitochondrial function following TNFα/IL1β inflammatory insult. A, Quantified rates of pyruvate-supported respiration in permeabilized Vec and oPHB transfected HL1c in the presence and absence of TNFα/IL1β. B, ATP generation was driven by a progressive titration of ADP (B shown 500μM ADP) and peaked between 200μM and 1mM ADP. Measurements of respiratory capacity and ATP generation allow us to calculate the P:O ratio, which is a measure of the efficiency of OxPHOS (C). D, Quantified rates of mitochondrial oxidant emitting potential during respiration supported by carbohydrate-based substrates. E, Quantified amount of total mitochondrial Ca^{2+} retained before opening of mitochondrial permeability transition pore (mPTP). F, Calculated RCR shows no difference in mitochondrial coupling Data are expressed as means ± SEM, n=3=6, * $P<0.05$ vs. Veh

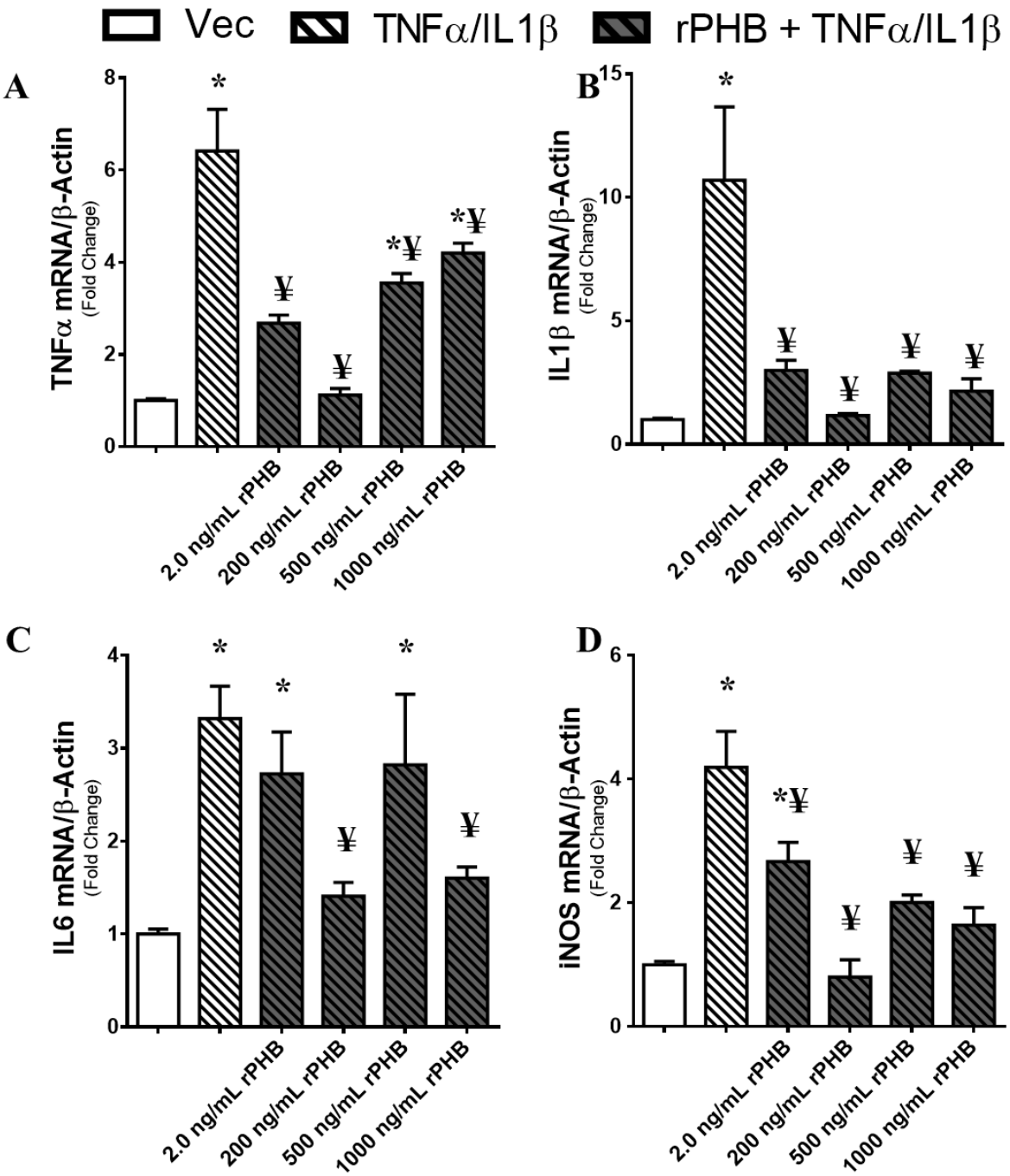
Vec
TNFα/IL1β
rPHB + TNFα/IL1β
A
TNFα mRNA/β-Actin
(Fold Change)
B
IL1β mRNA/β-Actin
(Fold Change)
C
IL6 mRNA/β-Actin
(Fold Change)
D
iNOS mRNA/β-Actin
(Fold Change)
2.0 ng/mL rPHB
200 ng/mL rPHB
500 ng/mL rPHB
1000 ng/mL rPHB

Figure 3.14 rPHB effects TNFα/IL1β-induced up-regulation of NFκB target gene expression

rPHB has varying effects on quantified gene expression of NFκB targets following activation with TNFα/IL1β. Data are expressed at means ± SEM, n=4-6, *P<0.05 vs. Vec, ¥P<0.05 vs. TNFα/IL1β

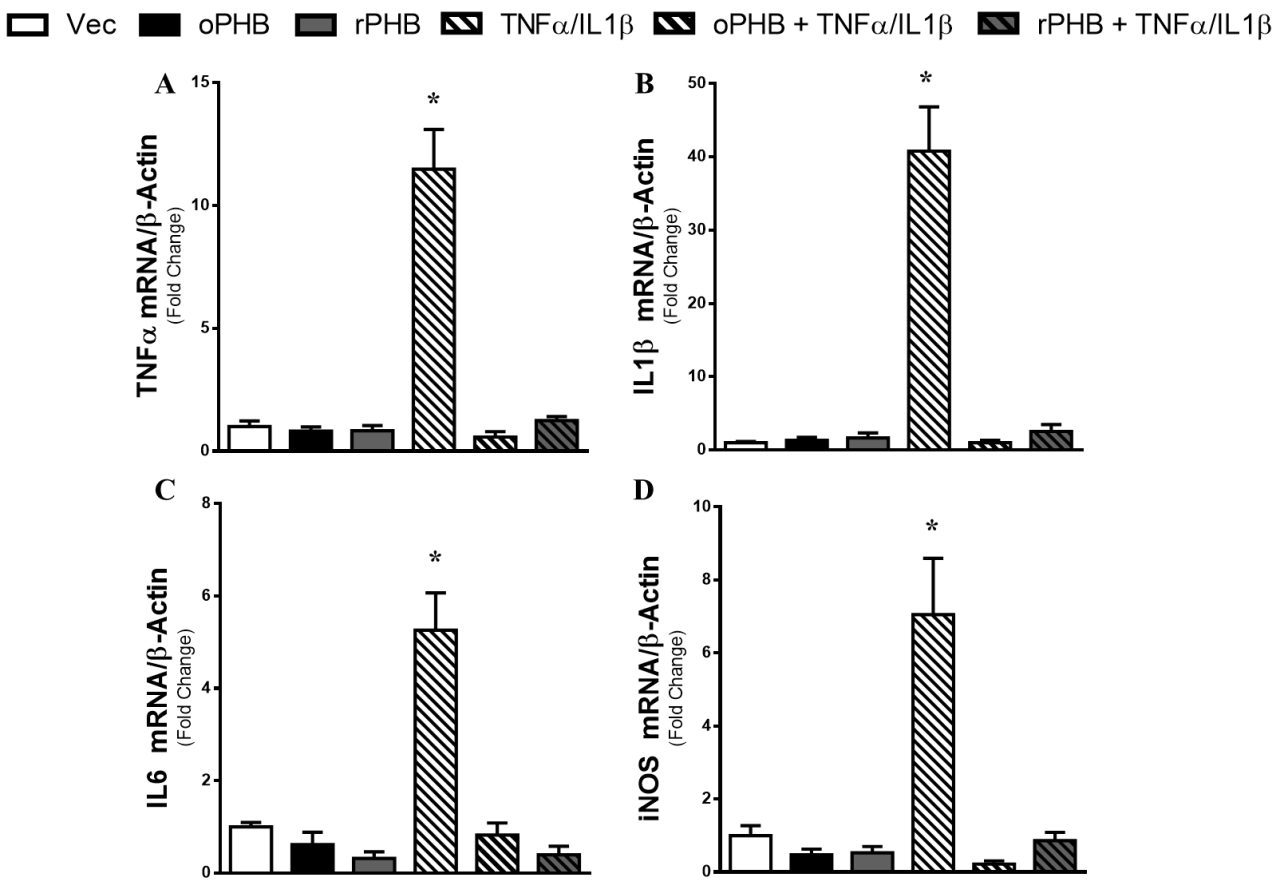
Vec
oPHB
rPHB
TNFα/IL1β
oPHB + TNFα/IL1β
rPHB + TNFα/IL1β
A
TNFα mRNA/β-Actin
(Fold Change)
B
IL1β mRNA/β-Actin
(Fold Change)
C
IL6 mRNA/β-Actin
(Fold Change)
D
iNOS mRNA/β-Actin
(Fold Change)
*

Figure 3.15 rPHB and oPHB attenuate NFκB driven gene expression

rPHB and oPHB attenuate quantified gene expression of NFκB targets following exposure to TNFα/IL1β for three hours. Data are expressed at means ± SEM, n=6, *P<0.05 vs. Vec, ¥P<0.05 vs. TNFα/IL1β

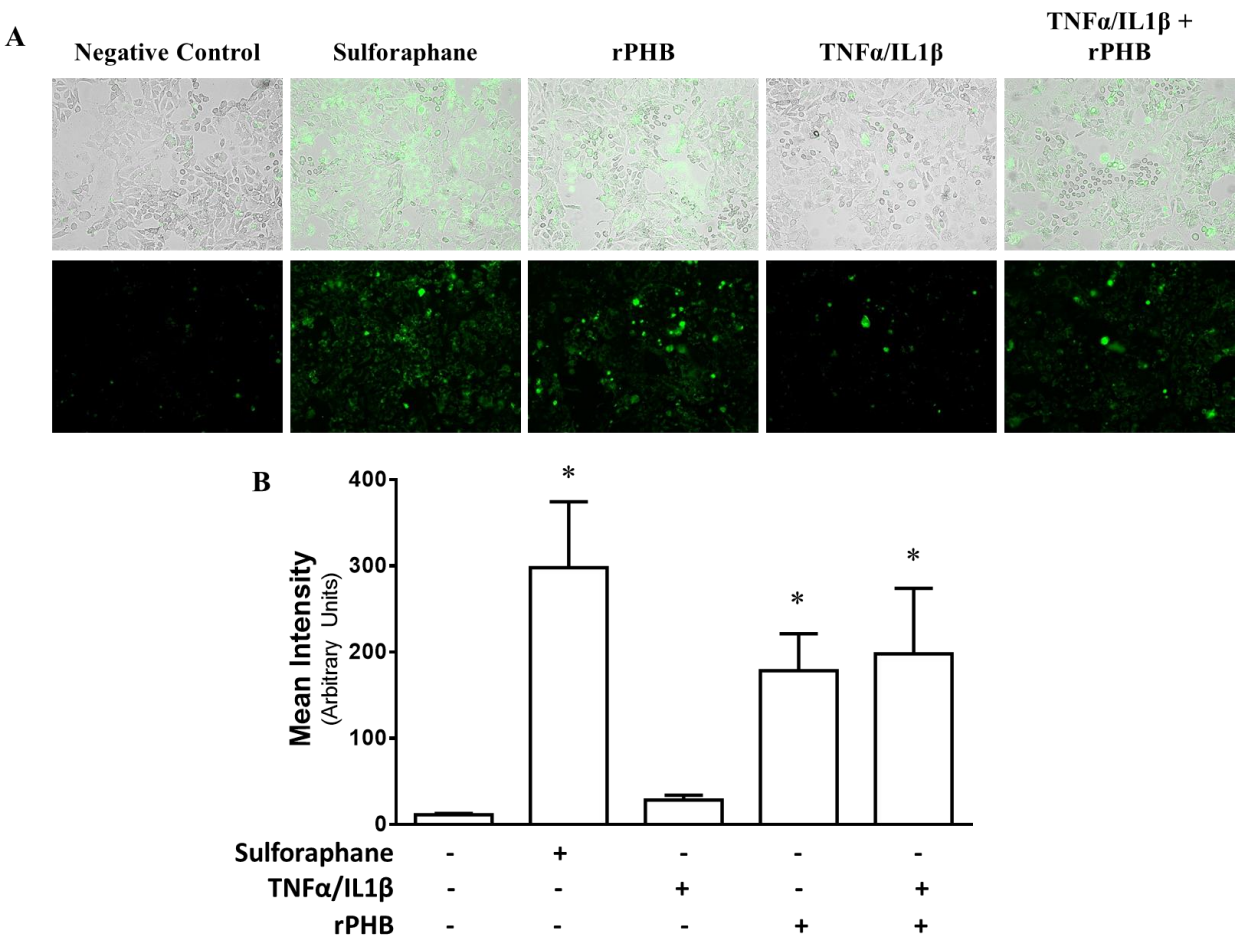
A
Negative Control
Sulforaphane
rPHB
TNFα/IL1β
TNFα/IL1β + rPHB
B
Mean Intensity
(Arbitrary Units)
400
300
200
100
0
*
*
*
Sulforaphane - + - - -
TNFα/IL1β - - + - +
rPHB - - - + +

Figure 3.16 rPHB activates the antioxidant response element (ARE).

A, Representative bright field and ARE driven GFP fluorescent images. Scale bars are 200μm. B, Quantified mean GFP fluorescent intensity. rPHB drives activation of the ARE in the presence and absence of TNFα/IL1β. Data expressed at means ± SEM. N=6, *P<0.05 vs ARE Only

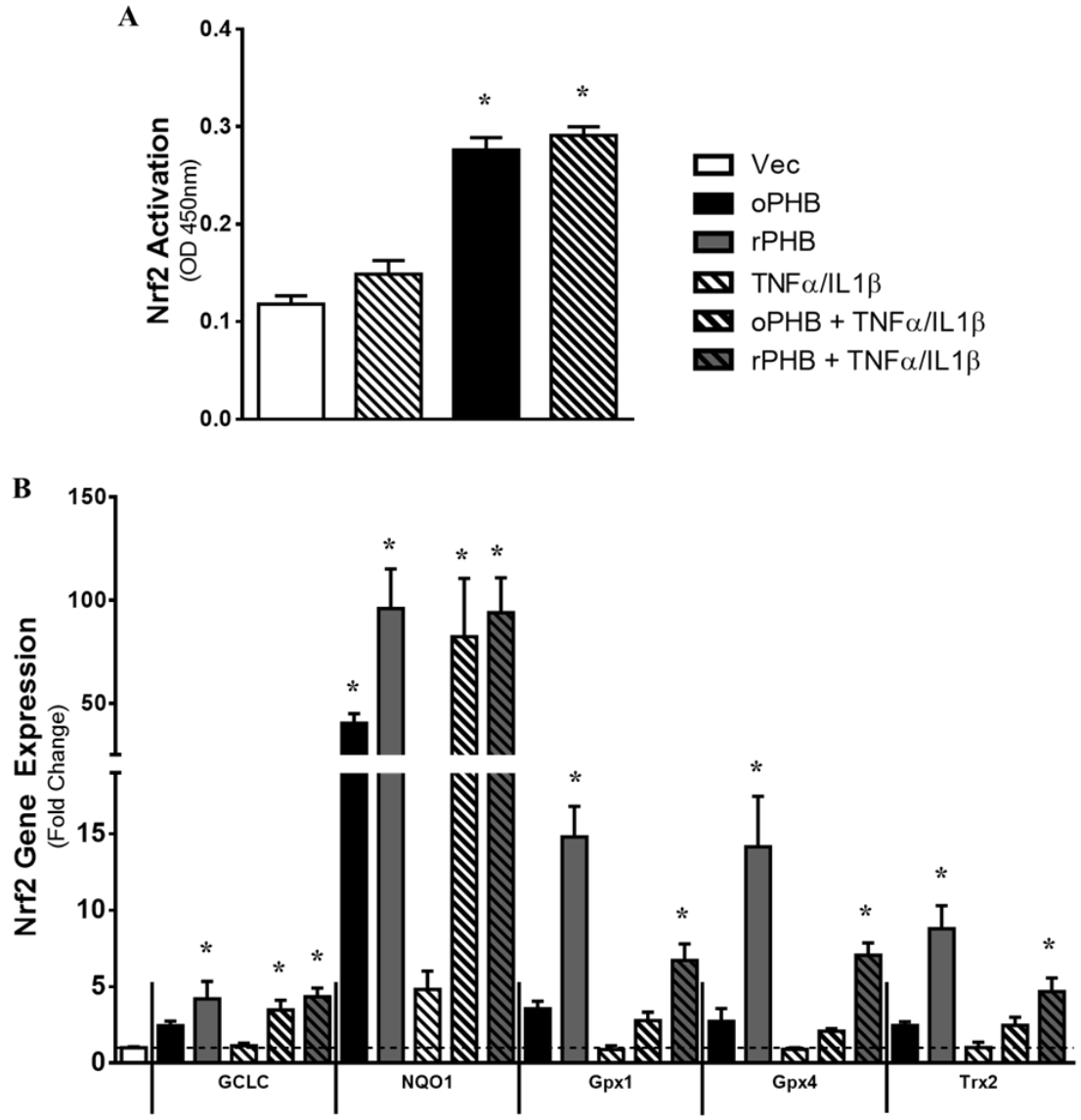
A
Nrf2 Activation
(OD 450nm)
0.4
0.3
0.2
0.1
0.0
Vec
oPHB
rPHB
TNFα/IL1β
oPHB + TNFα/IL1β
rPHB + TNFα/IL1β
B
Nrf2 Gene Expression
(Fold Change)
150
100
50
15
10
5
0
GCLC
NQO1
Gpx1
Gpx4
Trx2

Figure 3.17 PHB activates Nrf2 to increased gene transcription.

A, Quantified level of Nrf2 transactivation in the nuclear compartment of HL1c. oPHB induced increase in Nfr2 activation. B, Quantified gene expression of Nrf2 targets with rPHB treatment and oPHB in the presence and absence of TNFα/IL1β induced inflammatory stress. Data are expressed as means ± SEM. N=6-7, *P<0.05 vs. Vec

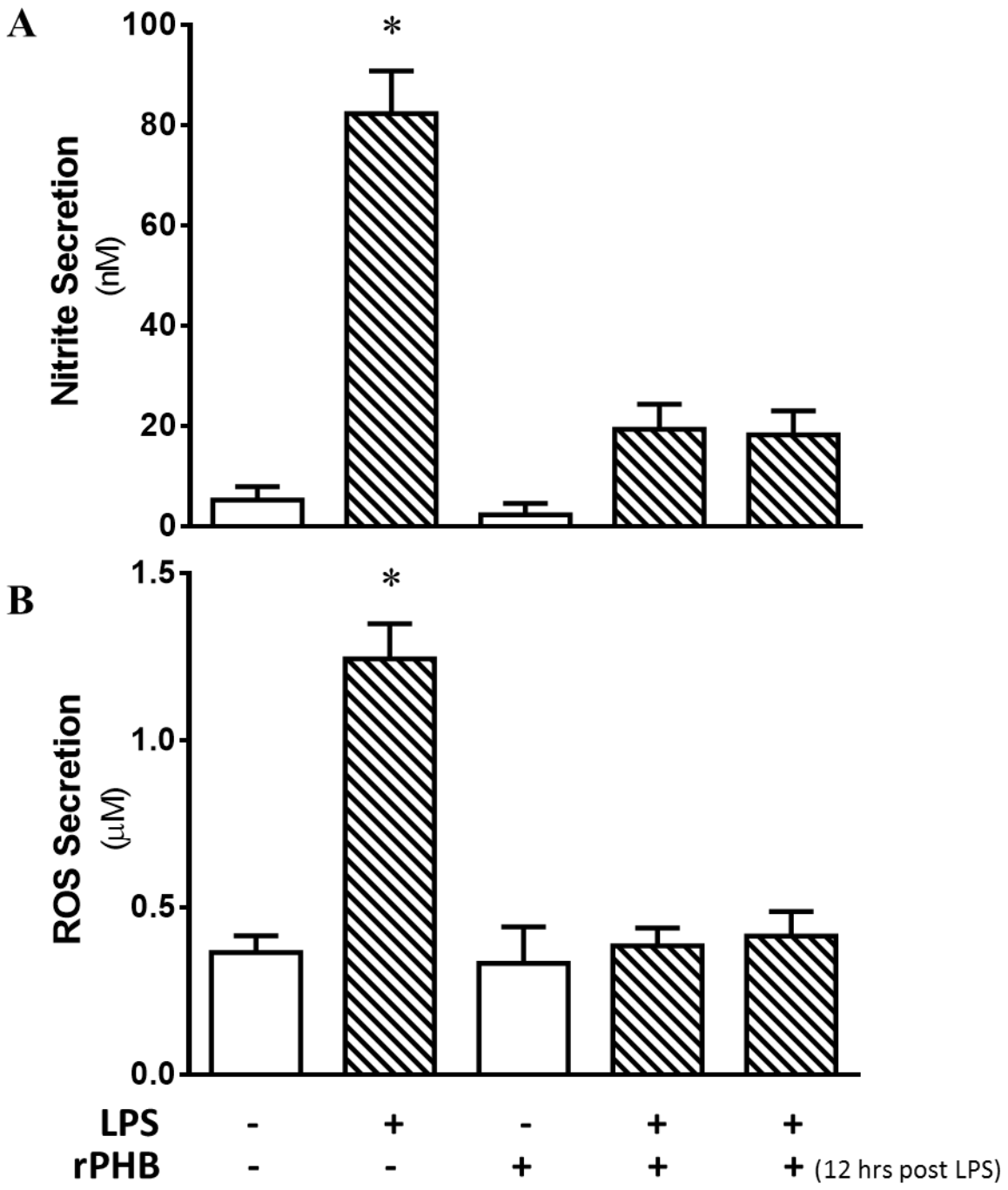
A
100
80
60
40
20
0
Nitrite Secretion
(nM)
*
B
1.5
1.0
0.5
0.0
ROS Secretion
(μM)
*
LPS - + - + +
rPHB - - + + + (12 hrs post LPS)

Figure 3.18 rPHB treatment suppresses LPS-activation of macrophage.

A, Concomitant and post-endotoxin rPHB treatment abolished NO secretion by LPS-activated RAW 264.7 macrophages. B, Concomitant and post-endotoxin rPHB treatment abolished ROS secretion by LPS-activated RAW 264.7 macrophages. Data are expressed as means ± SEM, N=8-16, * $P<0.05$ vs. Control.

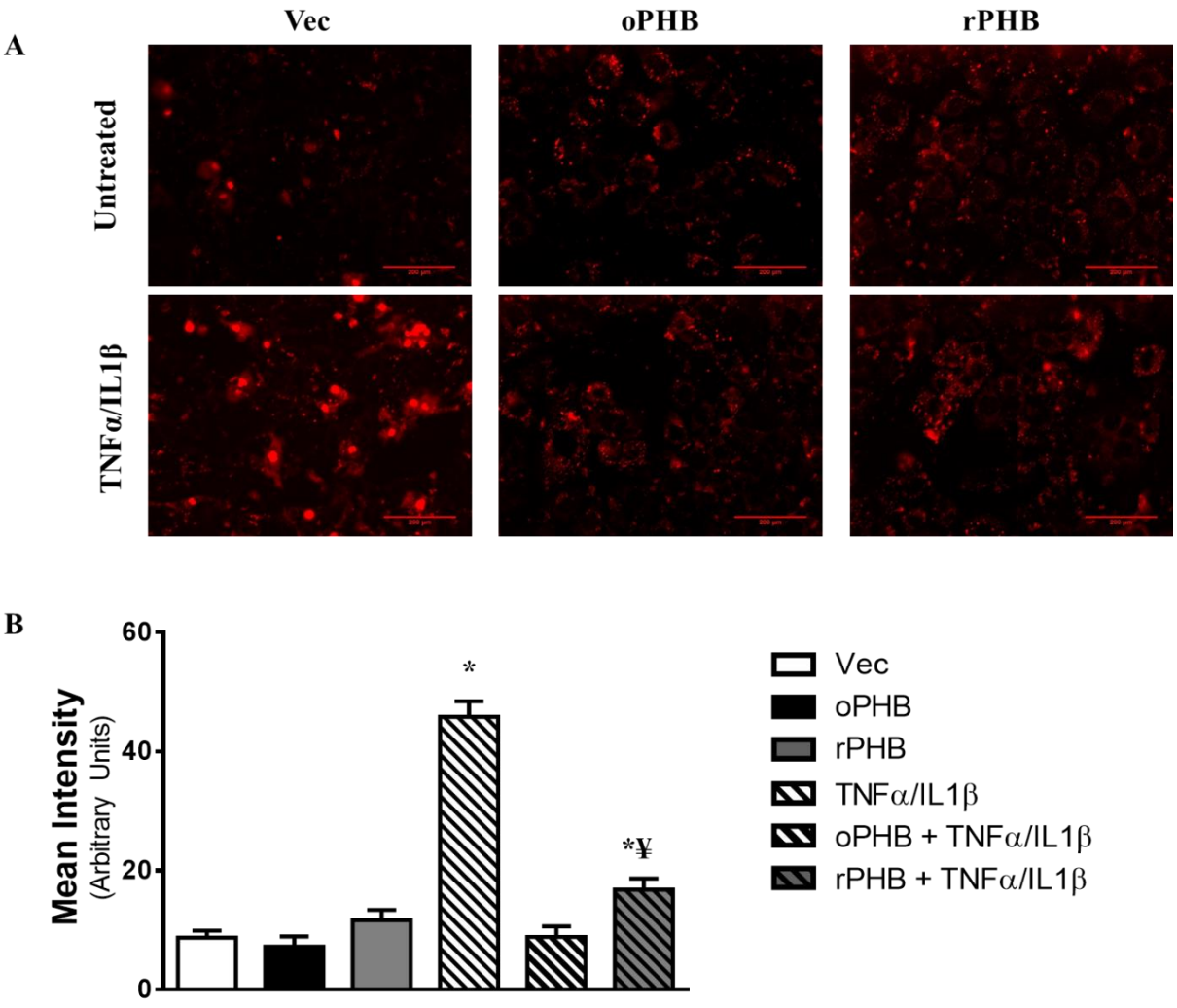
A
Vec
oPHB
rPHB
Untreated
TNFα/IL1β
B
Mean Intensity
(Arbitrary Units)
60
40
20
0
*
*¥
Vec
oPHB
rPHB
TNFα/IL1β
oPHB + TNFα/IL1β
rPHB + TNFα/IL1β

Figure 3.19 PHB abolishes TNFα/IL1β induced oxidative stress.

A, Representative images of MitoSox™ Red staining in HL1c with and without six hours of TNFα/IL1β treatment. Scale bars are 200μm. B, Quantified mean MitoSox™ Red fluorescent intensity. oPHB abolishes the TNFα/IL1β-mediated increase in oxidative stress as measured by MitoSox™ Red staining. rPHB attenuates TNFα/IL1β induced oxidative stress. Data expressed at means ± SEM. N=6, *P<0.05 vs Vec, ¥ P<0.05 vs. TNFα/IL1β.

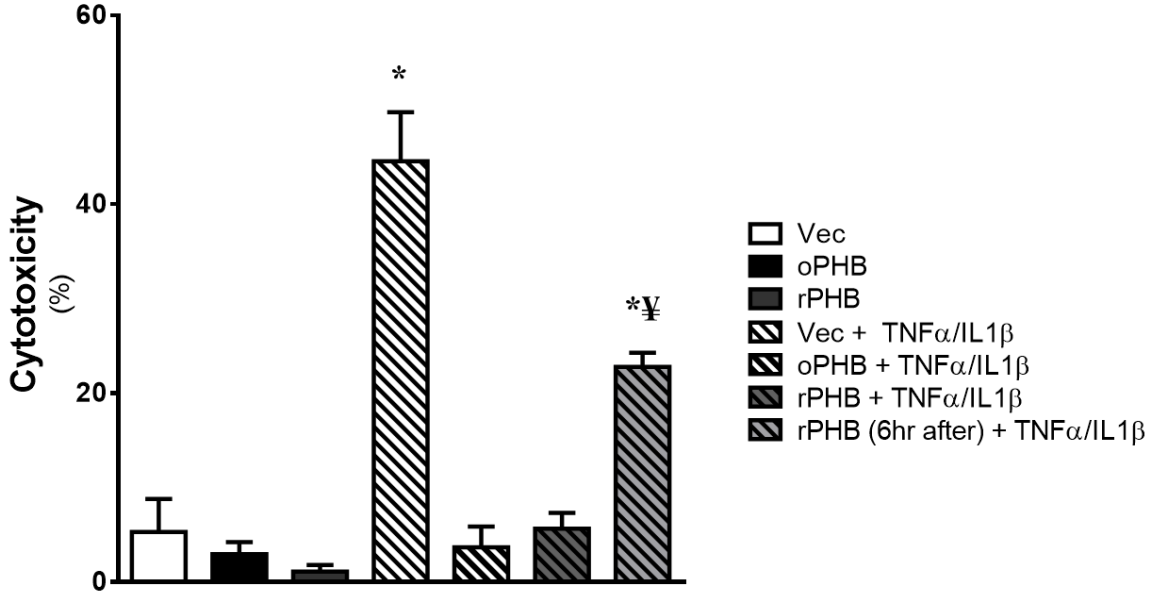
60
40
20
0
Cytotoxicity
(%)
*
*¥
Vec
oPHB
rPHB
Vec + TNFα/IL1β
oPHB + TNFα/IL1β
rPHB + TNFα/IL1β
rPHB (6hr after) + TNFα/IL1β

Figure 3.20 1 PHB prevents TNFα/IL1β induced cell death.

Percent cell death quantified using lactate dehydrogenase assay. HL1c are treated for 24 hours with TNFα/IL1β. oPHB and pretreatment with rPHB completely abolish TNFα/IL1β induced cell death. Treating cell with rPHB 6 hours after the exposure to TNFα/IL1β attenuates cell death. Data are expressed at means ± SEM. N=4-6, * $P<0.05$ vs. Vec, ¥ $P<0.05$ vs. TNFα/IL1β

CHAPTER FOUR – Recombinant PHB treatment attenuates LPS-induced systemic inflammation and cardiomyopathy.

Sepsis is characterized by the excessive production of inflammatory cytokines leading to alterations in cardiac mitochondria and collapse in cardiac function. Currently there are no therapies to prevent sepsis-induced cardiomyopathy. In the experiments described in the preceding chapter we described how PHB induces a broad anti-inflammatory/antioxidant response in macrophages and cardiomyocytes, while also preserving mitochondrial function during exposure to elevated cytokines in cardiomyocytes. Here, we moved to an *in vivo* model and tested the hypothesis that cytokine generation and inflammatory signaling induced by LPS challenge would be suppressed by rPHB treatment, mediated by Nrf2, leading to protection of cardiac mitochondria and recovery of cardiac function.

4.1 Study Design

C57 Black 6 (C57B/6) mice from Charles River Laboratory and Nrf2KO mice (a kind gift from Dr. Thomas Kensler) were used in this study to test the hypothesis that rPHB confers cardioprotection by attenuating inflammatory signaling and cytokine production during endotoxic shock induced by LPS challenge. Animals' ages and weights can be found in Table 4.1 Mice were randomly assigned to one of the following experimental groups: 1) WT Vehicle 2) WT rPHB Only 3) WT LPS Only 4)WT rPHB+LPS 5) Nrf2KO Vehicle 6) Nrf2KO LPS Only or 7) Nrf2KO rPHB+LPS. Once assigned, mice were given a minimum of five days to acclimate to the animal facility. A schematic representation of the experimental timeline can be found in figure 4.1 Baseline echocardiograms were recorded immediately prior LPS or Veh injection (all echocardiograms were recorded under anesthesia). LPS (12 mg/kg), resuspendend in 5% dextrose water, was given IP to animals in groups 3, 4, 6, and 7, while animals in groups 1, 2,

and 5 received an IP injection of 5% dextrose water. Two hours following the LPS or Veh injection, animals in groups 2, 4, and 7 received their first of three IP injection of 200 ng/mL rPHB (the amount of rPHB given was adjusted based off the animals estimated circulating blood volume (NC3Rs)) the subsequent rPHB injections were given at 8 hours and 14 hours post LPS injection. Animals in the remaining groups were given IP injections of saline along the same timeline described for rPHB injections. Echocardiograms were taken at 4, 8 and 14 hours post LPS/Veh injection (for the 8 and 14 hour time points' rPHB or Sal was given after the completion of the echocardiogram). Animals were euthanized at 16 hours post LPS/Veh injection using a sublethal dose of ketamine/xylazine followed by exsanguination and decapitation. Critical organs were immediately dissected and processed according to procedures described thoroughly in Chapter 2.

4.2 rPHB attenuated LPS-induced inflammation *in vivo*

To determine whether LPS caused changes in PHB expression and localization, we examined whole heart and nuclear PHB levels via western blotting. In contrast to what we saw in the rats and HL1c, LPS caused no significant change in whole heart or nuclear PHB expression (data not shown). However, similar to what we saw in the rats, LPS caused a sharp increase in circulating PHB (Figure 4.2). There was no difference between the circulating levels of PHB in the WT-Veh and Nrf2KO-Veh animals. Four hours following LPS exposure, circulating levels of PHB were elevated 8-fold in WT-LPS and WT-rPHB+LPS animals. Mice receiving rPHB alone also had substantially higher serum PHB. To our surprise, LPS had no effect on serum PHB levels in Nrf2KO animals at 4 hours following LPS exposure (Figure 4.2). Interestingly though, 16 hours following LPS exposure all groups, including the Nrf2KO mice,

showed a significant increase in serum PHB levels. These data suggest that Nrf2 may be critical for the early release of PHB into circulation.

Inflammation is a major component of sepsis and suppression of the inflammatory response has been proposed as a therapeutic approach. Here we sought to determine whether rPHB treatment suppressed LPS driven systemic inflammation *in vivo* by measuring levels of circulating proinflammatory cytokines IL6 and TNFα following LPS +/- rPHB injection. LPS caused a dramatic increase in these cytokines in both WT and Nrf2KO mice (Figure 4.3A). rPHB treatment in WT mice two hours after LPS challenge attenuated the LPS-induced spike in serum IL6 at 4 hours post-LPS challenge. However, rPHB had no effect on circulating IL6 levels in Nrf2KO mice (Figure 4.3A) at 4 hours post-LPS challenge. Similarly, the level of circulating TNFα in Veh animals was below the detection level while, rPHB only and Nrf2KO Veh animals had serum TNFα levels below 100 pg/mL (Figure 4.3B). LPS treatment increased the circulating levels of TNFα to nearly 1,000 pg/mL in WT mice and 800 pg/mL in Nrf2KO mice. rPHB treatment in WT mice attenuated the spike in serum TNFα level in response to LPS. Interestingly, rPHB caused a greater reduction in circulating TNFα levels in Nrf2KO mice than in WT mice, while the effect on TNFα appears to be independent of Nrf2.

Echocardiography has been commonly used to characterize sepsis-related cardiac dysfunction (Ramana et al., 2006; Zang et al., 2012; Drosatos et al., 2013). To determine if rPHB could rescue cardiac dysfunction associated with systemic inflammation, we preformed serial echocardiography on anesthetized mice. All cardiac function parameters were calculated from M-mode tracings (Figure 4.4). Four hours after LPS injection, LVeSD was increased by nearly 40% in WT mice and 25% in Nrf2KO mice. This increase was sustained at 8 hours in

WT and Nrf2KO mice and at 14 hours in WT mice, indicating a decrease in cardiac contractility (Table 4.1). Treatment with rPHB following LPS administration restored cardiac contractility. Fractional shortening (FS%) is the ratio between the diameter of the heart during systole and diastole and measure the pump function of the heart. Following four hours of LPS exposure, FS% is reduced by ~50% (Figure 4.5A). A similar decrease was observed in mice treated with LPS and rPHB at 4 hours post-LPS challenge; however, 14 hours after LPS treatment, rPHB treated mice showed complete recovery of FS compared to mice treated with LPS alone (Figure 4.5A). In Nrf2KO mice, LPS reduced FS to similar degree as WT. rPHB treatment in Nrf2 KO mice following LPS resulted in a similar decrease at four hours as WT, however at 8 hours Nrf2 KO mice demonstrated significant recovery compared to mice treated with only LPS (Figure 4.5B). These findings are the first to demonstrate that rPHB attenuates LPS-mediated systolic dysfunction.

4.3 rPHB suppresses LPS-induced NFκB and STAT3 activation in heart.

In order to determine whether rPHB would mitigate LPS-induced NFκB or STAT3 activation and subsequent cytokine production in the heart, we compared nuclear p65 and phospho-STAT3 (pSTAT3) activation and proinflammatory cytokines mRNA levels in myocardial tissue from mice that were treated with LPS alone or rPHB+LPS for four hours. LPS caused a four-fold increase in NFκB nuclear activation in WT and Nrf2KO hearts (Figure 4.6B). Similarly, LPS induced a ten-fold and seven fold increase in STAT3 activation, demonstrated by nuclear pSTAT3, in WT and Nrf2KO mice respectively (Figure 4.6C). Treatment of mice with rPHB two hours following LPS administration yielded suppression of NFκB and STAT3 activation, which occurred to equivalent extent in both WT and Nrf2 KO mice (Figures 4.6 B-C).

NFκB and STAT3 are both transcription factors that regulate the production of cytokines (Figure 1.1 and 1.2). Therefore, we examined the effect of rPHB on cytokine production in myocardium following four hours after LPS administration. As expected, LPS caused a marked increase in IL1β, IL6, and TNFα gene expression (Figure 4.7A-C). LPS caused a significantly higher induction of IL1β and IL6 (Figure 4.7A and B) in Nrf2KO mice. Treatment with rPHB two hours following LPS administration abolished LPS induced increases in IL1β, IL6, and TNFα gene expression in WT mice. rPHB treatment in Nrf2KO mice attenuated LPS-induced increases in IL1β, IL6, and TNFα (Figure 4.7A-C). These data suggest that rPHB suppresses activation of NFκB and STAT3 in heart following LPS challenge, thus attenuating the production of their downstream gene targets.

The mechanisms by which sepsis-related cardiac dysfunction develops remain incompletely understood. Clinical evidence has provided insight into a potential role for the endogenous potent vasodilator nitric oxide (NO) in the pathogenesis of sepsis-induced cardiac dysfunction (Avontuur et al., 1998; Flynn et al., 2010). NO synthesis occurs via three isoforms. Constitutive enzymes responsible for NO production include, endothelial cell derived nitric oxide synthase (eNOS) and neuronal derived nitric oxide synthase (nNOS). Under conditions of stress, including sepsis, inducible nitric oxide synthase (iNOS) leads to the production of large amounts of NO. To determine whether rPHB attenuates LPS-induced myocardial iNOS expression, we investigated the iNOS protein (Figure 4.8A) and mRNA expression in the myocardium following four hours of LPS exposure in the presence and absence of rPHB. As expected, LPS induced a four-fold increase in iNOS expression in WT mice (Figure 4.8B). Treatment with rPHB two hours following LPS administration completely abolished the LPS-induced increase in iNOS protein expression (Figure 4.8B). No significant increase in iNOS

expression was observed in Nrf2KO mice following LPS exposure, and Nrf2KO mice treated with rPHB two hours following LPS administration showed a significant increase in iNOS protein expression compared to Nrf2KO–Veh mice (Figure 4.8B). A four-fold and six-fold increase in iNOS mRNA levels in WT and Nrf2KO mice respectively, was observed at 4 hours post-LPS challenge (Figure 4.8C). rPHB treatment in WT mice completely abolished the LPS-induced increase in iNOS mRNA, while in Nrf2KO mice rPHB partially reversed the LPS-induced increase in iNOS mRNA (Figure 4.8C). LPS exposure for four hours did not increase nitrosylation of tyrosine residues in cardiac homogenate. However, rPHB treatment suppressed tyrosine nitrosylation below Vehicle levels in mice treated with LPS (Figure 4.9A and B). These data suggest that rPHB confers cardioprotection from LPS through suppression of myocardial inflammation and possibly through the inhibition iNOS expression. Future studies will be explore the role of iNOS inhibition in rPHB mediated cardioprotection.

4.4 rPHB inhibits activation of autophagy early in sepsis

Autophagy is an adaptive response intended to recycle redundant, defective, or unnecessary proteins and cellular components. These dysfunctional proteins and organelles are sequestered in double membrane bound vesicles called autophagosomes. Upon delivery to lysosomes, the contents of the autolysosome is degraded and recycled (Mofarrahi et al., 2012) (Figure 1.4). Autophagy has been implicated as an important pro-survival mechanism in late sepsis, critical for cellular hibernation, where alternative energy supplies are needed to promote cell survival (Singer, 2008). Activation of the TLR4 has been shown to increase activation of autophagy in cultured skeletal muscle cells (Doyle et al., 2011) and *in vivo* following LPS administration (Mofarrahi et al., 2012). To determine whether rPHB mitigates LPS-induced activation of autophagy, we examined several genes involved with autophagosome formation.

LPS exposure triggered a significant increase in mRNA expression of LC3B, Lamp2a, and Beclin-1, with no change in p62 mRNA expression (Figure 4.10 A-D) at 4 hours. rPHB treatment two hours after LPS administration resulted in a significant inhibition of autophagy marker mRNA expression (Figure 4.10 A-D). In contrast to the mRNA expression, four hours of LPS was not sufficient to induce changes in LC3B or p62 protein (Figure 4.11 B and C). Interestingly, rPHB treatment following LPS administration appeared to increase LC3B protein expression, however it was not statistically significant ($p=0.061$) (Figure 4.11 A and B).

4.5 rPHB protects mitochondrial function in heart during endotoxic shock

Mitochondrial dysfunction has been implicated in the pathogenesis of sepsis-associated multiple organ dysfunction. Functional deficiency, characterized by decreased oxidative phosphorylation (OxPhos), and excessive production of mitochondrial derived ROS/RNS are commonly recognized as mediators of MODS (Crouser, 2004; Exline and Crouser, 2008). Mitochondrial dysfunction in tissue samples taken from septic patients in the ICU has been associated with poor prognosis and death (Brealey et al., 2002). To determine if rPHB could preserve mitochondrial function during sepsis, we compared mitochondrial oxygen consumption (mO_2), mitochondrial ATP generation (mATP), and mitochondrial oxidant emitting potential (mH_2O_2) in mice 16 hours following LPS challenge, with and without subsequent rPHB treatment. As expected, LPS administration had a moderate but significant deleterious effect on mO_2 in WT mice, reducing ADP-stimulated respiration by ~30% compared to Veh-treated mice (Figure 4.12A). rPHB treatment was unable to rescue the LPS-induced decrease in mO_2 (Figure 4.12 A). In contrast, mATP was significantly decreased by LPS administration in both WT and Nrf2KO mice, and treatment with rPHB preserved mATP in mice treated with LPS in both WT and Nrf2KO mice (Figure 4.12 B). Simultaneous measurement of mO_2 and mATP allows us to

calculate the P:O ratio, the ratio of the number of ATP produced per oxygen consumed, which is a measure of mitochondrial OxPhos efficiency. Treatment with rPHB in both WT and Nrf2KO mice exposed to LPS resulted in preserved P:O ratio (Figure 4.12 C). The respiratory control ratio (RCR), which is a measure of mitochondrial coupling, was not different between groups, indicating that uncoupling of OxPhos was not likely to be the cause of the differences seen (Figure 4.12 D). Surprisingly, LPS or rPHB+LPS treatment did not yield significant changes in mH_2O_2 in either WT or Nrf2KO mice (data not shown). Collectively, these data suggest that rPHB mediated mitochondrial protection by preserving mATP generation capacity and mitochondrial OxPhos efficiency during LPS challenge.

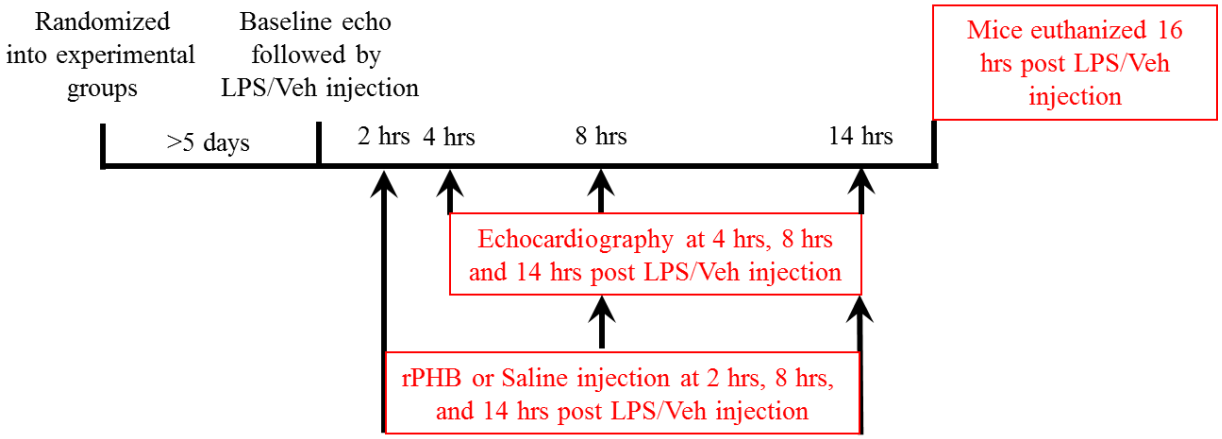
Randomized into experimental groups
Baseline echo followed by LPS/Veh injection
Mice euthanized 16 hrs post LPS/Veh injection
>5 days
2 hrs
4 hrs
8 hrs
14 hrs
Echocardiography at 4 hrs, 8 hrs and 14 hrs post LPS/Veh injection
rPHB or Saline injection at 2 hrs, 8 hrs, and 14 hrs post LPS/Veh injection

Figure 4.1 Schematic representation of study design.

Sixteen hour time-course of sepsis in WT and Nrf2KO mice.

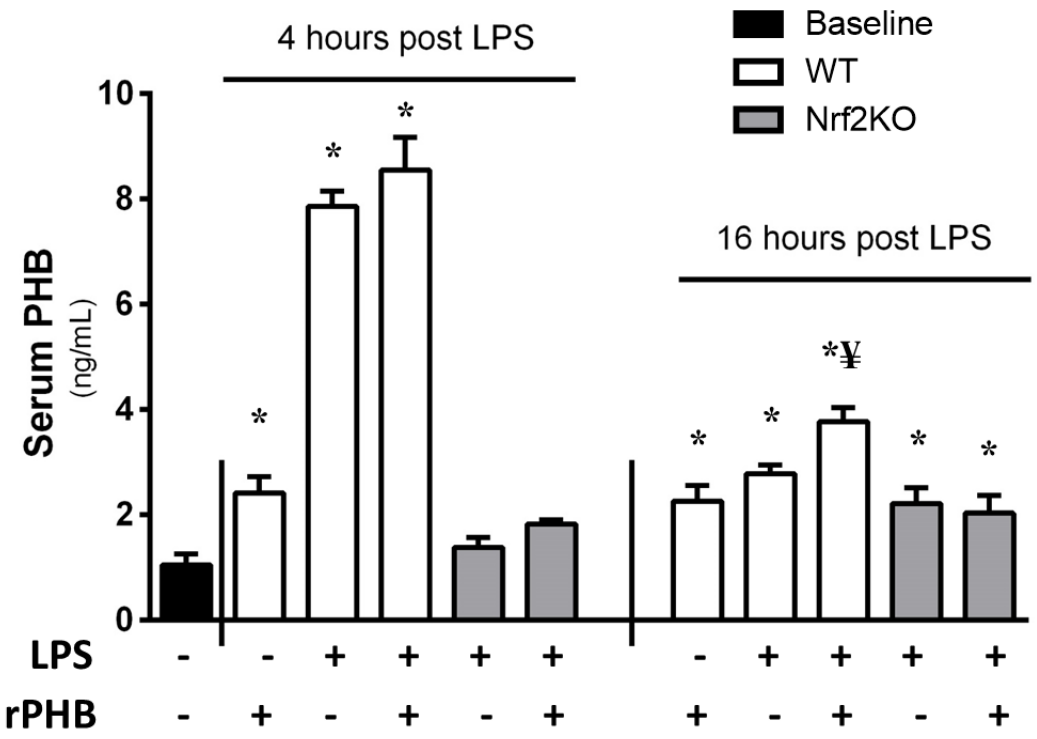
4 hours post LPS
16 hours post LPS
Baseline
WT
Nrf2KO
Serum PHB
(ng/mL)
10
8
6
4
2
0
*
*
*
*
*
*
*
*¥
*
*
LPS - - + + + + - + + + +
rPHB - + - + - + + - + - +

Figure 4.2 Serum PHB spikes in a time-dependent manner following administration of LPS.

LPS induces a rapid (≤ 4 hours) increase in circulating PHB which is dependent on Nrf2 (solid bars). Serum PHB level remain elevated 16 hours following LPS administration, with greater elevation in the WT LPS+rPHB mice (Stripped bars). There was no significant difference between WT sham and Nrf2KO sham, therefore they were grouped into one sham column. Data are expressed at means ± SEM. N=3-6, *P<0.05 vs. WT Vehicle, ¥ P<0.05 vs. WT LPS Only 16hr

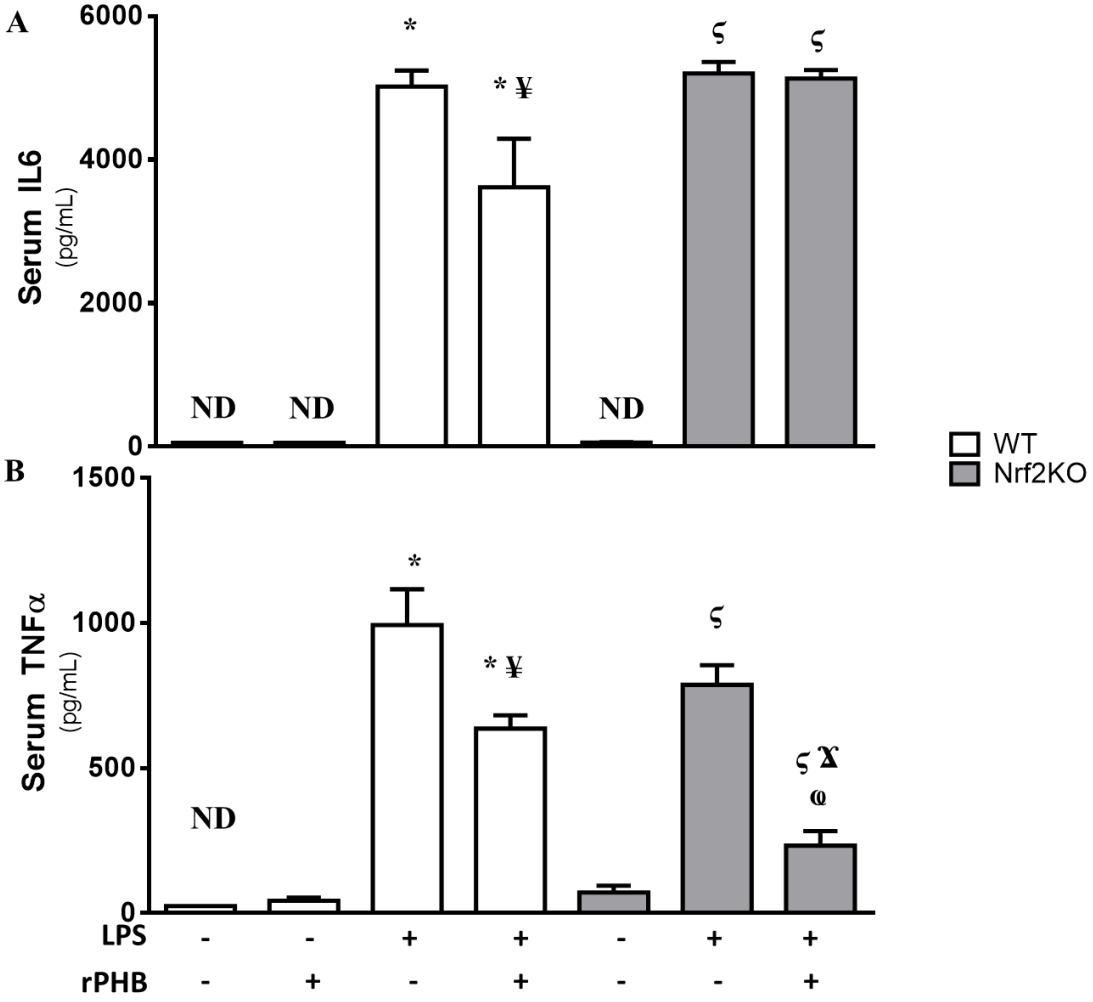
A
6000
4000
2000
0
Serum IL6
(pg/mL)
ND
ND
ND
*
* ¥
ς
ς
B
1500
1000
500
0
Serum TNFα
(pg/mL)
ND
*
* ¥
ς
ς ϰ
ϖ
LPS - - + + - + +
rPHB - + - + - - +
WT
Nrf2KO

Figure 4.3 rPHB administration attenuates circulating cytokines in LPS treated mice.

A. IL6 production was significantly reduced by an IP injection of rPHB (200ng/mL) two hours after LPS administration in WT mice treated LPS for four hours. However, no change of IL6 production was detected in Nrf2KO mice. B. Increased circulating TNFα levels were attenuated by an IP injection of rPHB (200ng/mL) two hours following LPS administration in both WT and Nrf2KO mice treated with LPS for four hours. Data are expressed at means ± SEM. N=3, * P<0.05 vs. WT Vechile, ¥ P<0.05 vs. WT LPS Only, ๏ P<0.05 vs WT rPHB+LPS, ς P<0.05 vs. Nrf2KO Vehicle, ⁑ P<0.05 vs. Nrf2KO LPS Only

A

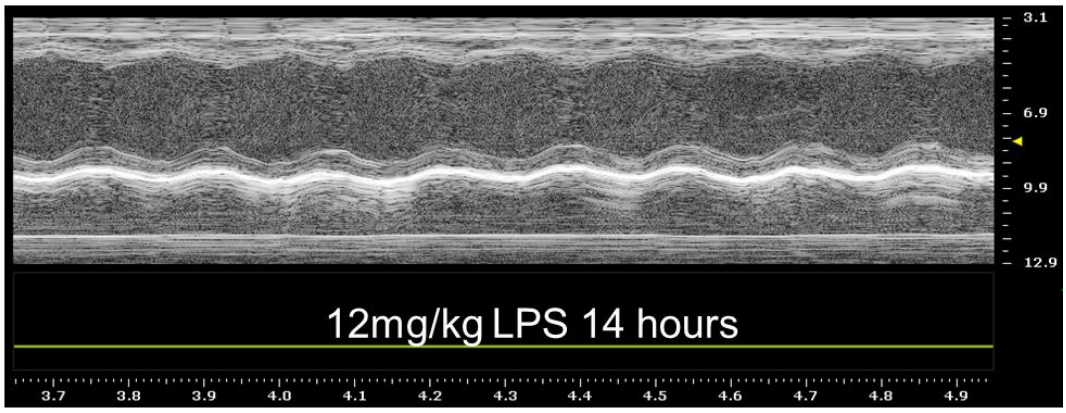
3.1
6.9
9.9
12.9
12mg/kg LPS 14 hours
3.7 3.8 3.9 4.0 4.1 4.2 4.3 4.4 4.5 4.6 4.7 4.8 4.9

B

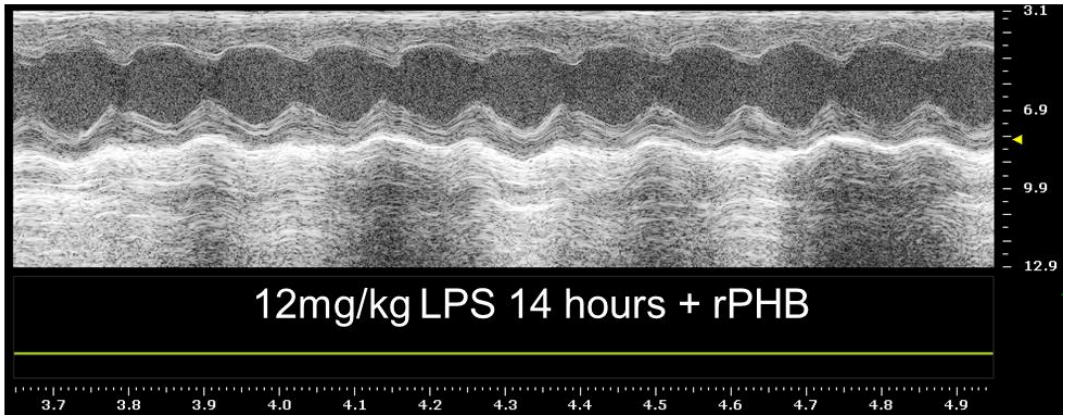
3.1
6.9
9.9
12.9
12mg/kg LPS 14 hours + rPHB
3.7 3.8 3.9 4.0 4.1 4.2 4.3 4.4 4.5 4.6 4.7 4.8 4.9

Figure 4.4 rPHB restores cardiac contractility.

Representative M-mode tracing images 14 hours after LPS alone (A) and rPHB+LPS (B) in WT mice.

	WT									Nrf2KO						
	Sham	**rPHB**			**LPS**			**rPHB +LPS**			**Sham**	**LPS**			**rPHB +LPS**		
Age (weeks)	11.60 ± 0.5	12.25 ± 1.0			11.60 ± 0.5			12.33 ± 0.8			9.50 ± 0.7	9.25 ± 0.5			9.50 ± 0.6		
Weight (g)	26.16 ± 2.3	27.60 ± 2.0			26.96 ± 1.0			26.65 ± 1.3			24.35 ± 1.5	23.96 ± 1.0			24.20 ± 1.6		
		4 hours	**8 hours**	**14 hours**	**4 hours**	**8 hours**	**14 hours**	**4 hours**	**8 hours**	**14 hours**		**4 hours**	**8 hours**	**14 hours**	**4 hours**	**8 hours**	**14 hours**
LVeSD (mm)	2.53 ± 0.3	2.46 ± 0.4	2.53 ± 0.3	2.39 ± 0.4	3.49 ± 0.4*	3.01 ± 0.2*	3.19 ± 0.3*	3.29 ± 0.3*	3.15 ± 0.4	2.12 ± 0.5	2.65 ± 0.3	3.24 ± 0.2ς	3.03 ± 0.3ς	2.79 ± 0.3	2.82 ± 0.1	2.33 ± 0.2	2.11 ± 0.5
LVeDD (mm)	3.99 ± 0.3	3.95 ± 0.4	3.97 ± 0.3	3.86 ± 0.3	4.16 ± 0.4	3.90 ± 0.2	4.14 ± 0.3	4.03 ± 0.2	4.05 ± 0.3	3.57 ± 0.4	4.34 ± 0.3	4.07 ± 0.2	3.88 ± 0.3	3.75 ± 0.3	3.84 ± 0.3	3.69 ± 0.2	3.77 ± 0.3
Heart Rate (bpm)	463.98 ± 42.6	531.14 ± 24.1	526.04 ± 28.9	505.99 ± 35.1	552.34 ± 40.8*	459.69 ± 22.4	412.35 ± 52.3	565.26 ± 36.0*	497.13 ± 57.9	482.52 ± 46.4	435.33 ± 40.1	527.55 ± 16.1ς	365.11 ± 33.8	370.89 ± 44.3	523.14 ± 17.0ς	433.76 ± 46.7	431.49 ± 31.3
Stroke Volume (µL)	46.82 ± 7.3	46.38 ± 6.8	45.64 ± 6.2	44.10 ± 5.3	26.00 ± 4.3*	30.78 ± 4.5*	35.45 ± 4.9*	27.37 ± 7.6*	32.27 ± 6.3*	38.33 ± 6.6	59.17 ± 7.0	30.78 ± 3.4ς	29.06 ± 3.3ς	30.10 ± 6.7ς	33.68 ± 11.5ς	38.87 ± 5.9ς	45.56 ± 5.6

Table 4.1 Echocardiographic Data

Echocardiogram was performed in anesthetized mice before LPS administration and again four, eight and 14 hours after LPS. Data shown as statistical analysis of echocardiography measurements means ± SD. Left-ventricle end systolic diameter (LVeSD), left-ventricle end diastolic diameter (LVeDD), N=4-6, * $P<0.05$ vs. WT Vehicle, ς $P<0.05$ vs. Nrf2KO Vehicle.

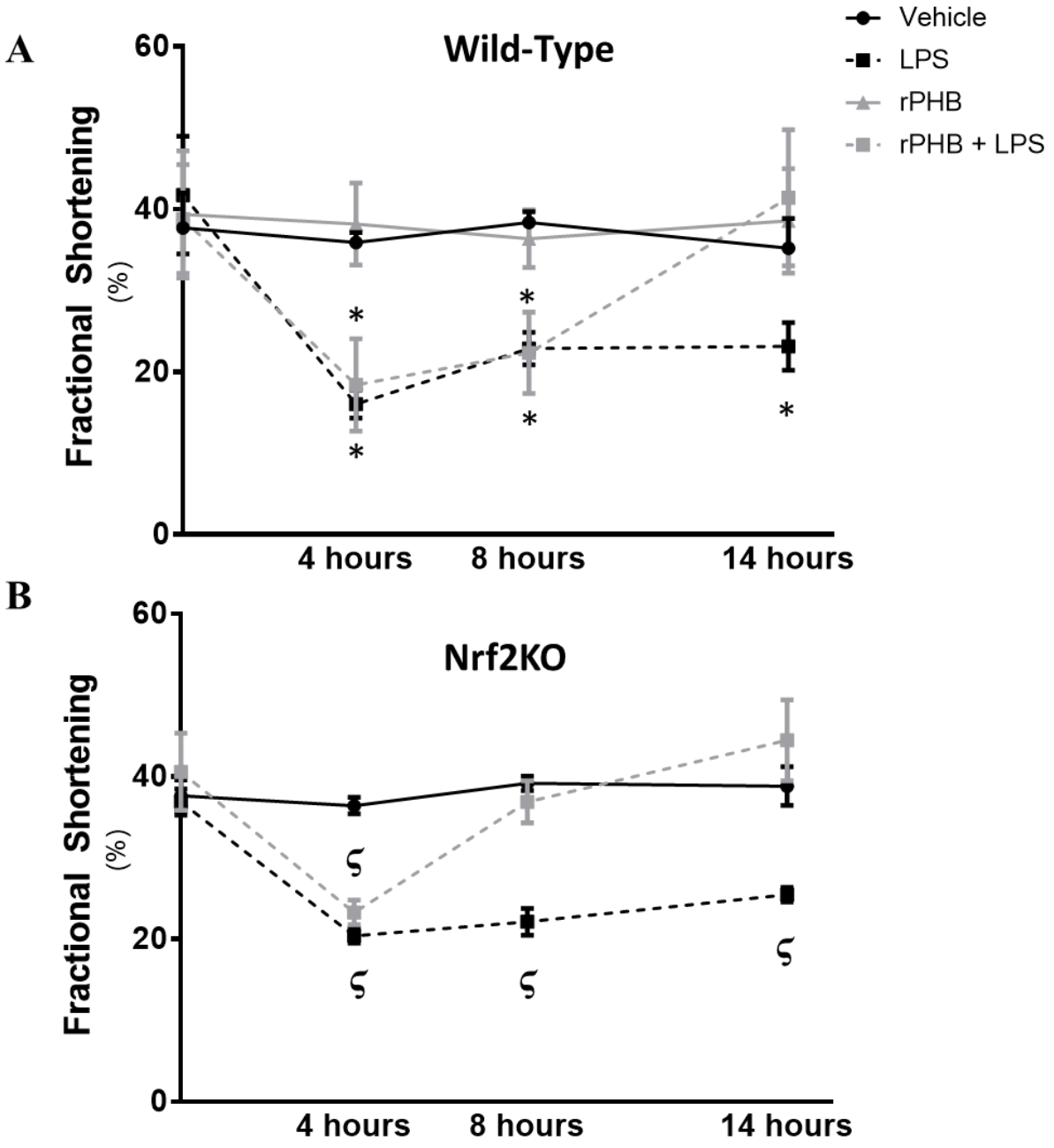
A
Wild-Type
Vehicle
LPS
rPHB
rPHB + LPS
Fractional Shortening (%)
60
40
20
0
4 hours
8 hours
14 hours
B
Nrf2KO
Fractional Shortening (%)
60
40
20
0
4 hours
8 hours
14 hours

Figure 4.5 rPHB improves recovery from LPS-mediated decrease in fractional shortening.

A, IP injection of LPS resulted in decreased FS%, as determined by M-mode echocardiographic tracings, as early as four hours after LPS in WT mice. rPHB treatment resulted in recovery of FS% by 14 hours in WT mice. B, IP injection of LPS resulted in decreased FS%, as determined by M-mode echocardiographic tracings, as early as four hours after LPS in Nrf2KO mice. rPHB treatment resulted in recovery of FS% by 8 hours in Nrf2KO mice. Data are expressed as means ± SEM, N=4-6, * $P<0.05$ vs. WT Vehicle, ς $P<0.05$ vs. Nrf2KO Vehicle.

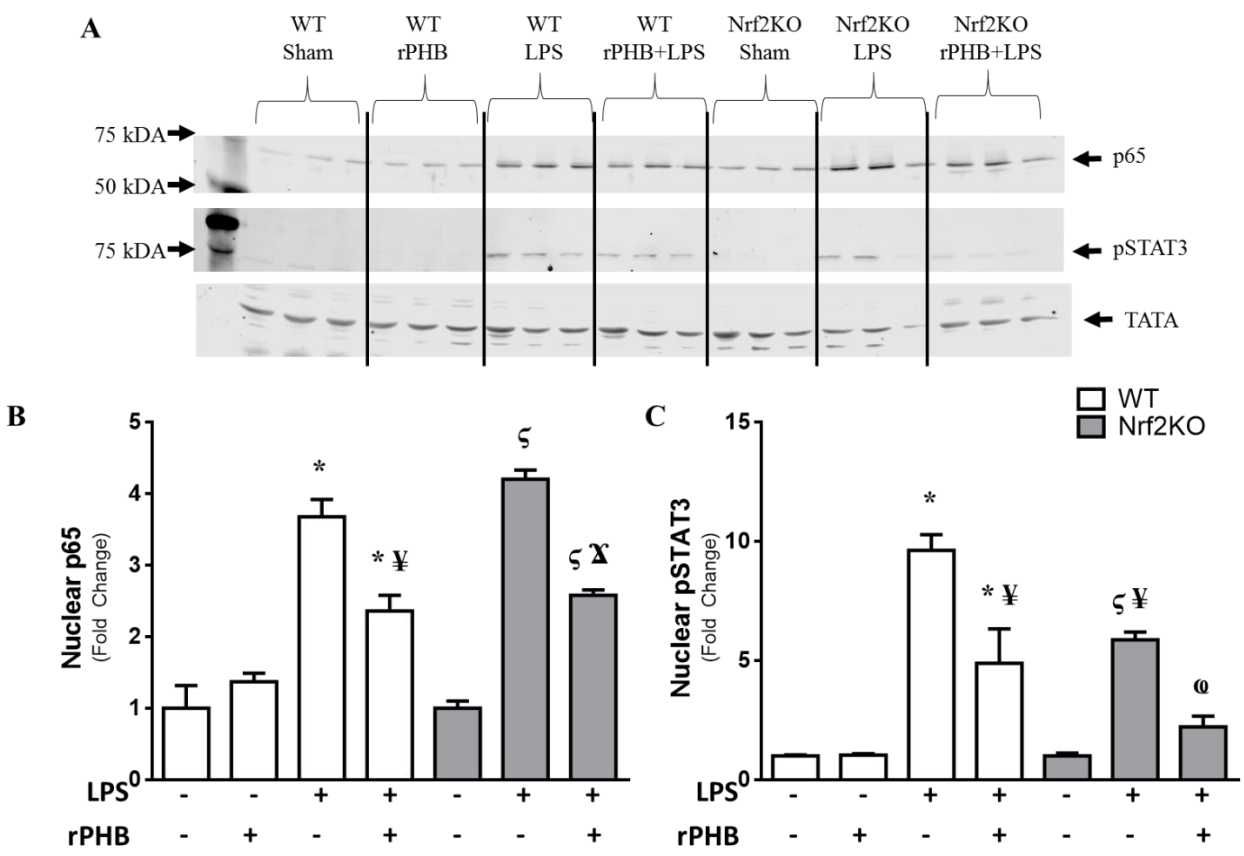
A
WT Sham
WT rPHB
WT LPS
WT rPHB+LPS
Nrf2KO Sham
Nrf2KO LPS
Nrf2KO rPHB+LPS
75 kDA
50 kDA
75 kDA
p65
pSTAT3
TATA
B
Nuclear p65
(Fold Change)
LPS
rPHB
C
WT
Nrf2KO
Nuclear pSTAT3
(Fold Change)
LPS
rPHB

Figure 4.6 rPHB attenuated LPS-induced NFκB and STAT3 activation independent of Nrf2. Mice given an IP injection of LPS or Veh followed two hours later with an IP injection of rPHB (200 ng/mL) or saline. A. Representative immunoblots of p65 and pSAT3 in isolated nuclei 4 hours following LPS administration. B. Quantified fold-change in p65 nuclear expression with respect to the genotype sham. C. Quantified fold-change of pSTAT3 nuclear expression with respect to the genotype sham. Data are expressed as means ± SEM. N=3, * P<0.05 vs. WT Vehicle, ¥ P<0.05 vs. WT LPS Only, ◎ P<0.05 vs. WT rPHB+LPS, ς P<0.05 vs. Nrf2KO Vehicle, Ϫ P<0.05 vs. Nrf2KO LPS Only

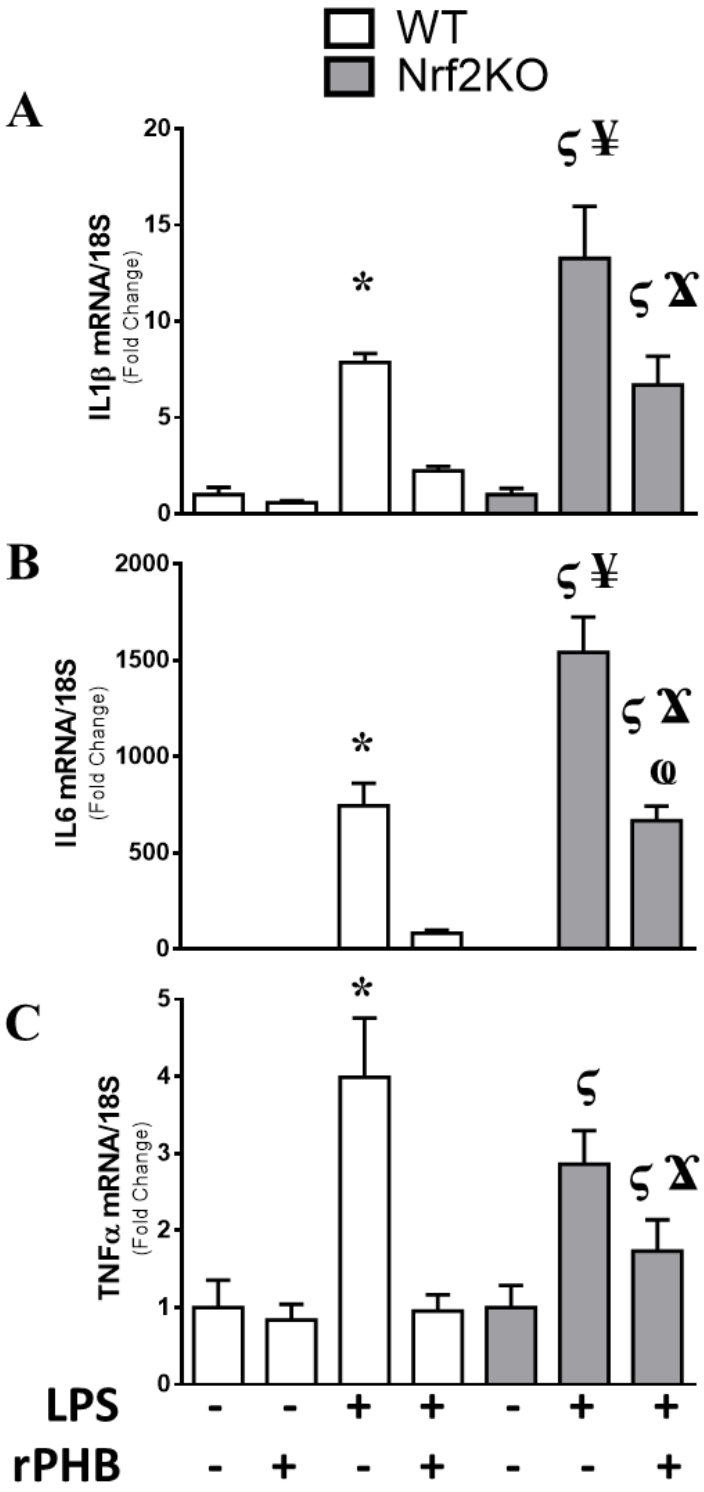
WT
Nrf2KO
A
IL1β mRNA/18S
(Fold Change)
20
15
10
5
0
*
ς ¥
ς χ
B
IL6 mRNA/18S
(Fold Change)
2000
1500
1000
500
0
*
ς ¥
ς χ
ϖ
C
TNFα mRNA/18S
(Fold Change)
5
4
3
2
1
0
*
ς
ς χ
LPS - - + + - + +
rPHB - + - + - - +

Figure 4.7 rPHB prevention LPS-driven cytokine production in cardiomyocytes partially dependent of Nrf2.

Following two hours of LPS or Veh administration, mice were given rPHB (200 ng/mL) or saline. Four hours of LPS induced a dramatic increase in IL1β (A), IL6 (B) and TNFα (C) gene expression which was completely abolished in WT animals receiving rPHB and partially inhibited in Nrf2KO animals receiving rPHB. Data are expressed at means ± SEM. N=3-4, * P<0.05 vs. WT Vehicle, ¥ P<0.05 vs. WT LPS Only, ɷ P<0.05 vs. WT rPHB+LPS, ς P<0.05 vs. Nrf2KO Vehicle, ϫ P<0.05 vs. Nrf2KO LPS Only

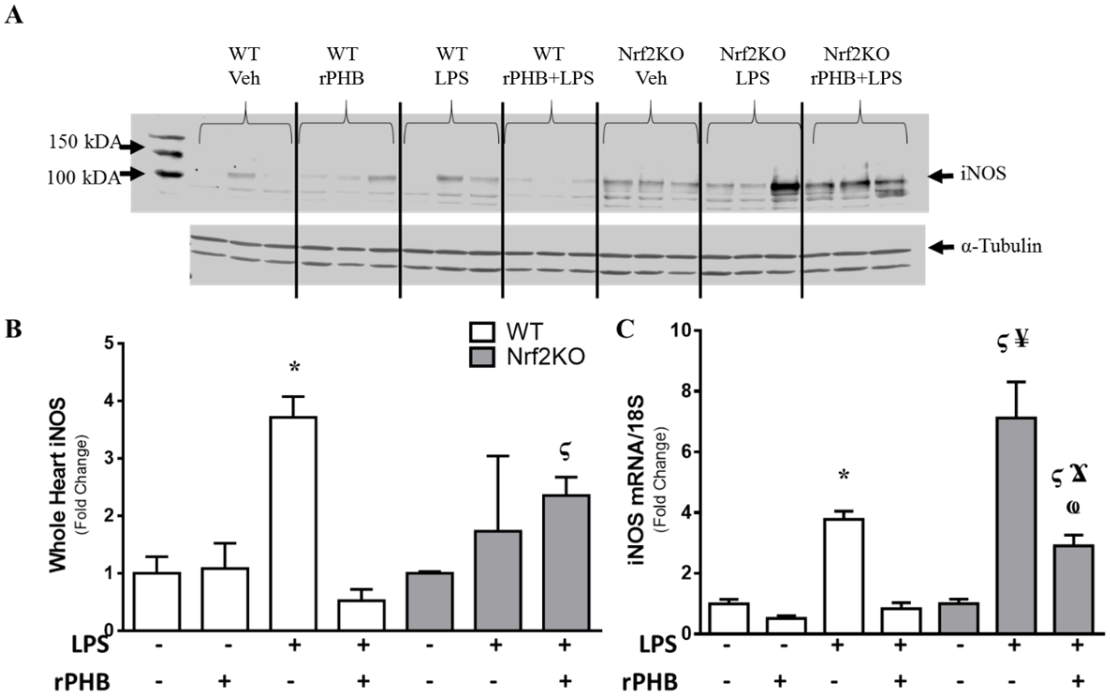
A
WT Veh
WT rPHB
WT LPS
WT rPHB+LPS
Nrf2KO Veh
Nrf2KO LPS
Nrf2KO rPHB+LPS
150 kDA
100 kDA
iNOS
α-Tubulin
B
WT
Nrf2KO
Whole Heart iNOS
(Fold Change)
LPS
rPHB
C
iNOS mRNA/18S
(Fold Change)
LPS
rPHB

Figure 4.8 rPHB attenuates iNOS gene and protein expression.

Two hours following administration of LPS or Veh mice received their first IP injection of Flag-tagged rPHB (200ng/mL) or saline. Four hours of LPS induced a significant increase in iNOS gene and protein expression. A. Representative immunoblots of iNOS and α-Tubulin. B. Quantified fold change of iNOS expression shows that rPHB inhibits LPS-induced iNOS expression in an Nrf2-dependent manner. C. Quantified fold change of iNOS gene expression shows rPHB inhibits LPS-induced gene expression. Data are expressed as mean ± SEM. N=3, * $P<0.05$ vs. WT Vehicle, ¥ $P<0.05$ vs. WT LPS Only, ⍬ $P<0.05$ vs. WT rPHB+LPS, ς $P<0.05$ vs. Nrf2KO Vehicle, Ϫ $P<0.05$ vs. Nrf2KO LPS Only

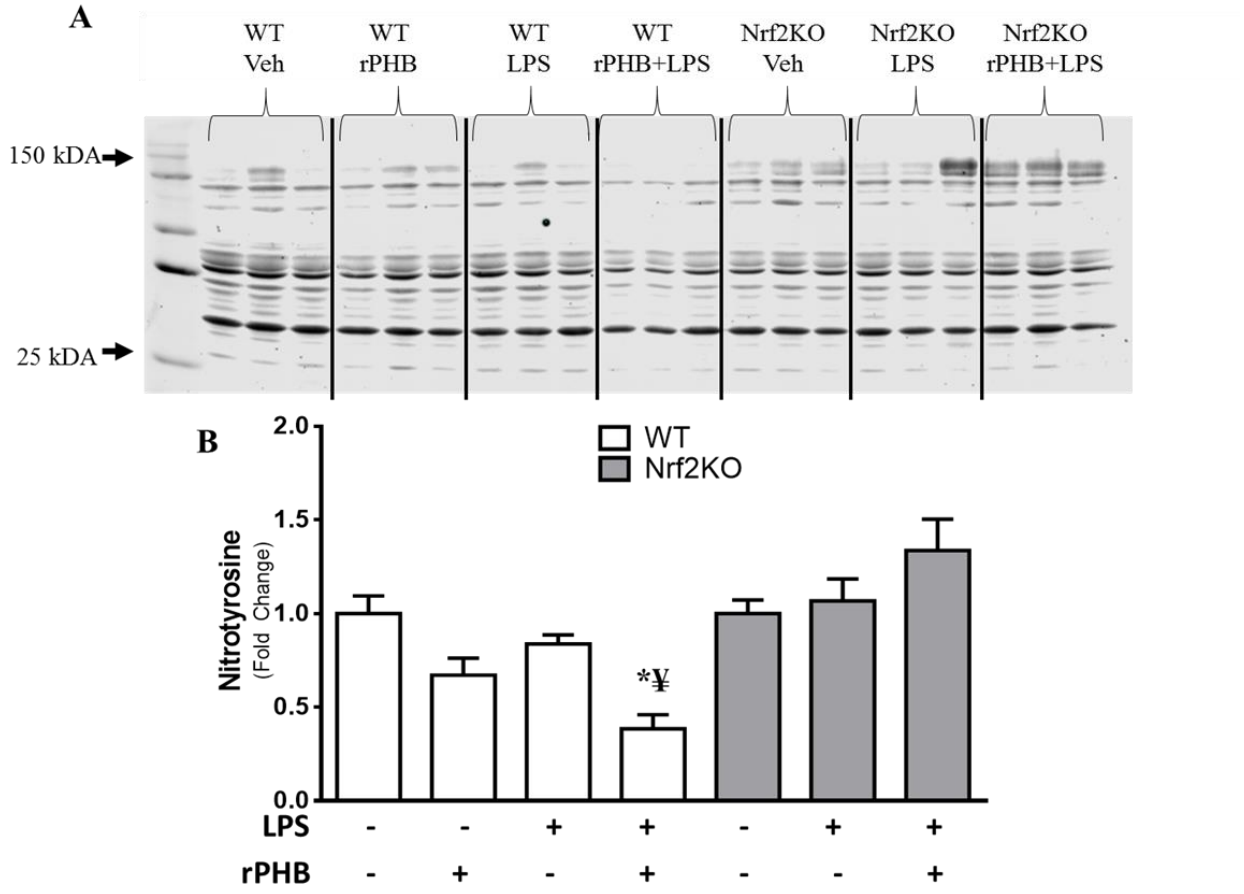
A
WT Veh
WT rPHB
WT LPS
WT rPHB+LPS
Nrf2KO Veh
Nrf2KO LPS
Nrf2KO rPHB+LPS
150 kDA
25 kDA
B
WT
Nrf2KO
Nitrotyrosine (Fold Change)
2.0
1.5
1.0
0.5
0.0
*¥
LPS - - + + - + +
rPHB - + - + - - +

Figure 4.9 rPHB inhibition of tyrosine nitroslyatation requires Nrf2.

Two hours following administration of LPS or Veh mice received their first IP injection of Flag-tagged rPHB (200ng/mL) or saline. A. Representative immunoblot of protein nitrosylation. B. Quantified fold change in nitrotyrosine expression shows that four hours of LPS exposure does not increase tyrosine nitrosylation however, rPHB treatment in WT mice exposed to LPS yields a decreased in tyrosine nitrosylation, that is not seen in Nrf2KO mice. Data are expressed as mean ± SEM. N=3, *P<0.05 vs. WT Vehicle, ¥ P<0.05 vs. WT LPS Only

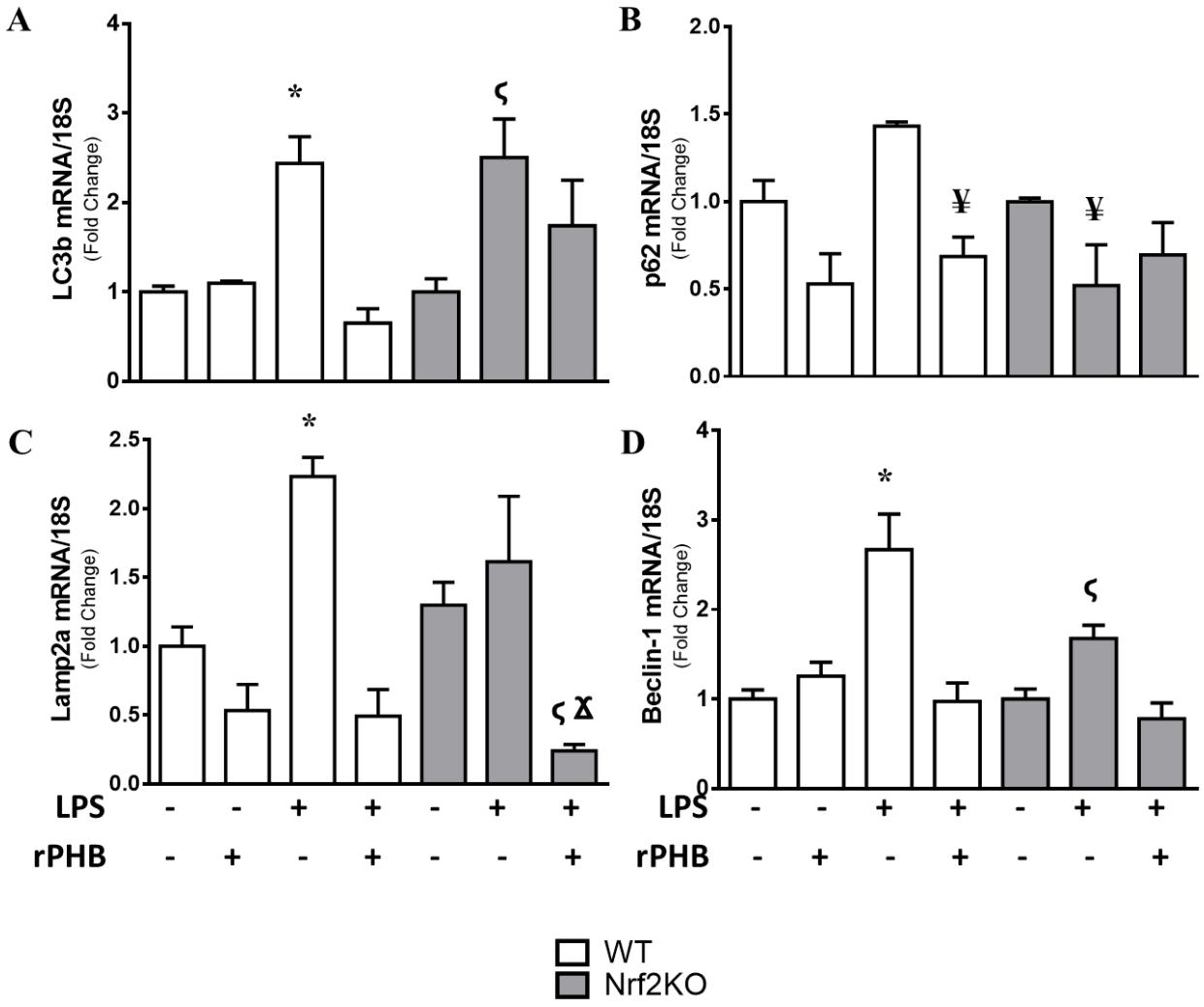
A
LC3b mRNA/18S
(Fold Change)
B
p62 mRNA/18S
(Fold Change)
C
Lamp2a mRNA/18S
(Fold Change)
D
Beclin-1 mRNA/18S
(Fold Change)
LPS
rPHB
WT
Nrf2KO

Figure 4.10 LPS induced upregulation of autophagy gene expression prevented by rPHB.

Four hours of LPS caused an increase in the gene expression of common autophagy markers LC3B (A) and Beclin-1 (D) in both C57B6 and Nrf2KO mice and Lamp2a (C) in C57B6 mice. LPS induced no change in p62 gene expression. rPHB treatment two hours after LPS administration abolished the increase in LC3B, Lamp2a, and beclin-1 gene expression in WT mice, but only abolished the LPS effect on Beclin-1 in Nrf2KO mice. Data are expressed as means ± SEM. N=3, *P<0.05 vs. WT Vehicle, ¥ P<0.05 vs. WT LPS Only, ς P<0.05 vs. Nrf2KO Vehicle

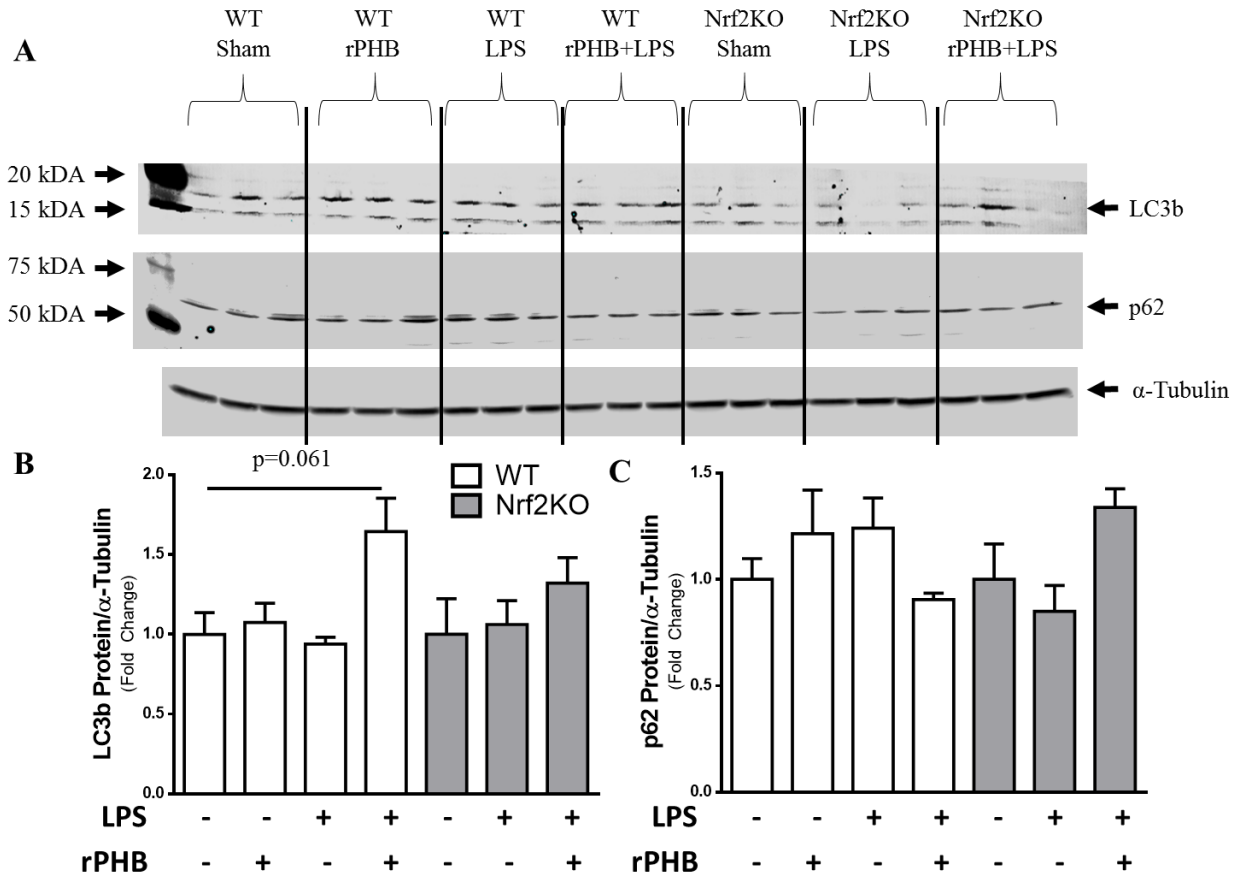
A
WT Sham
WT rPHB
WT LPS
WT rPHB+LPS
Nrf2KO Sham
Nrf2KO LPS
Nrf2KO rPHB+LPS
20 kDA
15 kDA
LC3b
75 kDA
50 kDA
p62
α-Tubulin
B
p=0.061
WT
Nrf2KO
LC3b Protein/α-Tubulin (Fold Change)
2.0
1.5
1.0
0.5
0.0
LPS - - + + - + +
rPHB - + - + - - +
C
p62 Protein/α-Tubulin (Fold Change)
1.5
1.0
0.5
0.0
LPS - - + + - + +
rPHB - + - + - - +

Figure 4.11 rPHB has no effect of protein expression of autophagy markers.

Despite changes in gene expression, LPS caused no change in LC3B or p62 protein express four hours after exposure. A. Representative immunoblots of Lc3B, p62 and α-tubulin in mice 4 hours after LPS or Veh administration. B. Quantified fold-change in LC3B protein expression. C. Quantified fold-change in p62 protein expression. Data are expressed as means ± SEM. N=3

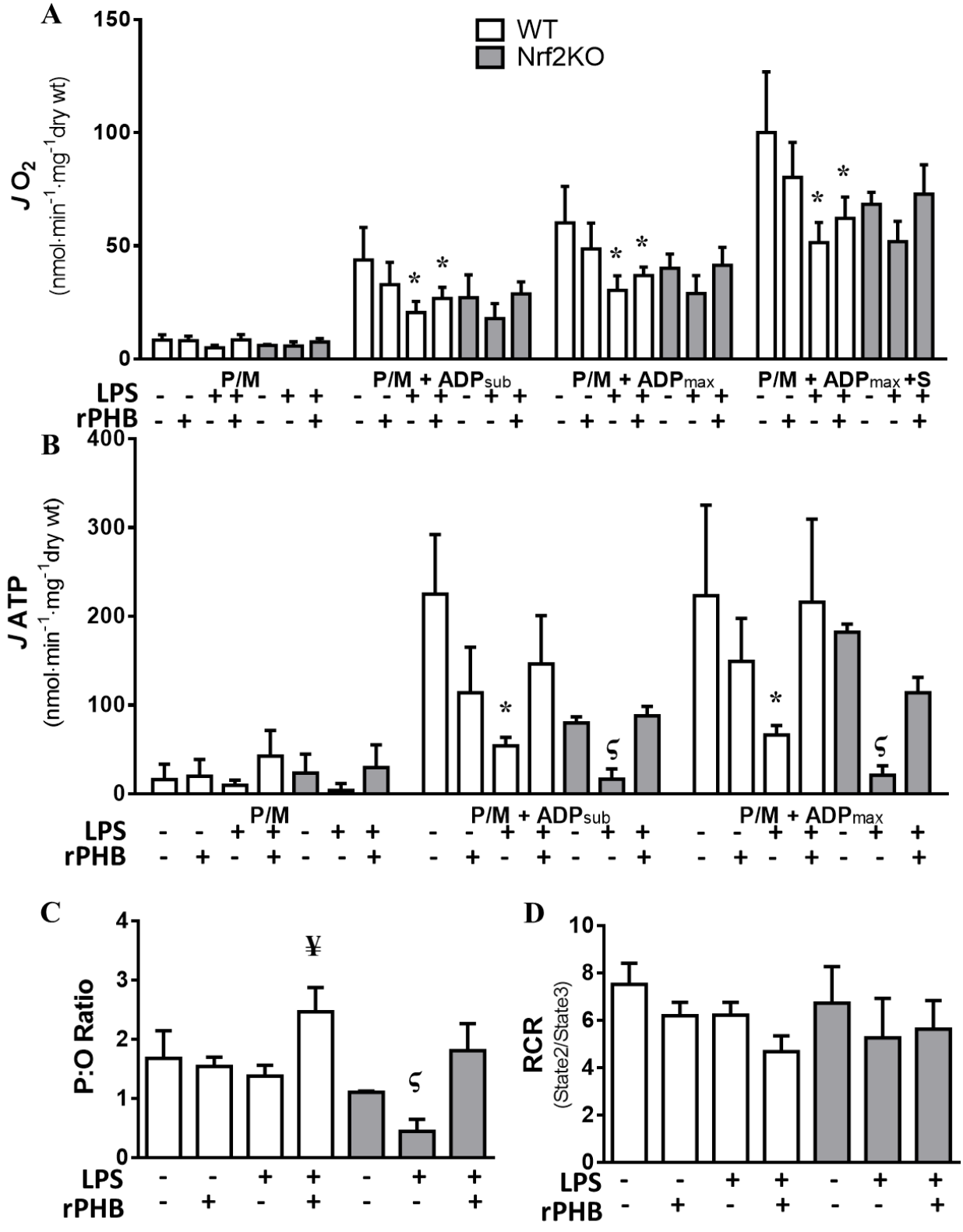
A
WT
Nrf2KO
$J O_2$
(nmol·min^{-1}·mg^{-1}dry wt)
150
100
50
0
P/M
P/M + ADP$_{sub}$
P/M + ADP$_{max}$
P/M + ADP$_{max}$ +S
LPS
rPHB
B
J ATP
(nmol·min^{-1}·mg^{-1}dry wt)
400
300
200
100
0
P/M
P/M + ADP$_{sub}$
P/M + ADP$_{max}$
LPS
rPHB
C
P:O Ratio
4
3
2
1
0
¥
ς
LPS
rPHB
D
RCR
(State2/State3)
10
8
6
4
2
0
LPS
rPHB

Figure 4.12 rPHB sustains ATP production in LPS exposed mice.

A. Quantified rates of substrate supported respiration in permeabilized LV myofibers from mice in all groups. LPS decreased complex I and complex II driven mO2 was not reversed with rPHB in WT mice. B. Quantified rates of complex I supported ATP generation in permeabilized LV myofibers from mice in all groups. LPS administration decreased ATP generation under both maximal and submaximal conditions in WT and Nrf2KO mice. C. Calculated P:O ratio. rPHB significantly increased the P:O ratio in mice exposed to LPS, with no change in mice treated with only LPS. LPS caused a small but significant decrease in P:O in Nrf2KO mice, that we abolished with rPHB. D. Calculated RCR showed no significant differences. Data are expressed as means ± SEM. N=4-6, * $P<0.05$ vs. WT Vehicle, ¥ $P<0.05$ vs. WT LPS Only, ς $P<0.05$ vs. Nrf2KO Vehicle

CHAPTER FIVE – Discussion

The broad objective of this project was to determine the role of PHB in preserving n mitochondrial function and mediating inflammatory/redox signaling within heart during severe inflammatory stress. Furthermore, a systematic experimental approach was utilized to investigate whether PHB acts in a Nrf2-dependent manner in the heart during endotoxic shock. In this context, the work presented in the preceding chapters is both novel and significant for a number of reasons. First, this study is the first to examine the role of PHB in the cardiovascular system, specifically the heart and blood, during endotoxic shock and inflammatory stress. It is also the first to examine effects of recombinant PHB administration *in vivo* during any disease and show that rPHB treatment induces protective effects on cardiac function during endotoxic shock. These findings are also novel in that they demonstrate that an inflammatory stimulus induces changes to endogenous PHB expression and localization in the heart, namely, causing a sharp rise in circulating levels of PHB. Third, this work shows that PHB mediates antioxidant and anti-inflammatory signaling events following exposure to inflammatory stimuli. Finally, these findings show that PHB protects mitochondria from inflammatory stress mediated dysfunction through direct measures of oxygen consumption, ATP generation and H_2O_2 emitting capacity. Together these results unveil a completely new biology concerning mitochondrial proteins, namely, that PHB, a mitochondrial inner-membrane protein, serves as a global anti-inflammatory/antioxidant signal, spanning from intracellular to paracrine to systemic level. While the diverse functions of PHB are still being elucidated, it is evident that this protein harbors a new avenue for therapeutic based research, in that the mechanisms by which PHB performs these functions can serve as novel targets. With implications in diseases ranging from cancer to diabetes, PHB's therapeutic potential seems to lie in altering its expression level and its

subcellular localization in affected cells. Importantly, PHB itself may be a viable therapeutic option for diseases with excessive inflammatory and oxidative stress.

5.1 Mitochondria's role in signaling with the innate immune system

The importance of mitochondrial function dates back to the 1946 discovery that respiratory chain function and energy production take place in mitochondria (HOGEBOOM et al., 1946). However, in the decades since it has become widely accepted that in addition to bioenergetics ATP production, mitochondria also actively participate in numerous biological process by initiating and transducing cell signaling. Mitochondrial regulation of cell signaling happens in two ways, 1) the outer mitochondrial membrane serves as physical platforms on which protein-protein signaling interactions occur and 2) by regulating the levels of intracellular signaling intermediates including mitochondrial metabolites (i.e cytochrome c, ATP, and ROS). Mitochondria have been implicated in cell death signaling, innate immunity and autophagy.

In response to microbial invasion cells of the immune system, such as macrophages, use pattern recognition receptors to detect pathogen-associated molecular patterns (PAMPs) on infectious agents and damage-associated molecular patterns (DAMPs) on proteins release from damaged cells. Recent evidence has shown that mitochondria regulate innate immunity by serving as damage-associated molecular patterns themselves or by responding as effectors through the generation of ROS (West et al., 2011). Mitochondria represent a large pool of DAMPs. For example, mitochondrial DNA (mtDNA) has been shown to act as an effective DAMP. When injected into the joints of mice, mtDNA was shown to induce a proinflammatory response (Collins et al., 2004). mtDNA, like bacterial DNA, possess hypomethylated CpG motifs which are required to activate PRRs including TLR (Medzhitov, 2007). Another

similarity between mtDNA and bacterial DNA is the use of *N*-formylmethionine to initiate protein synthesis. Mitochondrial N-formyl peptides are also effective DAMPs, acting through the same formyl peptide receptors as bacterial formyl peptides to stimulated neutrophil chemotaxis and cytokine secretion (Carp, 1982; Zhang et al., 2010). Trauma injury causes the release of mtDNA and formyl peptides into circulation. Evidence presented in 2010 by Zhang and colleagues demonstrated that circulating mtDNA and formyl peptides, release following trauma, stimulate polymorphonuclear neutrophils resulting in systemic inflammation (Zhang et al., 2010). The authors suggest that mitochondrial DAMPs drive the hyperactivity of the innate immune system which underlies the development of SIRS. In addition to mtDNA and formyl peptides, evidence also suggests that mitochondrially derived ATP and ROS can also act as DAMPs activating NLR family pyrin domain-containing 3 (NRLP3) inflammasomes. Mature inflammasomes are responsible for the cleavage and maturation of IL1β. Two studies have implicated mitochondria derived ROS in the activation of NLRP3 inflammasomes (Nakahira et al., 2011; Zhou et al., 2011). Zhou *et. al.* found that inhibition of oxidative phosphorylation drives mitochondrial ROS generation which was sufficient for NLRP3 activation, while inhibition of mitochondrial ROS generation blocked NLRP3 activation. Additionally, they demonstrated that inhibition of the mitophagy lead to increased ROS and NLRP3-driven IL1β release, which was consistent with earlier work showing autophagy-deficient macrophages stimulated with LPS released excessive amounts of IL1β (Saitoh et al., 2008; Nakahira et al., 2011; Zhou et al., 2011). Interestingly, release of mtDNA was also shown to facilitate NLRP3 activation (Nakahira et al., 2011). Taken together the evidence suggests a critical role for mitochondria as DAMPs activating NRLP3 inflammasomes and innate immune signaling.

The data discussed above are in sharp contrast to the work presented here. Our results show that the mitochondrial derived protein, prohibitin acts as a global mobile suppressor of inflammation. rPHB treatment *in vivo,* resulted in decreased systemic and local inflammation following an LPS challenge. With mounting evidence supporting the hypothesis that a decline in mitochondrial function is essential to the development of the inflammatory phenotype observed in both chronic and acute disease, it is interesting to speculate that PHB release from mitochondria could be acting as an early warning alarm for the system.

5.2 PHB and mitochondrial function

Mitochondria are responsible for greater than 90% of the body's total oxygen consumption for generation of ATP, making this organelle monumentally important in organs with high energy demand (i.e. the heart). Of late, keen interest has been placed on the determining the role of mitochondria in the cell's response to stress, resulting in evidence suggesting it plays a central role in the pathogenesis of diseases in which metabolic and inflammatory stresses result in altered cardiac function (Baines, 2010). The existence of mitochondrial dysfunction and increased oxidative stress in animal models of sepsis has been well characterized in the literature (Brealey et al., 2004; Crouser, 2004) and demonstrated in the data presented here making this organelle a target of therapeutic-based research. Excessive production of NO has been reported to bind and inhibit complex IV of the mitochondrial electron transport chain, thus decreasing mitochondrial respiration and increasing mitochondrial ROS production (Borutaite et al., 2001). The adverse effects of NO may be mediated in part by the generation of peroxynitrite, a highly reactive nitrogen species formed by the interaction of superoxide anions and NO. Peroxynitrite itself has toxic effects on complexes I, II and III of the electron transport chain (Rabuel and Mebazaa, 2006) and has been directly linked to

perturbations of calcium flux (Ishida et al., 1996; Khadour et al., 2002). These adverse effects on oxidative phosphorylation prevent cells from using molecular oxygen to produce ATP inducing bioenergetics failure. This phenomenon has been termed cytopathic hypoxia (Fink, 2001; Fink, 2002) and has been proposed as a mechanism for sepsis-induced organ failure (Levy, 2007).

Given that PHB's predominate cellular localization in the mitochondria and its most well-documented function is stabilizing mitochondrial proteins and maintaining proper mitochondrial morphology, we sought to determine how PHB would affect mitochondrial function and integrity during sepsis. In cardiomyocytes, TNFα/IL1β treatment resulted in a decrease in complex I supported respiration. These data are in line with others who have reported complex I specific mitochondrial dysfunction under cytokine stress (Brealey et al., 2002; Protti et al., 2007). Simultaneous measurement of mO_2 and mATP revealed that in concert with the decrease in mO_2, TNFα/IL1β treatment decreased mATP production, leading to compromised mitochondrial efficiency as indicated by the P:O ratio. Not surprising, over-expression of PHB in cardiomyocytes abolished the TNFα/IL1β-driven decrease in complex I-mediated mO_2 and mATP generation, resulting in sustained mitochondrial integrity (Figure 3.13). Similar results were obtained with rPHB treatment in the mouse model of sepsis. While rPHB treatment was unable to completely reverse the LPS-driven decrease in mO_2 in WT mice, it maintained ATP production despite impaired oxygen consumption in a mechanism that is independent of Nrf2, resulting in enhanced mitochondrial efficiency (Figure 4.13). These data are in line with previous reports that show exogenous PHB, when incubated with pancreatic β-cells, sustains mitochondrial electron transport chain enzyme activities following incubation with ethanol (Lee et al., 2010). Knock-down studies have shown that loss of PHB in endothelial cells induces

mitochondrial membrane depolarization and decreased complex-I activity (Schleicher et al., 2008). Similar results have been found in plants (Osman et al., 2009) and yeast (Coates et al., 1997). Additionally, PHB has been implicated as a chaperone for newly synthesized subunits of the mitochondrial election transport chain (Artal-Sanz et al., 2003). Its chaperone activity reduced proteolysis of these essential respiratory components (Nijtmans et al., 2000). Furthermore, studies have implicated mitochondrial uncoupling as a cause of cytopathic hypoxia (Fink, 2001). Mitochondrial uncoupling occurs when oxygen consumption is no longer tightly coupled to the production of ATP and has been reported in sepsis dating back to the early 1970s (Decker et al., 1971; Le Minh et al., 2009). While our findings do not directly investigate the impact of PHB on mitochondrial uncoupling during endotoxic shock, per se, the rPHB-mediated maintenance of ATP generation during LPS challenge suggests that PHB may preserve mitochondrial coupling during cytokine stress, either directly through interaction with mitochondrial transporters/enzymes, or indirectly via up-regulation of antioxidant enzymes.

5.3 PHB expression and antioxidant/anti-inflammatory signaling

The data presented here suggests a role for PHB in attenuating inflammation and is consistent with recent observations showing that PHB inhibits NFκB nuclear translocation, DNA binding, and NFκB–mediated gene transcription in epithelial cells during TNFα-induced inflammatory stress (Theiss et al., 2009). NFκB plays a central role in the initial inflammatory response and the feed-forward mechanism that causes the subsequent cytokine storm during sepsis (Kumar et al., 2001). Therapeutic strategies focusing on inhibition of NFκB activation during sepsis has resulted in a mass of evidence demonstrating reduced systemic release of TNFα, IL1β and IL6 and protection from a lethal dose of LPS in mice (Lauzurica et al., 1999; Li et al., 2009; Theiss et al., 2009; Mofarrahi et al., 2012; Liu et al., 2013). In 2007, a NFκB

binding site was identified in the PHB promoter (Theiss et al., 2007b). The findings presented in this dissertation, combined with others (Theiss et al., 2009) have shown that PHB expression is decreased in response to inflammatory mediators. Theiss *et al.* in 2009 reported that TNFα treatment in intestinal epithelial cells mediated a decrease in PHB promoter activation, mRNA and protein expression. Interestingly, responsiveness of PHB promoter activity to TNFα was dose-dependently decreased with the use of NFκB inhibitor pyrrolidine dithiocarbamate (PDTC) and abolished with mutation of the NFκB binding site (Theiss et al., 2009) demonstrating that the NFκB binding site is required for the TNFα mediated decrease in PHB promoter activity. Although not specifically examined in the present study, it is plausible that similar pathways *in vivo* could be responsible for the decrease in cardiac PHB following LPS insult.

Maintenance of proper mitochondrial function requires communication between nuclear and mitochondrial encoded genes, particularly under stress conditions. Our results suggest that PHB may fulfill dual roles, serving as a mitochondrial phospholipid scaffold and chaperone protein in the mitochondria and a mobile signal transducer and transcriptional regulator under stress conditions in the heart. The role of PHB in the mitochondria is well documented and evidence of interactions between prohibitin and phospholipids such as cardiolipin and PIP3 suggest that lipid binding may determine PHB's mitochondrial localization (Ande and Mishra, 2009; Osman et al., 2009; van Gestel et al., 2010). Interestingly, cardiolipin content decreases under conditions of oxidative stress (Sen et al., 2007; Wiswedel et al., 2010) and in experimental models of sepsis (Crouser et al., 2006) leading us to speculate that PHB translocation during sepsis could be mediated through a loss of cardiolipin content. This speculation is supported by recent work showing decreased cardiolipin and cardiolipin-prohibitin interaction following

H_2O_2-induced oxidative stress corresponding to an increase in nuclear PHB localization (Sripathi et al., 2011). PHB localization influences its multiple functions within a cell.

Because we hypothesized a protective role for PHB, we addressed whether sustained expression of PHB would diminish the effect of inflammatory stimuli on NFκB and STAT3-mediated signaling events. *In vivo* LPS increased nuclear accumulation of the NFκB protein p65, and phosphorylated STAT3 (pSTAT3) in the heart. In comparison, following LPS challenge, treatment with rPHB resulted in a ~30% reduction of p65 and a ~45% pSTAT3 nuclear expression through a mechanism independent of Nrf2. Similarly, Theiss and colleagues found following exposure to TNFα, transgenic mice specifically overexpressing PHB in intestinal epithelial cells exhibited a marked decrease in NFκB activation, p65 nuclear localization and NFκB/DNA binding when compared to WT mice (Theiss et al., 2009). While the mechanism of PHB-mediated inhibition of p65 is not entirely known, it has been reported that PHB has no effect on the degradation of IκB-α, the inhibitory protein which hold the NFκB dimer in the cytosol, following a TNFα insult *in vitro* (Theiss et al., 2009). This suggests that PHB interferes with an event downstream of NFκB release from its repressor protein. The nuclear pore complex responsible for the nuclear trafficking of protein containing arginine/lysine rich nuclear localization signals such as p65 is a heterodimer of importin α/β (Goldfarb et al., 2004). Evidence suggests that PHB inhibits p65 nuclear accumulation by inhibiting importin α3 expression. Forced expression of importin α3, in cells overexpressing PHB, restored NFκB activation and nuclear accumulation of p65 (Theiss et al., 2009) verifying that PHB interrupts p65 nuclear accumulation through the inhibition of importin α3. Interesting loss-of-function studies in the liver also supports a role for PHB in mediating an anti-inflammatory response. PHB heterozygous mice displayed more severe steatohepatitis and had elevated circulating levels

of proinflammatory cytokines and chemokines including TNFα, macrophage inflammatory protein 1 and vascular cell adhesion protein 1. The survival rate in WT mice 48 hours following an IP injection of 15 mg/kg LPS was 80%, while in PHB heterozygous mice it was reduced to 40% and the mice displayed decreased appetite, mobility and severe tremors (Sanchez-Quiles et al., 2012). Additionally, both the work presented here (Figures 3.16 and 4.8) and by others (Theiss et al., 2009; Kathiria et al., 2012) reveals an inhibitory role of PHB on NFκB-mediated gene transcription. Numerous reports have linked pathophysiological generation of NO to the development of cardiovascular dysfunction in sepsis. Elevated levels of nitrite and nitrate metabolites of NO in the serum of rats and humans during septic shock have been reported (Wagner et al., 1983; Ochoa et al., 1991; Gómez-Jiménez et al., 1995; Wong et al., 1995). Adverse cardiovascular effects associated with LPS or TNFα and IL1β administration *in vivo* were substantially reduced with NOS inhibition (Kilbourn et al., 1990a; Kilbourn et al., 1990b; Petros et al., 1991; Petros et al., 1994; Avontuur et al., 1998; Xu et al., 2012). Similarly, high-dose NO perfused through isolated hearts induces cardiac contractile dysfunction (Kelm et al., 1997). The work presented here demonstrates that PHB treatment *in vitro* and *in vivo* lessens the induction of iNOS following exposure to an inflammatory stimuli. These findings suggest that in addition to limiting systemic inflammatory mediators, rPHB treatment may improve cardiac function during sepsis by inhibiting the induction of iNOS and therefore reducing NO production.

Normally functioning mitochondria emit ROS and RNS, which are partially reduced oxygen species including superoxide, hydrogen peroxide and the hydroxyl radical. As discussed previously, NO can also be produced during the normal function of the mitochondrial respiratory chain as well as through the induction of NOS enzymes. The production of RNS occurs

following the interaction between super oxide and NO, to produce peroxynitrite. Interaction between proteins and peroxynitrite can result in the nitrosylated proteins. Interestingly, rPHB treatment in mice following LPS challenge reduced tyrosine nitrosylation of cardiac proteins. It is estimated that as much as 1% of the oxygen taken up under normal physiological conditions is converted to ROS or RNS (Du et al., 1998). When the production of ROS/RNS exceeds the cells detoxification systems, namely during diseases, the cell has reached a state of redox imbalance. Redox imbalance during sepsis has been amply reported in the literature. Interestingly, PHB has been implicated in the induction of Nrf2, a key regulator of cellular redox status. Nrf2KO mice have been reported to have dramatically higher mortality rates, and increased inflammatory mediators following LPS challenge (Thimmulappa et al., 2006). Theiss and colleagues shown decreased oxidative stress through sustained activation of Nrf2 in transgenic mice overexpressing PHB specifically in the intestine (Theiss et al., 2009) and through nanoparticale delivery of PHB (Theiss et al., 2007a; Theiss et al., 2011). Both models showed decrease incidence of colitis. The authors suggest that PHB is acting as a regulator of both the inflammatory and antioxidant response in the setting of inflammatory disease. This is a compelling argument that our data supports in the context of inflammatory stress in the heart. Our data demonstrates that PHB is protective against oxidative stress (Figure 3.18). Additionally, we show that PHB induces nuclear translocation of Nrf2, and up-regulates antioxidant gene transcription in the presence and absence of an inflammatory stimuli (Figure 3.17). With its known importance in regulating mitochondrial morphology and function, PHB has been the subject of investigation as mediator of cytoprotection in response to various stresses. Overexpression of PHB was shown to protect cardiomyocytes from hypoxia (Muraguchi et al., 2010) and H_2O_2-induced cell death (Liu et al., 2009) by suppressing

cytochrome c release and decreasing the Bax/Bcl-2 ratio in the mitochondria and β-cells from the apoptotic effects of ethanol (Lee et al., 2010). We demonstrate similar results, showing that overexpression of PHB and exogenously added rPHB can protect cardiomyocytes from TNFα/IL1β-mediated cell death.

5.4 PHB mobilization during inflammation

In addition to intracellular localization changes, the work presented here also demonstrates an increase in circulating PHB levels (Figures 3.8 and 4.2). Giving precedence to these findings, PHB levels in the serum of cancer patients were shown to be higher than in healthy patients (Mengwasser et al., 2004). However, little is known about the function of PHB in circulation or the mechanism of its release from cells. Recently it has been suggested that PHB can be released from adipocytes in lipid droplets (Brasaemle et al., 2004; Vessal et al., 2006). PHB has been implicated in some aspects of the immune response. Crosslinking studies demonstrated that PHB binds fragments of C3 and enhances complement activation (Mishra et al., 2007). PHB has been implicated as a critical mediator of T-cell mitochondrial function (Ross et al., 2008). More recently it was shown that PHB expression increases on the surface of activated T-cells (Yurugi et al., 2012) and B-cells (Lucas et al., 2013) where it modulates CD86 and CD3 signaling. Data presented here demonstrate that rPHB administration *in vivo* following LPS exposure decreases circulating levels of the proinflammatory cytokines TNFα and IL6 (Figure 4.3). This suggests that PHB in circulation may directly prevent cytokine generation by macrophages or other immune cells and the subsequent release into circulation. Clearly more investigative work is needed to establish the role of circulating PHB and the mechanism of its release.

Additionally, *in vitro* work (Lee et al., 2010) has shown that exogenously added PHB can enter cultured cells. Mechanisms of PHB internalization have yet to be discovered, however an association between PHB and EH domain 2 has been reported in isolated adipocytes (Vessal et al., 2006). EH domain-containing proteins function in intracellular trafficking and have been implicated in endocytosis and vesicle recycling (George et al., 2007). Additionally, PHB has been found on cell membranes in lipid rafts (Wu and Wu, 2012). Lipid rafts are involved in the internalization processes of various molecules (Mielenz et al., 2005; Staubach et al., 2009), which suggests that PHB uptake into cells may rely on EH domain 2 or lipid raft association.

5.5 Clinical ramifications of these findings

It is widely accepted that most septic patients have some degree of cardiac dysfunction (Krishnagopalan et al., 2002) and development of cardiac dysfunction is positively correlated to death (Merx and Weber, 2007). In some patients, cardiac dysfunction progresses to cardiac collapse, with output being severely reduced subsequently being the primary cause of death (Rudiger and Singer, 2007). Over the last 35 years significant progress has been made in identifying mechanisms involved in sepsis-induced cardiac dysfunction. The proposed mechanisms underlying the development of cardiac dysfunction include: 1) depression and deregulation of autonomic β-adrenergic receptors (Rudiger, 2010); 2) generation of a cytokine storm, characterized by excessive levels of proinflammatory cytokines (Kumar et al., 2001; Lichtenstern et al., 2012); 3) microvascular dysfunction with impaired microcirculatory flow and increased heterogeneity with reduced myocardial oxygen extraction (Doerschug et al., 2007); 4) mitochondrial dysfunction (Chopra et al., 2011); 5) NO-mediated depression, likely due to iNOS activity (Kumar et al., 2001; Araújo et al., 2012) and generation of peroxynitrite (Lancel et al., 2004); 6) apoptotic cell death in the heart via intrinsic (mitochondrial) and extrinsic (TNFα-

receptor associated) pathways (Iwata et al., 2011), and 7) altered calcium homeostasis, manifested through suppression of autonomic-related L-type calcium channels resulting in reduced cytosolic calcium (Stengl et al., 2010) and reduced ryanodine receptor type 2 density which causes reduced release of calcium from the sarcoplasmic reticulum (Dong et al., 2001). Recent therapeutic attempts to reduce the mortality rate of patients along the sepsis continuum have provided limited success (Levy et al., 2010; Fink, 2013) and the development of successful novel therapies for the treatment of sepsis will likely involve modulating multiple of the mechanisms mentioned above. These data provide evidence to suggest that PHB can play a beneficial role in the treatment of sepsis and other diseases associated with the production of excessive or maladaptive inflammation.

Using echocardiography, a tool used clinically to measure and monitor cardiac function, findings in the present work are consistent with commonly reported effects of LPS administration on the heart. LPS administration in both animals and humans reproduces many of the clinical characteristics of human sepsis (Kumar et al., 2001). Interestingly, compared to the vehicle-treated sepsis groups, rPHB treatment improve sepsis associated changes on cardiac contractility including FS (Figure 4.5), EF (data not shown) and left ventricular end systolic diameter (Table 4.1). In 1991, work by Snell and Parrillo resulted in the isolation and identification a circulating substance in humans and animals in septic shock, termed myocardial depressant factor (MDF) for its ability to induced cardiac dysfunction when injected in donor animals (Snell and Parrillo, 1991). Extensive investigation into the identity of MDF demonstrated it was a combination of TNFα and IL1β (Kumar et al., 2001). Studies found that TNFα and IL1β individually cause depression on cardiac contractile function. However, together the two work synergistically to decrease contractility at much lower concentrations.

Immuno-absorption studies found that removal of both cytokines (but not either alone) from the serum of 5 patients in septic shock reversed the depression in cardiac contractility (Kumar et al., 1996). Other compounds used to prevent the production and release of cytokines have also resulted in improved cardiac recovery to sepsis similar to the results shown here (Ramana et al., 2006; Lowes et al., 2008; Zang et al., 2012). Taken together, our results suggest that PHB mediates cardioprotection through decreased systemic inflammation, which subsequently lowers local inflammation in the heart, likely through decreased NFkB and STAT3 signaling, leading to suppression of iNOS expression and activity (Figure 5.1).

Our findings have clinical ramifications in that they provide a new therapeutic target for potent anti-inflammation action to mitigate organ failure, particularly cardiac, thereby reducing mortality caused by endotoxin-stimulated systemic inflammatory response syndrome. While sepsis is the most common clinical condition associated with a maladaptive hyper-inflammatory response, a variety of other clinical conditions are associated with extremely high concentrations of cytokines, including trauma, ischemia-reperfusion injury, antigen specific immune response and various auto-immune diseases (Landry and Oliver, 2001). The development of organ and tissue dysfunction in these clinical settings has been associated with excessive cytokine production and it could be suggested that use of PHB during these conditions could abate the maladaptive inflammatory response.

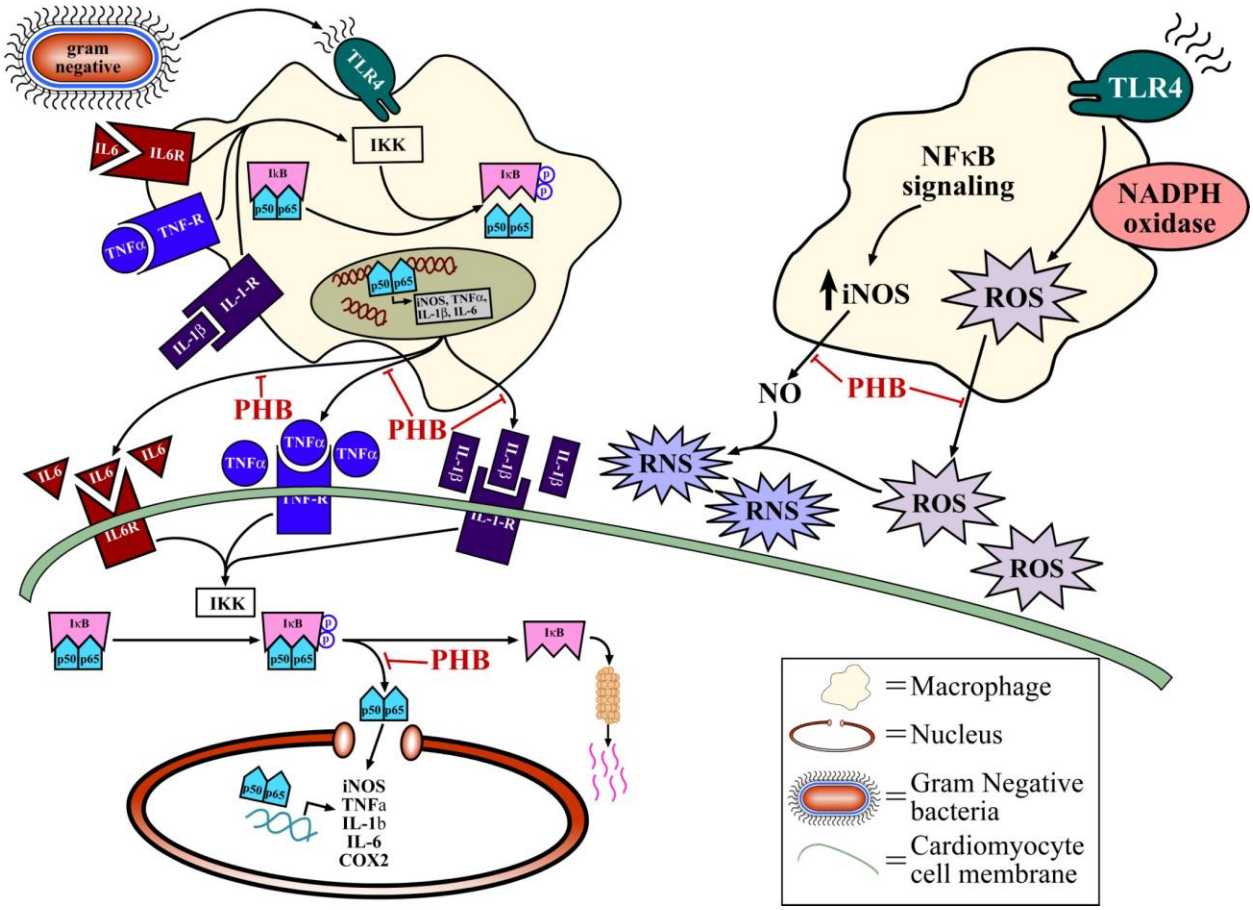
gram negative
TLR4
IKK
IL6
IL6R
TNF-R
TNFα
IL-1-R
IL-1β
IκB
p50 p65
iNOS, TNFα, IL-1β, IL-6
PHB
NFκB signaling
NADPH oxidase
iNOS
ROS
NO
RNS
=Macrophage
=Nucleus
=Gram Negative bacteria
=Cardiomyocyte cell membrane
iNOS
TNFa
IL-1b
IL-6
COX2

Figure 5.1 Proposed pathway for PHB-mediated cardioprotection in endotoxic shock.

Schematic representation of PHB-mediated decreases in systemic inflammation, leading to decreased local inflammation in the heart and preserved mitochondrial function.

Reference List

National Centre for the Replacement Refinement & Reduction of Animals in Research, in, London, England.

Abraham E (2003) Nuclear factor-kappaB and its role in sepsis-associated organ failure. *J Infect Dis* **187 Suppl 2**:S364-369.

Alexander HR, Sheppard BC, Jensen JC, Langstein HN, Buresh CM, Venzon D, Walker EC, Fraker DL, Stovroff MC and Norton JA (1991) Treatment with recombinant human tumor necrosis factor-alpha protects rats against the lethality, hypotension, and hypothermia of gram-negative sepsis. *J Clin Invest* **88**:34-39.

Ande SR, Gu Y, Nyomba BL and Mishra S (2009a) Insulin induced phosphorylation of prohibitin at tyrosine 114 recruits Shp1. *Biochim Biophys Acta* **1793**:1372-1378.

Ande SR and Mishra S (2009) Prohibitin interacts with phosphatidylinositol 3,4,5-triphosphate (PIP3) and modulates insulin signaling. *Biochem Biophys Res Commun* **390**:1023-1028.

Ande SR, Moulik S and Mishra S (2009b) Interaction between O-GlcNAc modification and tyrosine phosphorylation of prohibitin: implication for a novel binary switch. *PLoS One* **4**:e4586.

Ande SR, Xu Z, Gu Y and Mishra S (2012) Prohibitin has an important role in adipocyte differentiation. *Int J Obes (Lond)* **36**:1236-1244.

Anderson EJ and Neufer PD (2006) Type II skeletal myofibers possess unique properties that potentiate mitochondrial H(2)O(2) generation. *Am J Physiol Cell Physiol* **290**:C844-851.

Anderson EJ, Rodriguez E, Anderson CA, Thayne K, Chitwood WR and Kypson AP (2011) Increased propensity for cell death in diabetic human heart is mediated by mitochondrial-dependent pathways. *Am J Physiol Heart Circ Physiol* **300**:H118-124.

Angus DC, Linde-Zwirble WT, Lidicker J, Clermont G, Carcillo J and Pinsky MR (2001) Epidemiology of severe sepsis in the United States: analysis of incidence, outcome, and associated costs of care. *Crit Care Med* **29**:1303-1310.

Angus DC and van der Poll T (2013) Severe sepsis and septic shock. *N Engl J Med* **369**:840-851.

Araújo AV, Ferezin CZ, Pereira AeC, Rodrigues GJ, Grando MD, Bonaventura D and Bendhack LM (2012) Augmented nitric oxide production and up-regulation of endothelial nitric oxide synthase during cecal ligation and perforation. *Nitric Oxide* **27**:59-66.

Artal-Sanz M, Tsang WY, Willems EM, Grivell LA, Lemire BD, van der Spek H, Nijtmans LG and Sanz MA (2003) The mitochondrial prohibitin complex is essential for embryonic viability and germline function in Caenorhabditis elegans. *J Biol Chem* **278**:32091-32099.

Avontuur JA, Tutein Nolthenius RP, van Bodegom JW and Bruining HA (1998) Prolonged inhibition of nitric oxide synthesis in severe septic shock: a clinical study. *Crit Care Med* **26**:660-667.

Ayala A and Chaudry IH (1996) Immune dysfunction in murine polymicrobial sepsis: mediators, macrophages, lymphocytes and apoptosis. *Shock* **6 Suppl 1**:S27-38.

Baines CP (2010) The cardiac mitochondrion: nexus of stress. *AnnuRevPhysiol* **72**:61-80.

Barber AE, Coyle SM, Fischer E, Smith C, van der Poll T, Shires GT and Lowry SF (1995) Influence of hypercortisolemia on soluble tumor necrosis factor receptor II and

interleukin-1 receptor antagonist responses to endotoxin in human beings. *Surgery* **118**:406-410; discussion 410-401.

Berger KH and Yaffe MP (1998) Prohibitin family members interact genetically with mitochondrial inheritance components in Saccharomyces cerevisiae. *Mol Cell Biol* **18**:4043-4052.

Blanco J, Muriel-Bombín A, Sagredo V, Taboada F, Gandía F, Tamayo L, Collado J, García-Labattut A, Carriedo D, Valledor M, De Frutos M, López MJ, Caballero A, Guerra J, Alvarez B, Mayo A, Villar J and Intensivos GdEyAeC (2008) Incidence, organ dysfunction and mortality in severe sepsis: a Spanish multicentre study. *Crit Care* **12**:R158.

Bone RC, Balk RA, Cerra FB, Dellinger RP, Fein AM, Knaus WA, Schein RM and Sibbald WJ (1992) Definitions for sepsis and organ failure and guidelines for the use of innovative therapies in sepsis. The ACCP/SCCM Consensus Conference Committee. American College of Chest Physicians/Society of Critical Care Medicine. *Chest* **101**:1644-1655.

Bonfoco E, Krainc D, Ankarcrona M, Nicotera P and Lipton SA (1995) Apoptosis and necrosis: two distinct events induced, respectively, by mild and intense insults with N-methyl-D-aspartate or nitric oxide/superoxide in cortical cell cultures. *ProcNatlAcadSciUSA* **92**:7162-7166.

Borutaite V, Matthias A, Harris H, Moncada S and Brown GC (2001) Reversible inhibition of cellular respiration by nitric oxide in vascular inflammation. *Am J Physiol Heart Circ Physiol* **281**:H2256-2260.

Bourges I, Ramus C, Mousson de Camaret B, Beugnot R, Remacle C, Cardol P, Hofhaus G and Issartel JP (2004) Structural organization of mitochondrial human complex I: role of the

ND4 and ND5 mitochondria-encoded subunits and interaction with prohibitin. *Biochem J* **383**:491-499.

Boyle KE, Zheng D, Anderson EJ, Neufer PD and Houmard JA (2012) Mitochondrial lipid oxidation is impaired in cultured myotubes from obese humans. *IntJObes(Lond)* **36**:1025-1031.

Brasaemle DL, Dolios G, Shapiro L and Wang R (2004) Proteomic analysis of proteins associated with lipid droplets of basal and lipolytically stimulated 3T3-L1 adipocytes. *JBiolChem* **279**:46835-46842.

Brealey D, Brand M, Hargreaves I, Heales S, Land J, Smolenski R, Davies NA, Cooper CE and Singer M (2002) Association between mitochondrial dysfunction and severity and outcome of septic shock. *Lancet* **360**:219-223.

Brealey D, Karyampudi S, Jacques TS, Novelli M, Stidwill R, Taylor V, Smolenski RT and Singer M (2004) Mitochondrial dysfunction in a long-term rodent model of sepsis and organ failure. *AmJPhysiol RegulIntegrComp Physiol* **286**:R491-R497.

Calvin JE, Driedger AA and Sibbald WJ (1981) An assessment of myocardial function in human sepsis utilizing ECG gated cardiac scintigraphy. *Chest* **80**:579-586.

Celes MR, Torres-Duenas D, Prado CM, Campos EC, Moreira JE, Cunha FQ and Rossi MA (2010) Increased sarcolemmal permeability as an early event in experimental septic cardiomyopathy: a potential role for oxidative damage to lipids and proteins. *Shock* **33**:322-331.

Cerveny KL, Tamura Y, Zhang Z, Jensen RE and Sesaki H (2007) Regulation of mitochondrial fusion and division. *Trends Cell Biol* **17**:563-569.

Chander H, Halpern M, Resnick-Silverman L, Manfredi JJ and Germain D (2010) Skp2B attenuates p53 function by inhibiting prohibitin. *EMBO Rep* **11**:220-225.

Chiu CF, Ho MY, Peng JM, Hung SW, Lee WH, Liang CM and Liang SM (2013) Raf activation by Ras and promotion of cellular metastasis require phosphorylation of prohibitin in the raft domain of the plasma membrane. *Oncogene* **32**:777-787.

Chopra M, Golden HB, Mullapudi S, Dowhan W, Dostal DE and Sharma AC (2011) Modulation of Myocardial Mitochondrial Mechanisms during Severe Polymicrobial Sepsis in the Rat. *PLoSOne* **6**:e21285.

Christof O, Mathias H, Christoph P, Jonathan R, Phat Vinh D, Felix TW, Britta B, Benedikt W and Thomas L (2009) The genetic interactome of prohibitins: coordinated control of cardiolipin and phosphatidylethanolamine by conserved regulators in mitochondria. *The Journal of Cell Biology* **184**:583-596.

Clark JA and Coopersmith CM (2007) Intestinal crosstalk: a new paradigm for understanding the gut as the "motor" of critical illness. *Shock* **28**:384-393.

Clarke PG (1990) Developmental cell death: morphological diversity and multiple mechanisms. *Anat Embryol (Berl)* **181**:195-213.

Claycomb WC, Lanson NA, Jr., Stallworth BS, Egeland DB, Delcarpio JB, Bahinski A and Izzo NJ, Jr. (1998) HL-1 cells: a cardiac muscle cell line that contracts and retains phenotypic characteristics of the adult cardiomyocyte. *ProcNatlAcadSciUSA* **95**:2979-2984.

Coates PJ, Jamieson DJ, Smart K, Prescott AR and Hall PA (1997) The prohibitin family of mitochondrial proteins regulate replicative lifespan. *CurrBiol* **7**:607-610.

Coopersmith CM, Wunsch H, Fink MP, Linde-Zwirble WT, Olsen KM, Sommers MS, Anand KJ, Tchorz KM, Angus DC and Deutschman CS (2012) A comparison of critical care

research funding and the financial burden of critical illness in the United States. *Crit Care Med* **40**:1072-1079.

Cowley RA, Mergner WJ, Fisher RS, Jones RT and Trump BF (1979) The subcellular pathology of shock in trauma patients: studies using the immediate autopsy. *Am Surg* **45**:255-269.

Crimi E, Sica V, Slutsky AS, Zhang H, Williams-Ignarro S, Ignarro LJ and Napoli C (2006) Role of oxidative stress in experimental sepsis and multisystem organ dysfunction. *Free Radic Res* **40**:665-672.

Crouser E, Exline M, Knoell D and Wewers MD (2008) Sepsis: links between pathogen sensing and organ damage. *CurrPharmDes* **14**:1840-1852.

Crouser ED (2004) Mitochondrial dysfunction in septic shock and multiple organ dysfunction syndrome. *Mitochondrion* **4**:729-741.

Crouser ED, Julian MW, Huff JE, Struck J and Cook CH (2006) Carbamoyl phosphate synthase-1: a marker of mitochondrial damage and depletion in the liver during sepsis. *Crit Care Med* **34**:2439-2446.

Decker GA, Daniel AM, Blevings S and Maclean LD (1971) Effect of peritonitis on mitochondrial respiration. *J Surg Res* **11**:528-532.

Deryckere F and Gannon F (1994) A one-hour minipreparation technique for extraction of DNA-binding proteins from animal tissues. *Biotechniques* **16**:405.

Ding J, Song D, Ye X and Liu SF (2009) A pivotal role of endothelial-specific NF-kappaB signaling in the pathogenesis of septic shock and septic vascular dysfunction. *J Immunol* **183**:4031-4038.

Ding L, Liang XG, Zhu DY and Lou YJ (2007) Icariin promotes expression of PGC-1alpha, PPARalpha, and NRF-1 during cardiomyocyte differentiation of murine embryonic stem cells in vitro. *Acta Pharmacol Sin* **28**:1541-1549.

Ding WX, Ni HM, Li M, Liao Y, Chen X, Stolz DB, Dorn GW and Yin XM (2010) Nix is critical to two distinct phases of mitophagy, reactive oxygen species-mediated autophagy induction and Parkin-ubiquitin-p62-mediated mitochondrial priming. *J Biol Chem* **285**:27879-27890.

Dinkova-Kostova AT, Holtzclaw WD, Cole RN, Itoh K, Wakabayashi N, Katoh Y, Yamamoto M and Talalay P (2002) Direct evidence that sulfhydryl groups of Keap1 are the sensors regulating induction of phase 2 enzymes that protect against carcinogens and oxidants. *Proc Natl Acad Sci U S A* **99**:11908-11913.

Doerschug KC, Delsing AS, Schmidt GA and Haynes WG (2007) Impairments in microvascular reactivity are related to organ failure in human sepsis. *Am J Physiol Heart Circ Physiol* **293**:H1065-1071.

Doise JM, Aho LS, Quenot JP, Guilland JC, Zeller M, Vergely C, Aube H, Blettery B and Rochette L (2008) Plasma antioxidant status in septic critically ill patients: a decrease over time. *Fundam Clin Pharmacol* **22**:203-209.

Dombrovskiy VY, Martin AA, Sunderram J and Paz HL (2007) Rapid increase in hospitalization and mortality rates for severe sepsis in the United States: a trend analysis from 1993 to 2003. *Crit Care Med* **35**:1244-1250.

Dong LW, Wu LL, Ji Y and Liu MS (2001) Impairment of the ryanodine-sensitive calcium release channels in the cardiac sarcoplasmic reticulum and its underlying mechanism during the hypodynamic phase of sepsis. *Shock* **16**:33-39.

Doyle A, Zhang G, Abdel Fattah EA, Eissa NT and Li YP (2011) Toll-like receptor 4 mediates lipopolysaccharide-induced muscle catabolism via coordinate activation of ubiquitin-proteasome and autophagy-lysosome pathways. *FASEB J* **25**:99-110.

Drosatos K, Khan RS, Trent CM, Jiang H, Son NH, Blaner WS, Homma S, Schulze PC and Goldberg IJ (2013) Peroxisome proliferator-activated receptor-γ activation prevents sepsis-related cardiac dysfunction and mortality in mice. *Circ Heart Fail* **6**:550-562.

Du G, Mouithys-Mickalad A and Sluse FE (1998) Generation of superoxide anion by mitochondria and impairment of their functions during anoxia and reoxygenation in vitro. *Free Radic Biol Med* **25**:1066-1074.

Echtay KS, Roussel D, St-Pierre J, Jekabsons MB, Cadenas S, Stuart JA, Harper JA, Roebuck SJ, Morrison A, Pickering S, Clapham JC and Brand MD (2002) Superoxide activates mitochondrial uncoupling proteins. *Nature* **415**:96-99.

Erridge C (2010) Endogenous ligands of TLR2 and TLR4: agonists or assistants? *J Leukoc Biol* **87**:989-999.

Exline MC and Crouser ED (2008) Mitochondrial mechanisms of sepsis-induced organ failure. *Front Biosci* **13**:5030-5041.

Fallach R, Shainberg A, Avlas O, Fainblut M, Chepurko Y, Porat E and Hochhauser E (2010) Cardiomyocyte Toll-like receptor 4 is involved in heart dysfunction following septic shock or myocardial ischemia. *JMolCell Cardiol* **48**:1236-1244.

Fang FC (2004) Antimicrobial reactive oxygen and nitrogen species: concepts and controversies. *Nat Rev Microbiol* **2**:820-832.

Ferreira FL, Ladrière L, Vincent JL and Malaisse WJ (2000) Prolongation of survival time by infusion of succinic acid dimethyl ester in a caecal ligation and perforation model of sepsis. *Horm Metab Res* **32**:335-336.

Fink MP (2001) Cytopathic hypoxia. Mitochondrial dysfunction as mechanism contributing to organ dysfunction in sepsis. *Crit Care Clin* **17**:219-237.

Fink MP (2002) Cytopathic hypoxia. Is oxygen use impaired in sepsis as a result of an acquired intrinsic derangement in cellular respiration? *Crit Care Clin* **18**:165-175.

Fink MP (2013) Animal models of sepsis. *Virulence* **5**.

Fisher-Wellman KH, Mattox TA, Thayne K, Katunga LA, La Favor JD, Neufer PD, Hickner RC, Wingard CJ and Anderson EJ (2013) Novel role for thioredoxin reductase-2 in mitochondrial redox adaptations to obesogenic diet and exercise in heart and skeletal muscle. *J Physiol* **591**:3471-3486.

Flierl MA, Rittirsch D, Huber-Lang MS, Sarma JV and Ward PA (2008) Molecular events in the cardiomyopathy of sepsis. *MolMed* **14**:327-336.

Flynn A, Chokkalingam MB and Mather PJ (2010) Sepsis-induced cardiomyopathy: a review of pathophysiologic mechanisms. *Heart FailRev* **15**:605-611.

Fusaro G, Dasgupta P, Rastogi S, Joshi B and Chellappan S (2003) Prohibitin induces the transcriptional activity of p53 and is exported from the nucleus upon apoptotic signaling. *JBiolChem* **278**:47853-47861.

Galley HF (2011) Oxidative stress and mitochondrial dysfunction in sepsis. *BrJAnaesth* **107**:57-64.

Gamble SC, Odontiadis M, Waxman J, Westbrook JA, Dunn MJ, Wait R, Lam EW and Bevan CL (2004) Androgens target prohibitin to regulate proliferation of prostate cancer cells. *Oncogene* **23**:2996-3004.

Garrabou G, Moren C, Lopez S, Tobias E, Cardellach F, Miro O and Casademont J (2012) The effects of sepsis on mitochondria. *JInfectDis* **205**:392-400.

George M, Ying G, Rainey MA, Solomon A, Parikh PT, Gao Q, Band V and Band H (2007) Shared as well as distinct roles of EHD proteins revealed by biochemical and functional comparisons in mammalian cells and C. elegans. *BMC Cell Biol* **8**:3.

Ghosh S and Karin M (2002) Missing pieces in the NF-kappaB puzzle. *Cell* **109 Suppl**:S81-96.

Goldfarb DS, Corbett AH, Mason DA, Harreman MT and Adam SA (2004) Importin alpha: a multipurpose nuclear-transport receptor. *Trends Cell Biol* **14**:505-514.

Gosbell AD, Stefanovic N, Scurr LL, Pete J, Kola I, Favilla I and de Haan JB (2006) Retinal light damage: structural and functional effects of the antioxidant glutathione peroxidase-1. *Invest OphthalmolVisSci* **47**:2613-2622.

Gregory-Bass RC, Olatinwo M, Xu W, Matthews R, Stiles JK, Thomas K, Liu D, Tsang B and Thompson WE (2008) Prohibitin silencing reverses stabilization of mitochondrial integrity and chemoresistance in ovarian cancer cells by increasing their sensitivity to apoptosis. *IntJCancer* **122**:1923-1930.

Griparic L, van der Wel NN, Orozco IJ, Peters PJ and van der Bliek AM (2004) Loss of the intermembrane space protein Mgm1/OPA1 induces swelling and localized constrictions along the lengths of mitochondria. *J Biol Chem* **279**:18792-18798.

Gu Y, Ande SR and Mishra S (2011) Altered O-GlcNAc modification and phosphorylation of mitochondrial proteins in myoblast cells exposed to high glucose. *Arch Biochem Biophys* **505**:98-104.

Guha M and Mackman N (2001) LPS induction of gene expression in human monocytes. *Cell Signal* **13**:85-94.

Guha M, O'Connell MA, Pawlinski R, Hollis A, McGovern P, Yan SF, Stern D and Mackman N (2001) Lipopolysaccharide activation of the MEK-ERK1/2 pathway in human monocytic cells mediates tissue factor and tumor necrosis factor alpha expression by inducing Elk-1 phosphorylation and Egr-1 expression. *Blood* **98**:1429-1439.

Gómez-Jiménez J, Salgado A, Mourelle M, Martín MC, Segura RM, Peracaula R and Moncada S (1995) L-arginine: nitric oxide pathway in endotoxemia and human septic shock. *Crit Care Med* **23**:253-258.

Hamid T, Guo SZ, Kingery JR, Xiang X, Dawn B and Prabhu SD (2011) Cardiomyocyte NF-kappaB p65 promotes adverse remodelling, apoptosis, and endoplasmic reticulum stress in heart failure. *CardiovascRes* **89**:129-138.

Harrois A, Huet O and Duranteau J (2009) Alterations of mitochondiral function in sepsis and critical illness. *Current Opnion in Anaesthesiology* **22**:143-149.

Hassoun SM, Marechal X, Montaigne D, Bouazza Y, Decoster B, Lancel S and Neviere R (2008) Prevention of endotoxin-induced sarcoplasmic reticulum calcium leak improves mitochondrial and myocardial dysfunction. *Crit Care Med* **36**:2590-2596.

He B, Feng Q, Mukherjee A, Lonard DM, DeMayo FJ, Katzenellenbogen BS, Lydon JP and O'Malley BW (2008) A repressive role for prohibitin in estrogen signaling. *Mol Endocrinol* **22**:344-360.

Heo SJ, Yoon WJ, Kim KN, Ahn GN, Kang SM, Kang DH, Affan A, Oh C, Jung WK and Jeon YJ (2010) Evaluation of anti-inflammatory effect of fucoxanthin isolated from brown algae in lipopolysaccharide-stimulated RAW 264.7 macrophages. *Food Chem Toxicol* **48**:2045-2051.

Hersch M, Gnidec AA, Bersten AD, Troster M, Rutledge FS and Sibbald WJ (1990) Histologic and ultrastructural changes in nonpulmonary organs during early hyperdynamic sepsis. *Surgery* **107**:397-410.

Hossen MN, Kajimoto K, Akita H, Hyodo M, Ishitsuka T and Harashima H (2010) Ligand-based targeted delivery of a peptide modified nanocarrier to endothelial cells in adipose tissue. *J Control Release* **147**:261-268.

Hotchkiss RS and Karl IE (2003) The pathophysiology and treatment of sepsis. *N Engl J Med* **348**:138-150.

Hsieh CH, Pai PY, Hsueh HW, Yuan SS and Hsieh YC (2011) Complete induction of autophagy is essential for cardioprotection in sepsis. *Ann Surg* **253**:1190-1200.

Hsieh SY, Shih TC, Yeh CY, Lin CJ, Chou YY and Lee YS (2006) Comparative proteomic studies on the pathogenesis of human ulcerative colitis. *Proteomics* **6**:5322-5331.

Ihle JN (1995) Cytokine receptor signalling. *Nature* **377**:591-594.

Ikonen E, Fiedler K, Parton RG and Simons K (1995) Prohibitin, an antiproliferative protein, is localized to mitochondria. *FEBS Lett* **358**:273-277.

Ishida H, Ichimori K, Hirota Y, Fukahori M and Nakazawa H (1996) Peroxynitrite-induced cardiac myocyte injury. *Free Radic Biol Med* **20**:343-350.

Israël A (2010) The IKK complex, a central regulator of NF-kappaB activation. *Cold Spring Harb Perspect Biol* **2**:a000158.

Itoh K, Ishii T, Wakabayashi N and Yamamoto M (1999) Regulatory mechanisms of cellular response to oxidative stress. *Free Radic Res* **31**:319-324.

Iwata A, de Claro RA, Morgan-Stevenson VL, Tupper JC, Schwartz BR, Liu L, Zhu X, Jordan KC, Winn RK and Harlan JM (2011) Extracellular administration of BCL2 protein reduces apoptosis and improves survival in a murine model of sepsis. *PLoS One* **6**:e14729.

Jia Y, Zhou F, Deng P, Fan Q, Li C, Liu Y, Fu X, Zhou Y, Xu X and Sun X (2012) Interleukin 6 protects H(2)O(2)-induced cardiomyocytes injury through upregulation of prohibitin via STAT3 phosphorylation. *Cell Biochem Funct* **30**:426-431.

Jon AB, Bernhard H and Michael S (2005) Animal Models of Sepsis: Setting the Stage. *Nature* **4**:854-865.

Kang X, Zhang L, Sun J, Ni Z, Ma Y, Chen X, Sheng X and Chen T (2008) Prohibitin: a potential biomarker for tissue-based detection of gastric cancer. *J Gastroenterol* **43**:618-625.

Kao YH, Chen YC, Cheng CC, Lee TI, Chen YJ and Chen SA (2010) Tumor necrosis factor-alpha decreases sarcoplasmic reticulum Ca2+-ATPase expressions via the promoter methylation in cardiomyocytes. *Crit Care Med* **38**:217-222.

Karin M and Lin A (2002) NF-kappaB at the crossroads of life and death. *Nat Immunol* **3**:221-227.

Kathiria AS, Butcher LD, Feagins LA, Souza RF, Boland CR and Theiss AL (2012a) Prohibitin 1 modulates mitochondrial stress-related autophagy in human colonic epithelial cells. *PLoSOne* **7**:e31231.

Kathiria AS, Butcher MA, Hansen JM and Theiss AL (2013) Nrf2 is not required for epithelial prohibitin-dependent attenuation of experimental colitis. *Am J Physiol Gastrointest Liver Physiol*.

Kathiria AS, Neumann WL, Rhees J, Hotchkiss E, Cheng Y, Genta RM, Meltzer SJ, Souza RF and Theiss AL (2012b) Prohibitin Attenuates Colitis-Associated Tumorigenesis in Mice by Modulating p53 and STAT3 Apoptotic Responses. *Cancer Res* **72**:5778-5789.

Katsumi K, Eriko O, Yasuo K and Hitoshi E (2006) Mitochondrial functions and esterongen receptor-dependent nuclear translocation of pleiotropic human prohibitin2. *The Journal of Biological Chemistry* **281**:36401-36410.

Kelm M, Schäfer S, Dahmann R, Dolu B, Perings S, Decking UK, Schrader J and Strauer BE (1997) Nitric oxide induced contractile dysfunction is related to a reduction in myocardial energy generation. *Cardiovasc Res* **36**:185-194.

Khadour FH, Panas D, Ferdinandy P, Schulze C, Csont T, Lalu MM, Wildhirt SM and Schulz R (2002) Enhanced NO and superoxide generation in dysfunctional hearts from endotoxemic rats. *Am J Physiol Heart Circ Physiol* **283**:H1108-1115.

Kilbourn RG, Gross SS, Jubran A, Adams J, Griffith OW, Levi R and Lodato RF (1990a) NG-methyl-L-arginine inhibits tumor necrosis factor-induced hypotension: implications for the involvement of nitric oxide. *ProcNatlAcadSciUSA* **87**:3629-3632.

Kilbourn RG, Jubran A, Gross SS, Griffith OW, Levi R, Adams J and Lodato RF (1990b) Reversal of endotoxin-mediated shock by NG-methyl-L-arginine, an inhibitor of nitric oxide synthesis. *BiochemBiophysResCommun* **172**:1132-1138.

Kolonin MG, Saha PK, Chan L, Pasqualini R and Arap W (2004) Reversal of obesity by targeted ablation of adipose tissue. *NatMed* **10**:625-632.

Kong X, Thimmulappa R, Craciun F, Harvey C, Singh A, Kombairaju P, Reddy SP, Remick D and Biswal S (2011) Enhancing Nrf2 pathway by disruption of Keap1 in myeloid leukocytes protects against sepsis. *Am J Respir Crit Care Med* **184**:928-938.

Krishnagopalan S, Kumar A and Parrillo JE (2002) Myocardial dysfunction in the patient with sepsis. *Curr Opin Crit Care* **8**:376-388.

Kuhlmann MK, Shahmir E, Maasarani E, Akhtar S, Thevanayagam V, Vadgama JV and Kopple JD (1994) New experimental model of acute renal failure and sepsis in rats. *JPEN J Parenter Enteral Nutr* **18**:477-485.

Kuldo JM, Westra J, Asgeirsdottir SA, Kok RJ, Oosterhuis K, Rots MG, Schouten JP, Limburg PC and Molema G (2005) Differential effects of NF-{kappa}B and p38 MAPK inhibitors and combinations thereof on TNF-{alpha}- and IL-1{beta}-induced proinflammatory status of endothelial cells in vitro. *AmJPhysiol Cell Physiol* **289**:C1229-C1239.

Kumar A, Krieger A, Symeoneides S and Parrillo JE (2001) Myocardial dysfunction in septic shock: Part II. Role of cytokines and nitric oxide. *JCardiothoracVascAnesth* **15**:485-511.

Kumar A, Thota V, Dee L, Olson J, Uretz E and Parrillo JE (1996) Tumor necrosis factor alpha and interleukin 1beta are responsible for in vitro myocardial cell depression induced by human septic shock serum. *J Exp Med* **183**:949-958.

Kyriakis JM and Avruch J (2012) Mammalian MAPK signal transduction pathways activated by stress and inflammation: a 10-year update. *Physiol Rev* **92**:689-737.

Lancel S, Joulin O, Favory R, Goossens JF, Kluza J, Chopin C, Formstecher P, Marchetti P and Neviere R (2005) Ventricular myocyte caspases are directly responsible for endotoxin-induced cardiac dysfunction. *Circulation* **111**:2596-2604.

Lancel S, Tissier S, Mordon S, Marechal X, Depontieu F, Scherpereel A, Chopin C and Neviere R (2004) Peroxynitrite decomposition catalysts prevent myocardial dysfunction and inflammation in endotoxemic rats. *J Am Coll Cardiol* **43**:2348-2358.

Landry DW and Oliver JA (2001) The pathogenesis of vasodilatory shock. *N Engl J Med* **345**:588-595.

Larche J, Lancel S, Hassoun SM, Favory R, Decoster B, Marchetti P, Chopin C and Neviere R (2006) Inhibition of mitochondrial permeability transition prevents sepsis-induced myocardial dysfunction and mortality. *J Am Coll Cardiol* **48**:377-385.

Lauzurica P, Martinez-Martinez S, Marazuela M, Gomez del AP, Martinez C, Sanchez-Madrid F and Redondo JM (1999) Pyrrolidine dithiocarbamate protects mice from lethal shock induced by LPS or TNF-alpha. *EurJImmunol* **29**:1890-1900.

Le Minh K, Kuhla A, Abshagen K, Minor T, Stegemann J, Ibrahim S, Eipel C and Vollmar B (2009) Uncoupling protein-2 deficiency provides protection in a murine model of endotoxemic acute liver failure. *Crit Care Med* **37**:215-222.

Lee JH, Nguyen KH, Mishra S and Nyomba BL (2010) Prohibitin is expressed in pancreatic beta-cells and protects against oxidative and proapoptotic effects of ethanol. *FEBS J* **277**:488-500.

Lesnefsky EJ, Moghaddas S, Tandler B, Kerner J and Hoppel CL (2001) Mitochondrial dysfunction in cardiac disease: ischemia--reperfusion, aging, and heart failure. *J Mol Cell Cardiol* **33**:1065-1089.

Levine B and Deretic V (2007) Unveiling the roles of autophagy in innate and adaptive immunity. *Nat Rev Immunol* **7**:767-777.

Levy MM, Dellinger RP, Townsend SR, Linde-Zwirble WT, Marshall JC, Bion J, Schorr C, Artigas A, Ramsay G, Beale R, Parker MM, Gerlach H, Reinhart K, Silva E, Harvey M, Regan S and Angus DC (2010) The Surviving Sepsis Campaign: results of an international guideline-based performance improvement program targeting severe sepsis. *Intensive Care Med* **36**:222-231.

Levy RJ (2007) Mitochondrial dysfunction, bioenergetic impairment, and metabolic down-regulation in sepsis. *Shock* **28**:24-28.

Li N, Ragheb K, Lawler G, Sturgis J, Rajwa B, Melendez JA and Robinson JP (2003) Mitochondrial complex I inhibitor rotenone induces apoptosis through enhancing mitochondrial reactive oxygen species production. *J Biol Chem* **278**:8516-8525.

Li X, Su J, Cui X, Li Y, Barochia A and Eichacker PQ (2009) Can we predict the effects of NF-kappaB inhibition in sepsis? Studies with parthenolide and ethyl pyruvate. *Expert Opin Investig Drugs* **18**:1047-1060.

Li YP, Atkins CM, Sweatt JD and Reid MB (1999) Mitochondria mediate tumor necrosis factor-alpha/NF-kappaB signaling in skeletal muscle myotubes. *Antioxid Redox Signal* **1**:97-104.

Lichtenstern C, Brenner T, Bardenheuer HJ and Weigand MA (2012) Predictors of survival in sepsis: what is the best inflammatory marker to measure? *Curr Opin Infect Dis* **25**:328-336.

Liu JS, Jung F, Yang SH, Chou SS, Huang JL, Lu CL, Huang GL, Yang PC, Lin JC and Jow GM (2013) FJU-C4, a New 2-Pyridone Compound, Attenuates Lipopolysaccharide-Induced Systemic Inflammation via p38MAPK and NF-κB in Mice. *PLoS One* **8**:e82877.

Liu SF and Malik AB (2006) NF-kappa B activation as a pathological mechanism of septic shock and inflammation. *Am J Physiol Lung Cell Mol Physiol* **290**:L622-L645.

Liu XH, Ren Z, Zhan R, Wang X, Wang XM, Zhang ZQ, Leng X, Yang ZH and Qian L (2009) Prohibitin protects against oxidative stress-induced cell injury in cultured neonatal cardiomyocyte. *Cell Stress & Chaperones* **14**:319.

Lowes DA, Thottakam BM, Webster NR, Murphy MP and Galley HF (2008) The mitochondria-targeted antioxidant MitoQ protects against organ damage in a lipopolysaccharide-peptidoglycan model of sepsis. *Free RadicBiolMed* **45**:1559-1565.

Lowes DA, Webster NR, Murphy MP and Galley HF (2013) Antioxidants that protect mitochondria reduce interleukin-6 and oxidative stress, improve mitochondrial function, and reduce biochemical markers of organ dysfunction in a rat model of acute sepsis. *Br J Anaesth* **110**:472-480.

Lucas CR, Cordero-Nieves HM, Erbe RS, McAlees JW, Bhatia S, Hodes RJ, Campbell KS and Sanders VM (2013) Prohibitins and the Cytoplasmic Domain of CD86 Cooperate To Mediate CD86 Signaling in B Lymphocytes. *JImmunol* **190**:723-736.

Maechler P and Wollheim CB (2001) Mitochondrial function in normal and diabetic beta-cells. *Nature* **414**:807-812.

Mahmood V, Suresh M, Saby M and Liam JM (2006) Prohibitin attenuates insulin-stimulated glucose and fatty acid oxidation in adipose tissue by inhibition id pyruvate carboxylase. *The FASEB Journa* **273**:568-576.

Majno G (1991) The ancient riddle of sigma eta psi iota sigma (sepsis). *J Infect Dis* **163**:937-945.

Makowski L, Noland RC, Koves TR, Xing W, Ilkayeva OR, Muehlbauer MJ, Stevens RD and Muoio DM (2009) Metabolic profiling of PPARalpha-/- mice reveals defects in carnitine

and amino acid homeostasis that are partially reversed by oral carnitine supplementation. *FASEB J* **23**:586-604.

Malaisse WJ, Nadi AB, Ladriere L and Zhang TM (1997) Protective effects of succinic acid dimethyl ester infusion in experimental endotoxemia. *Nutrition* **13**:330-341.

Manjeshwar S, Branam DE, Lerner MR, Brackett DJ and Jupe ER (2003) Tumor suppression by the prohibitin gene 3'untranslated region RNA in human breast cancer. *Cancer Res* **63**:5251-5256.

Manjeshwar S, Lerner MR, Zang XP, Branam DE, Pento JT, Lane MM, Lightfoot SA, Brackett DJ and Jupe ER (2004) Expression of prohibitin 3' untranslated region suppressor RNA alters morphology and inhibits motility of breast cancer cells. *JMolHistol* **35**:639-646.

Marchetti P, Castedo M, Susin SA, Zamzami N, Hirsch T, Macho A, Haeffner A, Hirsch F, Geuskens M and Kroemer G (1996) Mitochondrial permeability transition is a central coordinating event of apoptosis. *J Exp Med* **184**:1155-1160.

Marhl M, Schuster S and Brumen M (1998) Mitochondria as an important factor in the maintenance of constant amplitudes of cytosolic calcium oscillations. *Biophys Chem* **71**:125-132.

Mariappan N, Soorappan RN, Haque M, Sriramula S and Francis J (2007) TNF-alpha-induced mitochondrial oxidative stress and cardiac dysfunction: restoration by superoxide dismutase mimetic Tempol. *AmJPhysiol Heart CircPhysiol* **293**:H2726-H2737.

McBride HM, Neuspiel M and Wasiak S (2006) Mitochondria: more than just a powerhouse. *Curr Biol* **16**:R551-560.

McClung JK, Danner DB, Stewart DA, Smith JR, Schneider EL, Lumpkin CK, Dell'Orco RT and Nuell MJ (1989) Isolation of a cDNA that hybrid selects antiproliferative mRNA from rat liver. *BiochemBiophysResCommun* **164**:1316-1322.

McDonough KH, Smith T, Patel K and Quinn M (1998) Myocardial dysfunction in the septic rat heart: role of nitric oxide. *Shock* **10**:371-376.

McKenzie SJ, Baker MS, Buffinton GD and Doe WF (1996) Evidence of oxidant-induced injury to epithelial cells during inflammatory bowel disease. *J Clin Invest* **98**:136-141.

Medvedev AE, Lentschat A, Kuhns DB, Blanco JC, Salkowski C, Zhang S, Arditi M, Gallin JI and Vogel SN (2003) Distinct mutations in IRAK-4 confer hyporesponsiveness to lipopolysaccharide and interleukin-1 in a patient with recurrent bacterial infections. *J Exp Med* **198**:521-531.

Melamed A and Sorvillo FJ (2009) The burden of sepsis-associated mortality in the United States from 1999 to 2005: an analysis of multiple-cause-of-death data. *Crit Care* **13**:R28.

Mengwasser J, Piau A, Schlag P and Sleeman JP (2004) Differential immunization identifies PHB1/PHB2 as blood-borne tumor antigens. *Oncogene* **23**:7430-7435.

Merkwirth C, Dargazanli S, Tatsuta T, Geimer S, Löwer B, Wunderlich FT, von Kleist-Retzow JC, Waisman A, Westermann B and Langer T (2008) Prohibitins control cell proliferation and apoptosis by regulating OPA1-dependent cristae morphogenesis in mitochondria. *Genes Dev* **22**:476-488.

Merkwirth C and Langer T (2009) Prohibitin function within mitochondria: essential roles for cell proliferation and cristae morphogenesis. *BiochimBiophysActa* **1793**:27-32.

Merx MW, Liehn EA, Janssens U, Lütticken R, Schrader J, Hanrath P and Weber C (2004) HMG-CoA reductase inhibitor simvastatin profoundly improves survival in a murine model of sepsis. *Circulation* **109**:2560-2565.

Merx MW and Weber C (2007) Sepsis and the heart. *Circulation* **116**:793-802.

Mielenz D, Vettermann C, Hampel M, Lang C, Avramidou A, Karas M and Jäck HM (2005) Lipid rafts associate with intracellular B cell receptors and exhibit a B cell stage-specific protein composition. *J Immunol* **174**:3508-3517.

Mishra S, Ande SR and Nyomba G (2010) The role of prohibitin in cell signaling. *The FASEB Journal* **277**:3937-3946.

Mishra S, Moulik S and Murphy LJ (2007) Prohibitin binds to C3 and enhances complement activation. *MolImmunol* **44**:1897-1902.

Mishra V (2007) Oxidative stress and role of antioxidant supplementation in critical illness. *Clin Lab* **53**:199-209.

MITCHELL P (1961) Coupling of phosphorylation to electron and hydrogen transfer by a chemi-osmotic type of mechanism. *Nature* **191**:144-148.

Mizushima N, Levine B, Cuervo AM and Klionsky DJ (2008) Autophagy fights disease through cellular self-digestion. *Nature* **451**:1069-1075.

Mofarrahi M, Sigala I, Guo Y, Godin R, Davis EC, Petrof B, Sandri M, Burelle Y and Hussain SN (2012) Autophagy and skeletal muscles in sepsis. *PLoS One* **7**:e47265.

Muraguchi T, Kawawa A and Kubota S (2010) Prohibitin protects against hypoxia-induced H9c2 cardiomyocyte cell death. *Biomedical Research* **31**:113-122.

Natanson C, Fink MP, Ballantyne HK, MacVittie TJ, Conklin JJ and Parrillo JE (1986) Gram-negative bacteremia produces both severe systolic and diastolic cardiac dysfunction in a canine model that simulates human septic shock. *J Clin Invest* **78**:259-270.

NC3Rs National Centre for the Replacement Refinement & Reduction of Animals in Research, in, London, England.

Nijtmans LG, Artal SM, Grivell LA and Coates PJ (2002) The mitochondrial PHB complex: roles in mitochondrial respiratory complex assembly, ageing and degenerative disease. *Cell MolLife Sci* **59**:143-155.

Nijtmans LG, de JL, Artal SM, Coates PJ, Berden JA, Back JW, Muijsers AO, van der Spek H and Grivell LA (2000) Prohibitins act as a membrane-bound chaperone for the stabilization of mitochondrial proteins. *EMBO J* **19**:2444-2451.

Niu J, Azfer A, Rogers LM, Wang X and Kolattukudy PE (2007) Cardioprotective effects of cerium oxide nanoparticles in a transgenic murine model of cardiomyopathy. *CardiovascRes* **73**:549-559.

O'Neill LA (2002) Signal transduction pathways activated by the IL-1 receptor/toll-like receptor superfamily. *Curr Top Microbiol Immunol* **270**:47-61.

Ochoa JB, Udekwu AO, Billiar TR, Curran RD, Cerra FB, Simmons RL and Peitzman AB (1991) Nitrogen oxide levels in patients after trauma and during sepsis. *Ann Surg* **214**:621-626.

Ohsumi Y (2001) Molecular dissection of autophagy: two ubiquitin-like systems. *Nat Rev Mol Cell Biol* **2**:211-216.

Opal SM, Laterre PF, Francois B, LaRosa SP, Angus DC, Mira JP, Wittebole X, Dugernier T, Perrotin D, Tidswell M, Jauregui L, Krell K, Pachl J, Takahashi T, Peckelsen C,

Cordasco E, Chang CS, Oeyen S, Aikawa N, Maruyama T, Schein R, Kalil AC, Van Nuffelen M, Lynn M, Rossignol DP, Gogate J, Roberts MB, Wheeler JL, Vincent JL and Group AS (2013) Effect of eritoran, an antagonist of MD2-TLR4, on mortality in patients with severe sepsis: the ACCESS randomized trial. *JAMA* **309**:1154-1162.

Osman C, Haag M, Potting C, Rodenfels J, Dip PV, Wieland FT, Brügger B, Westermann B and Langer T (2009a) The genetic interactome of prohibitins: coordinated control of cardiolipin and phosphatidylethanolamine by conserved regulators in mitochondria. *J Cell Biol* **184**:583-596.

Osman C, Merkwirth C and Langer T (2009b) Prohibitins and the functional compartmentalization of mitochondrial membranes. *JCell Sci* **122**:3823-3830.

P.J.Coates, R.Nenutil, McGregor A, M.Picksley, D.H.Crouch, P.A.Hall and Wright EG (2001) Mammalian prohibitin proeins responf to mitochondrial stress and decrease during cellular sencence. *Experimental Cell Research* **265**:262-273.

Pan Z, Zhao W, Zhang X, Wang B, Wang J, Sun X, Liu X, Feng S, Yang B and Lu Y (2011) Scutellarin alleviates interstitial fibrosis and cardiac dysfunction of infarct rats by inhibiting TGFβ1 expression and activation of p38-MAPK and ERK1/2. *Br J Pharmacol* **162**:688-700.

Park SE, Xu J, Frolova A, Liao L, O'Malley BW and Katzenellenbogen BS (2005) Genetic deletion of the repressor of estrogen receptor activity (REA) enhances the response to estrogen in target tissues in vivo. *Mol Cell Biol* **25**:1989-1999.

Parrillo JE, Parker MM, Natanson C, Suffredini AF, Danner RL, Cunnion RE and Ognibene FP (1990) Septic shock in humans. Advances in the understanding of pathogenesis, cardiovascular dysfunction, and therapy. *AnnInternMed* **113**:227-242.

Patel N, Chatterjee SK, Vrbanac V, Chung I, Mu CJ, Olsen RR, Waghorne C and Zetter BR (2010) Rescue of paclitaxel sensitivity by repression of Prohibitin1 in drug-resistant cancer cells. *Proc Natl Acad Sci U S A* **107**:2503-2508.

Paul A, Ko KW, Li L, Yechoor V, McCrory MA, Szalai AJ and Chan L (2004) C-reactive protein accelerates the progression of atherosclerosis in apolipoprotein E-deficient mice. *Circulation* **109**:647-655.

Perera S, Holt MR, Mankoo BS and Gautel M (2011) Developmental regulation of MURF ubiquitin ligases and autophagy proteins nbr1, p62/SQSTM1 and LC3 during cardiac myofibril assembly and turnover. *Dev Biol* **351**:46-61.

Perry CG, Kane DA, Lin CT, Kozy R, Cathey BL, Lark DS, Kane CL, Brophy PM, Gavin TP, Anderson EJ and Neufer PD (2011) Inhibiting myosin-ATPase reveals a dynamic range of mitochondrial respiratory control in skeletal muscle. *Biochem J* **437**:215-222.

Petros A, Bennett D and Vallance P (1991) Effect of nitric oxide synthase inhibitors on hypotension in patients with septic shock. *Lancet* **338**:1557-1558.

Petros A, Lamb G, Leone A, Moncada S, Bennett D and Vallance P (1994) Effects of a nitric oxide synthase inhibitor in humans with septic shock. *CardiovascRes* **28**:34-39.

Petrozzi L, Ricci G, Giglioli NJ, Siciliano G and Mancuso M (2007) Mitochondria and neurodegeneration. *Biosci Rep* **27**:87-104.

Picard C, Pellicelli M, Taheri M, Lavoie JF, Doucet R, Wang D, Bernard L, Bouhanik S, Lavigne P and Moreau A (2013) Nuclear accumulation of prohibitin 1 in osteoarthritic chondrocytes down-regulates PITX1 expression. *Arthritis Rheum* **65**:993-1003.

Poelaert J, Declerck C, Vogelaers D, Colardyn F and Visser CA (1997) Left ventricular systolic and diastolic function in septic shock. *Intensive Care Med* **23**:553-560.

Poulton J, O'Rahilly S, Morten KJ and Clark A (1995) Mitochondrial DNA, diabetes and pancreatic pathology in Kearns-Sayre syndrome. *Diabetologia* **38**:868-871.

Protti A, Carre J, Frost MT, Taylor V, Stidwill R, Rudiger A and Singer M (2007) Succinate recovers mitochondrial oxygen consumption in septic rat skeletal muscle. *Crit Care Med* **35**:2150-2155.

Rabuel C and Mebazaa A (2006) Septic shock: a heart story since the 1960s. *Intensive Care Med* **32**:799-807.

Rachmilewitz D, Stamler JS, Bachwich D, Karmeli F, Ackerman Z and Podolsky DK (1995) Enhanced colonic nitric oxide generation and nitric oxide synthase activity in ulcerative colitis and Crohn's disease. *Gut* **36**:718-723.

Raffaello A, Milan G, Masiero E, Carnio S, Lee D, Lanfranchi G, Goldberg AL and Sandri M (2010) JunB transcription factor maintains skeletal muscle mass and promotes hypertrophy. *J Cell Biol* **191**:101-113.

Rajalingam K and Rudel T (2005) Ras-Raf signaling needs prohibitin. *Cell Cycle* **4**:1503-1505.

Rajalingam K, Wunder C, Brinkmann V, Churin Y, Hekman M, Sievers C, Rapp UR and Rudel T (2005) Prohibitin is required for Ras-induced Raf-MEK-ERK activation and epithelial cell migration. *Nat Cell Biol* **7**:837-843.

Ramana KV, Willis MS, White MD, Horton JW, DiMaio JM, Srivastava D, Bhatnagar A and Srivastava SK (2006) Endotoxin-induced cardiomyopathy and systemic inflammation in mice is prevented by aldose reductase inhibition. *Circulation* **114**:1838-1846.

Rastogi S, Joshi B, Fusaro G and Chellappan S (2006) Camptothecin induces nuclear export of prohibitin preferentially in transformed cells through a CRM-1-dependent mechanism. *JBiolChem* **281**:2951-2959.

Ren HZ, Wang JS, Wang P, Pan GQ, Wen JF, Fu H and Shan XZ (2010) Increased expression of prohibitin and its relationship with poor prognosis in esophageal squamous cell carcinoma. *PatholOncolRes* **16**:515-522.

Ren J, Ren BH and Sharma AC (2002) Sepsis-induced depressed contractile function of isolated ventricular myocytes is due to altered calcium transient properties. *Shock* **18**:285-288.

Rittirsch D, Huber-Lang MS, Flierl MA and Ward PA (2009) Immunodesign of experimental sepsis by cecal ligation and puncture. *Nat Protoc* **4**:31-36.

Roshon MJ, Kline JA, Thornton LR and Watts JA (2003) Cardiac UCP2 expression and myocardial oxidative metabolism during acute septic shock in the rat. *Shock* **19**:570-576.

Ross JA, Nagy ZS and Kirken RA (2008) The PHB1/2 phosphocomplex is required for mitochondrial homeostasis and survival of human T cells. *JBiolChem* **283**:4699-4713.

Rudiger A (2010) Beta-block the septic heart. *Crit Care Med* **38**:S608-612.

Rudiger A and Singer M (2007) Mechanisms of sepsis-induced cardiac dysfunction. *Crit Care Med* **35**:1599-1608.

Saitoh T, Fujita N, Jang MH, Uematsu S, Yang BG, Satoh T, Omori H, Noda T, Yamamoto N, Komatsu M, Tanaka K, Kawai T, Tsujimura T, Takeuchi O, Yoshimori T and Akira S (2008) Loss of the autophagy protein Atg16L1 enhances endotoxin-induced IL-1beta production. *Nature* **456**:264-268.

Saks V, Dos Santos P, Gellerich FN and Diolez P (1998) Quantitative studies of enzyme-substrate compartmentation, functional coupling and metabolic channelling in muscle cells. *Mol Cell Biochem* **184**:291-307.

Sanchez-Quiles V, Segura V, Bigaud E, He B, O'Malley BW, Santamaria E, Prieto J and Corrales FJ (2012) Prohibitin-1 deficiency promotes inflammation and increases sensitivity to liver injury. *JProteomics* **75**:5783-5792.

Sato T, Sakamoto T, Takita K, Saito H, Okui K and Nakamura Y (1993) The human prohibitin (PHB) gene family and its somatic mutations in human tumors. *Genomics* **17**:762-764.

Schleicher M, Shepherd BR, Suarez Y, Fernandez-Hernando C, Yu J, Pan Y, Acevedo LM, Shadel GS and Sessa WC (2008) Prohibitin-1 maintains the angiogenic capacity of endothelial cells by regulating mitochondrial function and senescence. *J Cell Biol* **180**:101-112.

Schumer W, Erve PR and Obernolte RP (1971) Endotoxemic effect on cardiac and skeletal muscle mitochondria. *Surg Gynecol Obstet* **133**:433-436.

Scott MJ, Godshall CJ and Cheadle WG (2002) Jaks, STATs, Cytokines, and Sepsis. *Clin Diagn Lab Immunol* **9**:1153-1159.

Sen T, Sen N, Jana S, Khan FH, Chatterjee U and Chakrabarti S (2007) Depolarization and cardiolipin depletion in aged rat brain mitochondria: relationship with oxidative stress and electron transport chain activity. *Neurochem Int* **50**:719-725.

Seok J, Warren HS, Cuenca AG, Mindrinos MN, Baker HV, Xu W, Richards DR, McDonald-Smith GP, Gao H, Hennessy L, Finnerty CC, López CM, Honari S, Moore EE, Minei JP, Cuschieri J, Bankey PE, Johnson JL, Sperry J, Nathens AB, Billiar TR, West MA, Jeschke MG, Klein MB, Gamelli RL, Gibran NS, Brownstein BH, Miller-Graziano C, Calvano SE, Mason PH, Cobb JP, Rahme LG, Lowry SF, Maier RV, Moldawer LL, Herndon DN, Davis RW, Xiao W, Tompkins RG and Inflammation and Host Response

to Injury LrSCRP (2013) Genomic responses in mouse models poorly mimic human inflammatory diseases. *Proc Natl Acad Sci U S A* **110**:3507-3512.

Sharma A and Qadri A (2004) Vi polysaccharide of Salmonella typhi targets the prohibitin family of molecules in intestinal epithelial cells and suppresses early inflammatory responses. *ProcNatlAcadSciUSA* **101**:17492-17497.

Sharma AC (2007) Sepsis-induced myocardial dysfunction. *Shock* **28**:265-269.

Shoffner JM, Lott MT, Voljavec AS, Soueidan SA, Costigan DA and Wallace DC (1989) Spontaneous Kearns-Sayre/chronic external ophthalmoplegia plus syndrome associated with a mitochondrial DNA deletion: a slip-replication model and metabolic therapy. *Proc Natl Acad Sci U S A* **86**:7952-7956.

Singer M (2008) Cellular dysfunction in sepsis. *Clin Chest Med* **29**:655-660, viii-ix.

Snell RJ and Parrillo JE (1991) Cardiovascular dysfunction in septic shock. *Chest* **99**:1000-1009.

Sripathi SR, He W, Atkinson CL, Smith JJ, Liu Z, Elledge BM and Jahng WJ (2011) Mitochondrial-nuclear communication by prohibitin shuttling under oxidative stress. *Biochemistry* **50**:8342-8351.

Staubach S, Razawi H and Hanisch FG (2009) Proteomics of MUC1-containing lipid rafts from plasma membranes and exosomes of human breast carcinoma cells MCF-7. *Proteomics* **9**:2820-2835.

Steglich G, Neupert W and Langer T (1999) Prohibitins regulate membrane protein degradation by the m-AAA protease in mitochondria. *Mol Cell Biol* **19**:3435-3442.

Stengl M, Bartak F, Sykora R, Chvojka J, Benes J, Krouzecky A, Novak I, Sviglerova J, Kuncova J and Matejovic M (2010) Reduced L-type calcium current in ventricular myocytes from pigs with hyperdynamic septic shock. *Crit Care Med* **38**:579-587.

Suffredini AF, Reda D, Banks SM, Tropea M, Agosti JM and Miller R (1995) Effects of recombinant dimeric TNF receptor on human inflammatory responses following intravenous endotoxin administration. *J Immunol* **155**:5038-5045.

Suliman HB, Welty-Wolf KE, Carraway M, Tatro L and Piantadosi CA (2004) Lipopolysaccharide induces oxidative cardiac mitochondrial damage and biogenesis. *Cardiovasc Res* **64**:279-288.

Supinski GS, Murphy MP and Callahan LA (2009) MitoQ administration prevents endotoxin-induced cardiac dysfunction. *AmJPhysiol RegulIntegrComp Physiol* **297**:R1095-R1102.

Svistunenko DA, Davies N, Brealey D, Singer M and Cooper CE (2006) Mitochondrial dysfunction in patients with severe sepsis: an EPR interrogation of individual respiratory chain components. *BiochimBiophysActa* **1757**:262-272.

Takeda K, Clausen BE, Kaisho T, Tsujimura T, Terada N, Förster I and Akira S (1999) Enhanced Th1 activity and development of chronic enterocolitis in mice devoid of Stat3 in macrophages and neutrophils. *Immunity* **10**:39-49.

Takeyama N, Takagi D, Matsuo N, Kitazawa Y and Tanaka T (1989) Altered hepatic fatty acid metabolism in endotoxicosis: effect of L-carnitine on survival. *Am J Physiol* **256**:E31-38.

Tanida I (2011) Autophagosome formation and molecular mechanism of autophagy. *Antioxid Redox Signal* **14**:2201-2214.

Tatsuta T, Model K and Langer T (2005) Formation of membrane-bound ring complexes by prohibitins in mitochondria. *Mol Biol Cell* **16**:248-259.

Taveira da Silva AM, Kaulbach HC, Chuidian FS, Lambert DR, Suffredini AF and Danner RL (1993) Brief report: shock and multiple-organ dysfunction after self-administration of Salmonella endotoxin. *N Engl J Med* **328**:1457-1460.

Tavener SA, Long EM, Robbins SM, McRae KM, Van Remmen H and Kubes P (2004) Immune cell Toll-like receptor 4 is required for cardiac myocyte impairment during endotoxemia. *Circ Res* **95**:700-707.

Taylor SW, Fahy E, Zhang B, Glenn GM, Warnock DE, Wiley S, Murphy AN, Gaucher SP, Capaldi RA, Gibson BW and Ghosh SS (2003) Characterization of the human heart mitochondrial proteome. *NatBiotechnol* **21**:281-286.

Theiss AL, Idell RD, Srinivasan S, Klapproth JM, Jones DP, Merlin D and Sitaraman SV (2007a) Prohibitin protects against oxidative stress in intestinal epithelial cells. *FASEB J* **21**:197-206.

Theiss AL, Jenkins AK, Okoro NI, Klapproth JM, Merlin D and Sitaraman SV (2009a) Prohibitin inhibits tumor necrosis factor alpha-induced nuclear factor-kappa B nuclear translocation via the novel mechanism of decreasing importin alpha3 expression. *MolBiolCell* **20**:4412-4423.

Theiss AL, Laroui H, Obertone TS, Chowdhury I, Thompson WE, Merlin D and Sitaraman SV (2011) Nanoparticle-based therapeutic delivery of prohibitin to the colonic epithelial cells ameliorates acute murine colitis. *InflammBowelDis* **17**:1163-1176.

Theiss AL, Obertone TS, Merlin D and Sitaraman SV (2007b) Interleukin-6 transcriptionally regulates prohibitin expression in intestinal epithelial cells. *JBiolChem* **282**:12804-12812.

Theiss AL, Vijay-Kumar M, Obertone TS, Jones DP, Hansen JM, Gewirtz AT, Merlin D and Sitaraman SV (2009b) Prohibitin is a novel regulator of antioxidant response that attenuates colonic inflammation in mice. *Gastroenterology* **137**:199-208, 208.

Thimmulappa RK, Lee H, Rangasamy T, Reddy SP, Yamamoto M, Kensler TW and Biswal S (2006) Nrf2 is a critical regulator of the innate immune response and survival during experimental sepsis. *J Clin Invest* **116**:984-995.

Thundathil J, Filion F and Smith LC (2005) Molecular control of mitochondrial function in preimplantation mouse embryos. *Mol Reprod Dev* **71**:405-413.

Tsai HW, Chow NH, Lin CP, Chan SH, Chou CY and Ho CL (2006) The significance of prohibitin and c-Met/hepatocyte growth factor receptor in the progression of cervical adenocarcinoma. *Hum Pathol* **37**:198-204.

Tsien RY (1988) Fluorescence measurement and photochemical manipulation of cytosolic free calcium. *Trends Neurosci* **11**:419-424.

van Gestel RA, Rijken PJ, Surinova S, O'Flaherty M, Heck AJ, Killian JA, de Kroon AI and Slijper M (2010) The influence of the acyl chain composition of cardiolipin on the stability of mitochondrial complexes; an unexpected effect of cardiolipin in alpha-ketoglutarate dehydrogenase and prohibitin complexes. *J Proteomics* **73**:806-814.

Vanasco V, Cimolai MC, Evelson P and Alvarez S (2008) The oxidative stress and the mitochondrial dysfunction caused by endotoxemia are prevented by alpha-lipoic acid. *Free RadicRes* **42**:815-823.

Venugopal R and Jaiswal AK (1996) Nrf1 and Nrf2 positively and c-Fos and Fra1 negatively regulate the human antioxidant response element-mediated expression of NAD(P)H:quinone oxidoreductase1 gene. *Proc Natl Acad Sci U S A* **93**:14960-14965.

Verma IM, Stevenson JK, Schwarz EM, Van Antwerp D and Miyamoto S (1995) Rel/NF-kappa B/I kappa B family: intimate tales of association and dissociation. *Genes Dev* **9**:2723-2735.

Vessal M, Mishra S, Moulik S and Murphy LJ (2006) Prohibitin attenuates insulin-stimulated glucose and fatty acid oxidation in adipose tissue by inhibition of pyruvate carboxylase. *FEBS J* **273**:568-576.

Vincent JL, Nelson DR and Williams MD (2011) Is worsening multiple organ failure the cause of death in patients with severe sepsis? *Crit Care Med* **39**:1050-1055.

Wagner DA, Young VR and Tannenbaum SR (1983) Mammalian nitrate biosynthesis: incorporation of 15NH3 into nitrate is enhanced by endotoxin treatment. *Proc Natl Acad Sci U S A* **80**:4518-4521.

Wallace CJ, Mascagni P, Chait BT, Collawn JF, Paterson Y, Proudfoot AE and Kent SB (1989) Substitutions engineered by chemical synthesis at three conserved sites in mitochondrial cytochrome c. Thermodynamic and functional consequences. *J Biol Chem* **264**:15199-15209.

Wang P, Mariman E, Keijer J, Bouwman F, Noben JP, Robben J and Renes J (2004) Profiling of the secreted proteins during 3T3-L1 adipocyte differentiation leads to the identification of novel adipokines. *Cell MolLife Sci* **61**:2405-2417.

Wang S, Fusaro G, Padmanabhan J and Chellappan SP (2002a) Prohibitin co-localizes with Rb in the nucleus and recruits N-CoR and HDAC1 for transcriptional repression. *Oncogene* **21**:8388-8396.

Wang S, Nath N, Adlam M and Chellappan S (1999a) Prohibitin, a potential tumor suppressor, interacts with RB and regulates E2F function. *Oncogene* **18**:3501-3510.

Wang S, Nath N, Fusaro G and Chellappan S (1999b) Rb and prohibitin target distinct regions of E2F1 for repression and respond to different upstream signals. *MolCell Biol* **19**:7447-7460.

Wang S, Zhang B and Faller DV (2002b) Prohibitin requires Brg-1 and Brm for the repression of E2F and cell growth. *EMBO J* **21**:3019-3028.

Werdan K, Schmidt H, Ebelt H, Zorn-Pauly K, Koidl B, Hoke RS, Heinroth K and Muller-Werdan U (2009) Impaired regulation of cardiac function in sepsis, SIRS, and MODS. *CanJPhysiol Pharmacol* **87**:266-274.

White SM and Claycomb WC (2003) Cardiac cell transplantation: protocols and applications. *Methods MolBiol* **219**:83-95.

White SM, Constantin PE and Claycomb WC (2004) Cardiac physiology at the cellular level: use of cultured HL-1 cardiomyocytes for studies of cardiac muscle cell structure and function. *AmJPhysiol Heart CircPhysiol* **286**:H823-H829.

Winter A, Kämäräinen O and Hofmann A (2007) Molecular modeling of prohibitin domains. *Proteins* **68**:353-362.

Winter BK, Fiskum G and Gallo LL (1995) Effects of L-carnitine on serum triglyceride and cytokine levels in rat models of cachexia and septic shock. *Br J Cancer* **72**:1173-1179.

Wiswedel I, Gardemann A, Storch A, Peter D and Schild L (2010) Degradation of phospholipids by oxidative stress--exceptional significance of cardiolipin. *Free Radic Res* **44**:135-145.

Wondergem R, Graves BM, Ozment-Skelton TR, Li C and Williams DL (2010) Lipopolysaccharides directly decrease Ca2+ oscillations and the hyperpolarization-activated nonselective cation current If in immortalized HL-1 cardiomyocytes. *Am J Physiol Cell Physiol* **299**:C665-671.

Wong HR, Carcillo JA, Burckart G, Shah N and Janosky JE (1995) Increased serum nitrite and nitrate concentrations in children with the sepsis syndrome. *Crit Care Med* **23**:835-842.

Wu Q and Wu S (2012) Lipid rafts association and anti-apoptotic function of prohibitin in ultraviolet B light-irradiated HaCaT keratinocytes. *Exp Dermatol* **21**:640-642.

Wu TF, Wu H, Wang YW, Chang TY, Chan SH, Lin YP, Liu HS and Chow NH (2007) Prohibitin in the pathogenesis of transitional cell bladder cancer. *Anticancer Res* **27**:895-900.

Xie Z and Klionsky DJ (2007) Autophagosome formation: core machinery and adaptations. *Nat Cell Biol* **9**:1102-1109.

Xu C, Yi C, Wang H, Bruce IC and Xia Q (2012) Mitochondrial nitric oxide synthase participates in septic shock myocardial depression by nitric oxide overproduction and mitochondrial permeability transition pore opening. *Shock* **37**:110-115.

Yang S and Hauptman JG (1994) The efficacy of heparin and antithrombin III in fluid-resuscitated cecal ligation and puncture. *Shock* **2**:433-437.

Yeo M, Kim DK, Park HJ, Oh TY, Kim JH, Cho SW, Paik YK and Hahm KB (2006) Loss of transgelin in repeated bouts of ulcerative colitis-induced colon carcinogenesis. *Proteomics* **6**:1158-1165.

Yurugi H, Tanida S, Ishida A, Akita K, Toda M, Inoue M and Nakada H (2012) Expression of prohibitins on the surface of activated T cells. *BiochemBiophysResCommun* **420**:275-280.

Zacharowski K, Olbrich A, Cuzzocrea S, Foster SJ and Thiemermann C (2000) Membrane-permeable radical scavenger, tempol, reduces multiple organ injury in a rodent model of gram-positive shock. *Crit Care Med* **28**:1953-1961.

Zang QS, Sadek H, Maass DL, Martinez B, Ma L, Kilgore JA, Williams NS, Frantz DE, Wigginton JG, Nwariaku FE, Wolf SE and Minei JP (2012) Specific inhibition of

mitochondrial oxidative stress suppresses inflammation and improves cardiac function in a rat pneumonia-related sepsis model. *AmJPhysiol Heart CircPhysiol* **302**:H1847-H1859.

Zheng X, Shoffner JM, Lott MT, Voljavec AS, Krawiecki NS, Winn K and Wallace DC (1989) Evidence in a lethal infantile mitochondrial disease for a nuclear mutation affecting respiratory complexes I and IV. *Neurology* **39**:1203-1209.

Zhu B, Zhai J, Zhu H and Kyprianou N (2010) Prohibitin regulates TGF-beta induced apoptosis as a downstream effector of Smad-dependent and -independent signaling. *Prostate* **70**:17-26.

Zhu H, Jia Z, Misra BR, Zhang L, Cao Z, Yamamoto M, Trush MA, Misra HP and Li Y (2008) Nuclear factor E2-related factor 2-dependent myocardiac cytoprotection against oxidative and electrophilic stress. *CardiovascToxicol* **8**:71-85.

Zou L, Feng Y, Chen YJ, Si R, Shen S, Zhou Q, Ichinose F, Scherrer-Crosbie M and Chao W (2010) Toll-like receptor 2 plays a critical role in cardiac dysfunction during polymicrobial sepsis. *Crit Care Med* **38**:1335-1342.

APPENDIX A: Animal Care and Use Committee Approval Letters

East Carolina University

Animal Care and Use Committee
212 Ed Warren Life Sciences Building
East Carolina University
Greenville, NC 27834

252-744-2436 office
252-744-2355 fax

September 19, 2011

Ethan Anderson, Ph.D.
Department of Pharmacology
Brody 6S-11
ECU Brody School of Medicine

Dear Dr. Anderson:

Your Animal Use Protocol entitled, "Rat Model for Studies on the Effect of TNFα Scavenging on the Development of Cardiac and Mitochondrial Dysfunction in Sepsis" (AUP #W230) was reviewed by this institution's Animal Care and Use Committee on 9/19/11. The following action was taken by the Committee:

"Approved as submitted"

A copy is enclosed for your laboratory files. Please be reminded that all animal procedures must be conducted as described in the approved Animal Use Protocol. Modifications of these procedures cannot be performed without prior approval of the ACUC. The Animal Welfare Act and Public Health Service Guidelines require the ACUC to suspend activities not in accordance with approved procedures and report such activities to the responsible University Official (Vice Chancellor for Health Sciences or Vice Chancellor for Academic Affairs) and appropriate federal Agencies.

Sincerely yours,

Scott E. Gordon, Ph.D.
Chairman, Animal Care and Use Committee

SEG/jd

enclosure

East Carolina University

Animal Care and Use Commitee
212 Ed Warren Life Sciences Building
East Carolina University
Greenville, NC 27834

252-744-2436 office
252-744-2355 fax

August 30, 2012

Ethan Anderson, Ph.D.
Department of Pharmacology
Brody 6S-10
ECU Brody School of Medicine

Dear Dr. Anderson:

The Amendment to your Animal Use Protocol entitled, "Rat Model for Studies on the Effect of TNFα Scavenging on the Development of Cardiac and Mitochondrial Dysfunction in Sepsis", (AUP #W230) was reviewed by this institution's Animal Care and Use Committee on 8/30/12. The following action was taken by the Committee:

"Approved as amended"

****Please contact Dale Aycock prior to any hazard use**

A copy of the Amendment is enclosed for your laboratory files. Please be reminded that all animal procedures must be conducted as described in the approved Animal Use Protocol. Modifications of these procedures cannot be performed without prior approval of the ACUC. The Animal Welfare Act and Public Health Service Guidelines require the ACUC to suspend activities not in accordance with approved procedures and report such activities to the responsible University Official (Vice Chancellor for Health Sciences or Vice Chancellor for Academic Affairs) and appropriate federal Agencies.

Sincerely yours,

SBMcRae

Susan McRae, Ph.D.
Chair, Animal Care and Use Committee

SM/jd

enclosure

East Carolina University

Animal Care and Use Committee
212 Ed Warren Life Sciences Building
East Carolina University
Greenville, NC 27834
252-744-2436 office
252-744-2355 fax

February 27, 2013

Ethan Anderson, Ph.D.
Department of Pharmacology
Brody 6S-10
ECU Brody School of Medicine

Dear Dr. Anderson:

The Amendment to your Animal Use Protocol entitled, "Rat Model for Studies on the Effect of TNFα Scavenging on the Development of Cardiac and Mitochondrial Dysfunction in Sepsis", (AUP #W230) was reviewed by this institution's Animal Care and Use Committee on 2/27/13. The following action was taken by the Committee:

"Approved as amended"

****Please contact Dale Aycock prior to any hazard use**

A copy of the Amendment is enclosed for your laboratory files. Please be reminded that all animal procedures must be conducted as described in the approved Animal Use Protocol. Modifications of these procedures cannot be performed without prior approval of the ACUC. The Animal Welfare Act and Public Health Service Guidelines require the ACUC to suspend activities not in accordance with approved procedures and report such activities to the responsible University Official (Vice Chancellor for Health Sciences or Vice Chancellor for Academic Affairs) and appropriate federal Agencies.

Sincerely yours,

Susan McRae, Ph.D.
Chair, Animal Care and Use Committee

SM/jd

enclosure

East Carolina University

Animal Care and Use Committee
212 Ed Warren Life Sciences Building
East Carolina University
Greenville, NC 27834

252-744-2436 office
252-744-2355 fax

June 12, 2013

Ethan Anderson, Ph.D.
Department of Pharmacology
Brody 6S-10
ECU Brody School of Medicine

Dear Dr. Anderson:

The Amendment to your Animal Use Protocol entitled, "Rat Model for Studies on the Effect of TNFα Scavenging on the Development of Cardiac and Mitochondrial Dysfunction in Sepsis", (AUP #W230) was reviewed by this institution's Animal Care and Use Committee on 6/12/13. The following action was taken by the Committee:

"Approved as amended"

****Please contact Dale Aycock prior to any hazard use**

A copy of the Amendment is enclosed for your laboratory files. Please be reminded that all animal procedures must be conducted as described in the approved Animal Use Protocol. Modifications of these procedures cannot be performed without prior approval of the ACUC. The Animal Welfare Act and Public Health Service Guidelines require the ACUC to suspend activities not in accordance with approved procedures and report such activities to the responsible University Official (Vice Chancellor for Health Sciences or Vice Chancellor for Academic Affairs) and appropriate federal Agencies.

Sincerely yours,

SBMcRae

Susan McRae, Ph.D.
Chair, Animal Care and Use Committee

SM/jd

enclosure

East Carolina University

Animal Care and Use Commitee
212 Ed Warren Life Sciences Building
East Carolina University
Greenville, NC 27834

252-744-2436 office
252-744-2355 fax

November 20, 2013

Ethan Anderson, Ph.D.
Department of Pharmacology
Brody 6S-10
ECU Brody School of Medicine

Dear Dr. Anderson:

The Amendment to your Animal Use Protocol entitled, "Rat Model for Studies on the Effect of TNFα Scavenging on the Development of Cardiac and Mitochondrial Dysfunction in Sepsis", (AUP #W230) was reviewed by this institution's Animal Care and Use Committee on 11/20/13. The following action was taken by the Committee:

"Approved as amended"

****Please contact Dale Aycock prior to any hazard use**

A copy of the Amendment is enclosed for your laboratory files. Please be reminded that all animal procedures must be conducted as described in the approved Animal Use Protocol. Modifications of these procedures cannot be performed without prior approval of the ACUC. The Animal Welfare Act and Public Health Service Guidelines require the ACUC to suspend activities not in accordance with approved procedures and report such activities to the responsible University Official (Vice Chancellor for Health Sciences or Vice Chancellor for Academic Affairs) and appropriate federal Agencies.

Sincerely yours,

Susan McRae, Ph.D.
Chair, Animal Care and Use Committee

SM/jd

enclosure